Universidad Carlos III de Madrid
www.uc3m.es

TESIS DOCTORAL

Manufacturing, Characterization and Modelling of Biodegradable Composite Materials

Autor:

Ángel Rubio López

Director y Tutor:

Prof. Dr. D. Carlos Santiuste Romero

DEPARTAMENTO DE MECÁNICA DE MEDIOS CONTÍNUOS Y TEORÍA DE ESTRUCTURAS

Leganés, Octubre 2016

Universidad Carlos III de Madrid
www.uc3m.es

TESIS DOCTORAL

Manufacturing, Characterization and Modelling of Biodegradable Composite Materials

Autor: Ángel Rubio López

Director: Prof. Dr. D. Carlos Santiuste Romero

Firma del Tribunal Calificador:

Firma

Presidente:

Vocal:

Secretario:

Calificación:

Leganés, 7 de Octubre de 2016

Contents

Acknowledgements

Para India y Alba

Author gratefully acknowledge the support of Spanish Ministry of Economy under the project DPI2013-43994-R and the Carlos III of Madrid University for the financial support during the last three years. Also acknowledge Dr. Mark Staiger and University of Canterbury in New Zealand for the teaching on the manufacturing of ACC's.

Gracias a Carlos, por tu paciencia, disponibilidad y por confiar en mí. Ha sido mucho lo que he aprendido de tu talento y motivación.

Recordaré con mucho cariño los momentos compartidos en el B12 con Javi, Mahy, Dani, Damián, Chon, Vila, Lore, Mata, Pablo, Oscar y compañía.

Gracias a todos aquellos que de una forma u otra han puesto su grano de arena para que esta tesis sea una realidad.

Abstract

In the recent decades, there has been a high rise in the development of renewable materials due to awareness in environmental care. Part of the research in such materials has focused on the development of biodegradable composites using natural fibres as reinforcement of 'green' plastics. The use of biocomposites means a major reduction in the environmental impact of industrial components after their life cycle, thus, the development of tools for design with biocomposites could mean a breakthrough for its implementation in the industry.

In this thesis, the basis for the development of tools for modelling the mechanical behaviour of biocomposites have been arise for first time through the development of a constitutive model based on the simulation of the mechanical behaviour through rheological elements. The seven model parameters have been adjusted by quasi-static tensile tests, while the model has been successfully validated by tensile tests at different strain rates. The constitutive model has proved to be valid for composites reinforced with cotton, flax and jute, allowing a greater understanding of the behaviour of those biocomposites, as the fact that the viscoplastic behaviour is mainly produced by fibres behaviour. The existence of a constitutive model for biocomposites opens the doors to its application in structural components of responsibility greatly reducing design costs.

Four different biocomposites were chosen to test the versatility of the constitutive model. Biodegradable PLA composites were manufactured by compression moulding combining two types of PLA as matrix and three natural fibres (flax, cotton and jute) as reinforcement. Moreover, the ACC's were manufactured by solving the surface cellulose of the fibres, which after a regeneration process forms the composite matrix. Thus, four different biocomposites were successfully manufactured in this thesis.

The parameters influencing the PLA based biocomposites manufacturing process (temperature, pressure, number of layers, type of fibre and matrix type) have been optimized to obtain a material with a strength greater than 100 MPa, indicating their potential application for replacing traditional composites, especially glass fibre composites. This could mean a large increase in the use of biocomposites in industrial applications such as automotive or aviation. However, it has been observed that biocomposites presents a viscoplastic behaviour with permanent deformations, which is far from the linear elastic behaviour until failure of traditional composites. This has motivated the development of computational tools for biocomposites to predict their behaviour under dynamic conditions such as impacts or machining.

Impact test in drop tower were conducted in flax/PLA biocomposites, revealing a high energy absorption, above the absorbed by carbon fibre composites in the range of energies analysed. The main failure mode was fibre failure, while delaminations were not found. Due to this differences in failure modes, the normalized residual strength observed in biocomposites was higher than that reported in carbon fibre reinforced composites.

Two different Finite Element Models were developed. First, a linear elastic model was used to reproduce the impact behaviour of ACC plates. Second, a model considering the influence of strain rate on the plastic behaviour of biocomposites was implemented to reproduce the impact behaviour of flax/PLA biodegradable composites

Finally, the different mechanisms of damage induced in drilling had been studied. For this, the damage induced under different cutting speeds, advances and drill geometries was analysed, noting that in this case delaminations were neither found as failure mode, revealing a good cohesion between fibre and matrix. Is also detachable the damage reduction with increasing drill feed rate, which is a novelty that can reduce the processing times of these materials in the industry. These machining tests are the basis for the application of a numerical model based on the constitutive model defined in this work.

Resumen

En las últimas décadas se ha producido un gran auge en el desarrollo de materiales renovables debido a la concienciación en el cuidado del medio ambiente. Parte de la investigación en dichos materiales se ha focalizado en el desarrollo de materiales compuestos biodegradables, empleando fibras naturales como refuerzo de plásticos 'verdes'. El uso de los biocomposites puede suponer una gran reducción en el impacto ambiental de componentes industriales tras su ciclo de vida, por lo que el desarrollo de herramientas para el diseño con biocomposites significaría un gran avance para su implementación en la industria.

En el presente trabajo se han planteado por primera vez las bases para el desarrollo de herramientas para el modelizado de los biocomposites desarrollando un modelo constitutivo que los defina, basándose dicho modelo en la simulación de su comportamiento mecánico por medio de elementos reológicos. Los siete parámetros del modelo han sido ajustados mediante ensayos a tracción cuasi-estáticos, mientras que la validación de los mismos se ha realizado con éxito por medio de ensayos de tracción a distintas velocidades de deformación. El modelo constitutivo ha demostrado ser válido para biocomposites reforzados con algodón, lino y yute, permitiendo una mayor comprensión del comportamiento de los biocomposites, tal como el hecho de que los comportamientos viscoplásticos tienen origen en las fibras y no en la matriz. La existencia de un modelo constitutivo para biocomposites abre las puertas a su aplicación en componentes de responsabilidad estructural reduciendo enormemente los costes de diseño.

Se han fabricado distintos materiales para comprobar la versatilidad del modelo constitutivo. Los materiales compuestos biodegradables de PLA se han fabricado mediante modelizado por compresión en caliente, empleando dos tipos de PLA y tres fibras naturales (lino, algodón y yute). Por otro lado, los ACC han sido fabricados mediante la disolución de la celulosa superficial de las fibras, que tras una regeneración conforma la matriz del compuesto. Por lo tanto, se han fabricado con éxito cuatro biocomposites diferentes en el marco de la tesis.

Los parámetros que influyen en el proceso de fabricación de los compuestos de PLA (temperatura, presión, número de capas, tipo de fibra y tipo de matriz) han sido optimizados para la obtención de un material con una resistencia superior a los 100 MPa, lo que revela su potencial aplicación para la sustitución de los materiales compuestos tradicionales, especialmente los compuestos de fibra de vidrio. Esto hace prever un gran incremento en su uso en aplicaciones industriales tales como la automoción o la aviación. Sin embargo, también se ha podido observar que los biocomposites presentan un comportamiento viscoso con deformaciones permanentes, lo que dista del comportamiento elástico lineal hasta rotura de los materiales compuestos tradicionales. Esto ha motivado el desarrollo de herramientas de cálculo para los biosomposites para la predicción de su comportamiento en condiciones dinámicas tales como impactos o mecanizados.

Se han realizado ensayos de impactos en torre de caída en compuestos de lino/PLA, lo que ha revelado una gran absorción de energía de los mismos, superior a la absorbida por compuestos de fibra de carbono en el rango de energías analizado. El principal modo de fallo localizado en los

biocomposites es la rotura de fibras, mientras que no se han encontrado delaminaciones. Debido a esta diferencia en los modos de fallo la resistencia residual normalizada es mayor en biocomposites que en compuestos de fibra de carbono estudiados.

Se han desarrollado dos modelos de elementos finitos. En primer lugar, se han reproducido impactos en placas de ACC por medio de un modelo elástico lineal. En segundo lugar, se ha desarrollado un modelo que tiene en cuenta la influencia de la velocidad de deformación en el comportamiento plástico de los biocomposites, el cual fue implementado para reproducir el comportamiento ante impactos de compuestos de lino/PLA.

Por último, se han estudiado los distintos mecanismos de daño inducidos en el taladrado de compuestos de PLA. Para ello, se ha estudiado el daño ante distintas velocidades de corte, avances y geometrías de broca, destacando que en este caso tampoco se han localizado delaminaciones como modo de fallo, revelando una buena cohesión entre fibra y matriz. También cabe destacar que se ha determinado una reducción del daño con el incremento de la velocidad de avance, lo que supone una novedad que puede reducir los tiempos de procesado de estos materiales en la industria. Estos ensayos son la base para la aplicación de un modelo numérico basado en el modelo constitutivo definido en este trabajo.

Chapter 1
Introduction

1.1 Motivation

Materials used in industry are always in evolution due to improvement in product specifications, cost reduction or compliance of new legislations. Awareness by climate change makes the authorities enact new laws by which they force the use of recyclable and reusable materials to avoid the solid waste landfills. For example, only the waste produced by the automotive industry due to the end of life of the vehicles in the European Community are between 8 and 9 million tons per year [1], and the best way to manage these wastes in order to reduce their environmental impact, is recycling. In this way, European Guideline 2000/53/EC [1], enacted by the European Commission, stablished that for 2005 the recyclability of a motor vehicle had to be 85% of the weight, while for 2015, this ratio was increased up to 95%. The 2005/64/EC [2] directive stablished the type-approval of motor vehicles with regard to their reusability and recoverability, through the ISO 22628: 2002 standard, without which is not possible to certificate a car in the European countries.

In the last years, the research of new green materials has experience a great expansion [3] based on the use of natural resources as natural fibres or bioplastics in order to substitute petroleum based materials [3]. As an example of this development, the U.S. agricultural, forestry and chemical communities published the Plant/Crop-based renewable resources 2020, a Vision to Enhance U.S. Economic Security Through Renewable Plant/Crop-based Resource Use [4], in which is targeted to achieve the use of at least 10% of basic chemical blocks arising from plant-derived renewables by 2020, and 50% in 2050.

Thus, Natural Fibre Composites (NFC) are being applied widely, showing really promising properties and being suitable for the substitution of glass fibre in most of its applications [5], so it can be expected a great expansion in its use in order to accomplish the objectives formulated by authorities. NFC represent not only recyclability advantages [6], but also a reduction on weight and costs. Figure 1.1 shows a comparison between some natural fibres, traditional fibres and steel in terms of specific tensile strength and costs. Typical synthetic fibres are glass, aramid or carbon fibres, being remarkable the similar specific strength between some plant fibres and fiberglass, which covers 95% of whole composites applications [7]. These similarities become unbalance when costs (Figure 1.1) and renewability are considered. Moreover, energy needed to produce natural fibres is really reduced (4 GJ/ton in plant fibres and 30 GJ/ton for fibreglass [8]) and they are less harmful for health and environment during its production and handling comparing with synthetic fibres. In addition, it should be considered that these fibres are often wasted by other industries, as in case of bagasse and rice husk, which are wasted in the production of sugar and rice, what means a next step in materials reuse [8]. Moreover, these fibres show better behaviour as thermal and acoustic insulators due to its hollowed structure [8], what implies potential applications for the construction industry. Another advantage to be considered is that these materials are produced in

terms of millions of tons per year [9], generally in developing countries, what means a potential increment of their economy.

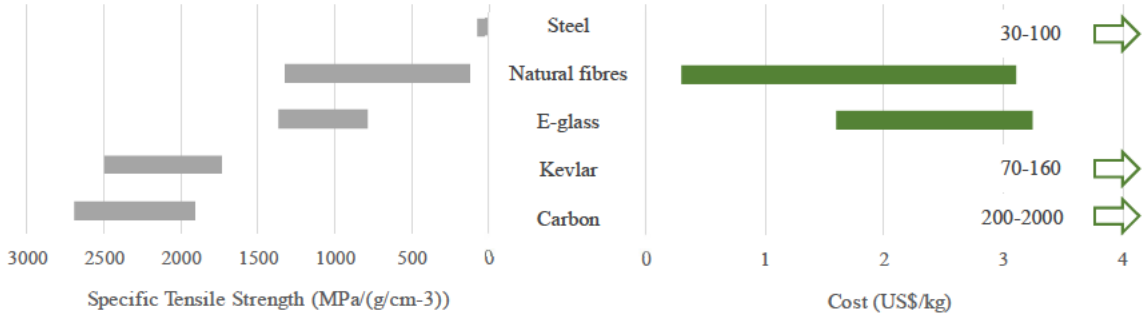

Figure 1.1. Specific tensile strength and costs comparative between natural fibres and other materials. Data included are extracted form [3, 7, 9-12]. Natural fibres includes flax, hemp, cotton and bamboo. This comparison is extended in Chapter 2.

Nevertheless, some disadvantages of NFC must be taken in consideration. Natural fibres are hydrophilic, what increase its biodegradability but limits their applications and is also translated to a poor bonding when combined with some matrixes, especially petroleum based ones. Nonetheless, this adhesion can be improved through modifying the natural fibre surface by physical or chemical treatments, improving considerably the mechanical performance of the NFC [3]. Moreover, plant fibres are sensible to temperatures over around 200ºC, depending on the fibre, what prevents its use with some oil based polymers. Also, there exists a great dispersion on the properties between two different fibres, being especially sensible to the weather conditions during the crop growth. For example, flax fibres length ranges between 5 and 900 mm and the fibre diameter does between 20 and 600 μm [3], what affects to the fibres processing.

One of the applications of biocomposites is the substitution of the traditional non-biodegradable composites in automotive industry. Traditional fibres are widely extended in components of cars, planes and in the aerospace sector. In order to reduce weight and costs and according with recyclability legislations, during the last two decades natural fibres have been introduced to substitute traditional fibres in interior panels of cars. For example, Mercedes Benz used in 1996 jute fibres as reinforcement of an epoxy matrix in its E-class door panels and Toyota uses a 100 % of bioplastics in all their cars [9]. Being the exterior panels subjected to weather conditions, natural fibres are more complicated to include using a biodegradable plastic, but combined with petrochemical matrixes were used, for example, in A-class Mercedes-Benz in 2004, in which abaca fibres combined with polypropylene (PP) were applied instead of fiberglass for the spare tire well production [9]. A recent example of natural fibres application is the 'Be.e' electric scooter, which structural body is made of flax fibres, Figure 1.2.a [16]. The present application of natural fibres does not remain in the motor vehicle industry, as there exist many goods which are incorporating this green technology, for example the 'Artengo TR890', a tennis racket which incorporates a 14% of flax to reduce damping (Figure 1.2.b) [17]. Other examples are the 'El Capitan Blackbird Guitar' (Figure 1.2.c), in which a high durability of the instrument is remarked, and it is also made of flax composites [18]. Flax seems to play an important role as is also found in the 'Le Ventoux' bamboo-flax bike (Figure 1.2.c) [19] and the 'Caperlan' flax jig fishing rod (Figure 1.2.d) [20-21].

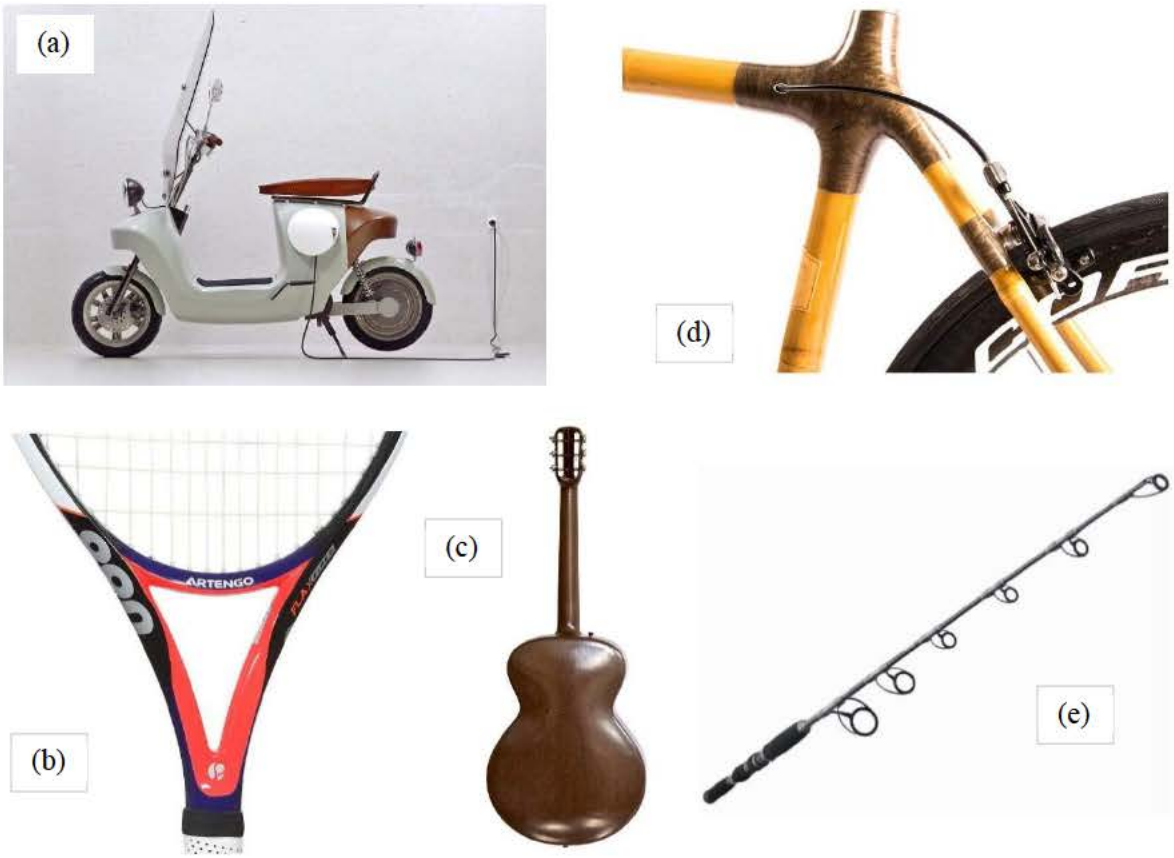

Figure 1.2. Natural fibres applied in: (a) Be.e electric scooter [16] © Waarmakers Product Design, (b) Artengo TR890 racket [17] © Decathlon (c) El Capitan Blackbird Guitar [18] © BLACKBIRD (d) Le Ventoux bamboo-flax bike [19] © INBO (e) Caperlan flax jig fishing rod [20] © Decathlon.

For all the mentioned applications, a good mechanical performance is needed, as products can be subjected to high stresses or impacts. There exist many works reporting the strength of different natural fibres [3, 5, 8], underlining the variety of the mechanical properties [8], being some of them, as flax, suitable for the substitution of traditional composites [5]. The matrix-fibre bonding has been widely studied to reduce the moisture absorption or to increase the tensile properties [3, 8]. In addition, many composites are characterized under Charpy or Izod impact tests in order to compare the energy absorbed by different natural fibres and matrixes configurations [3].

Nonetheless, the present and potential applications of biocomposites imply that components are subjected to dynamic conditions during its life service, what means the necessity of a deeper study on its mechanical properties. Two studies can help to understand the response of biocomposites under these conditions. First, a strain rate tensile dependence with permanent deformations was reported by Poilane et al [22], so a viscoplastic behaviour is present on biocomposites. Also, Huber et al. [23] studied the impact response of biocomposites under low-velocity impact tests, reporting a good impact performance based on a high energy absorption.

However, there is a lack of studies to fully understand the dynamic behaviour of biocomposites. A constitutive model based on the physics of the material would help to understand the response under dynamic applications as machining, impacts, fatigue, etc. Only a few predictive models for NFC have been reported, but only Poilane et al [22] defines a macromechanical constitutive model for flax/epoxy composites. Thus, exist a need of defining models for fully biodegradable composites.

A deep study of biocomposites properties through the definition of a constitutive model is the main motivation for this work. Understanding the behaviour of the composites is the first step for the development of design tools, which could mean a high reduction on the costs of production of biocomposite components and would open its applications to structural responsible parts in automotive or aerospace industry.

1.2 Project objectives

The objectives of this work are defined inside a project for the development of numerical tools for biocomposites, named BIOCOMPDYN (Biocomposites Dynamics). Three thesis are involved in the project, establishing in the present work the basis for the other two.

The BIOCOMPDYN project is divided in some goals as follows in Figure 1.3:

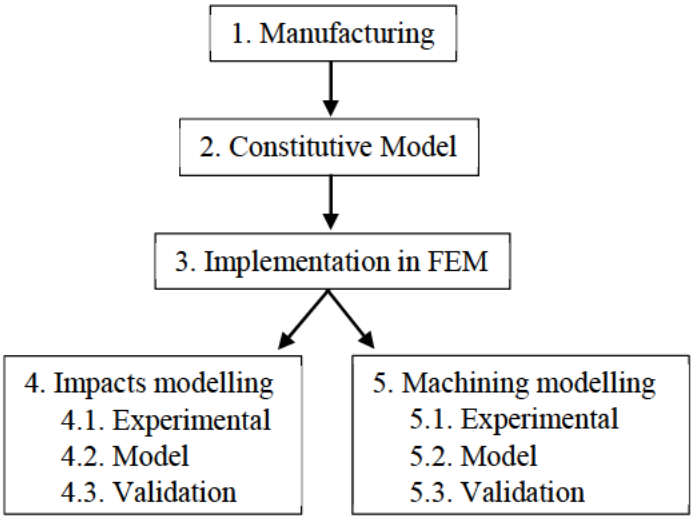

Figure 1.3. Scheme of the objectives planned for the BIOCOMPDYN project

In the present thesis, points 1 and 2 were fully developed while point 3 was approached though a material model implementation including strain rate influence and plastic behaviour, however, a user subroutine should be developed in the future for a further implementation in FEM. Goal 4 was developed with the approached models and goal 5 was partially accomplished, having performed experimental drilling operations. Detailed tasks of the works developed in this work are presented in Section 1.3 once an overview of the project is given in this section.

1.3 Thesis objectives

As presented in Section 1.2, the objective of this thesis can be divided in five goals, with some tasks inside each one. The highlight purpose of this work is goal 3, the definition a constitutive model for biocomposites in order to get a better understand of their mechanical behaviour, base for the numerical modelling of biocomposites.

1. Manufacturing. The first objective for this work is to obtain or produce the materials under study. As biocomposites are novel materials, its production is limited for research or for its application in final products, so it is not easy to find a supplier of the manufactured product. Thus, the

material has to be manufactured from scratch in a first step. To this end, the tasks in this point are:

1.1 Selection after comparison of materials and manufacturing methods.
1.2 Development of a manufacturing method to obtain the final product, studying different possibilities and having into consideration the complexity of the different processes and the costs.
1.3 Optimization of the the manufacturing method to maximize the mechanical properties of the final products in terms of tensile strength.

2. Constitutive model. The second goal of this work is to define a constitutive model to predict the behaviour of the material under dynamic conditions. The tasks considered to this purpose are:

2.1 Study of the models for biocomposites developed by other authors.
2.2 Definition of the model, studying the basic models and collecting the proper elements.
2.3 Calibration of the constitutive model through tensile tests for all the manufactured materials.
2.4 Validation of the model considering the strain rate influence.

3. Implementation in FEM. To analyse the behaviour of biocomposites under different dynamic conditions, FEM tools are used, and a definition of the biocomposites behaviour has to be defined in that tools. Thus, two approaches were done to this end:

3.1 Linear elastic approach, as used in traditional composites, to explore the limits of such assumption.
3.2 Biocomposites approach including a strain rate dependence.

4. Impacts modelling. The implementations in FEM done in point 3 can be applied in simulations of impacts on biocomposites.

4.1 Experimental tests to determine the behaviour of biocomposites under impacts, studying the energy absorption capability of biocomposites.
4.2 Modelling of the biocomposites behaviour with the approaches implemented in FEM.
4.3 Validation of the impact models, considering the experimental tests for this purpose and having present the limits of using approached models.

5. Machining modelling. This objective is focused on the definition of the machining properties of biocomposites for the future modelling of those properties.

5.1 Experimental tests to determine the behaviour of biocomposites under drilling, studying the damage induced during the drilling.

1.4 Contents description

The presented objectives have been distributed throughout this work.

In the second chapter, *State of the Art* (obj. 2.1), are describe the existing different options in materials properties and manufacturing processes regarding biocomposites in order to know the works done by other authors regarding the manufacturing, characterization and modelling of biocomposites. Once the manufacturing possibilities were studied, chapter three is presented,

Parametric study of Compression Moulding manufacturing conditions (obj. 1), defining the optimization process of the different parameters which influence in the compression moulding manufacturing process.

Chapter four presents works concerning the constitutive model definition under the title *Analytical model to predict the dynamic behaviour of biocomposites* (obj. 2.2 - 2.4), where a rheological model with seven parameters is introduced for a better understanding of biocomposites behaviour. The constitutive model was successfully validated with experimental works considering plasticity and viscoelasticity.

In the fifth chapter, *Low-velocity impact behaviour of biocomposites: Experimental study* (obj. 4.1), the results of dynamic impact properties of biocomposites are exposed, presenting the promising properties under impacts of PLA/flax composites. Chapter six, *Low-velocity impact behaviour of biocomposites: Numerical model* (obj. 3.1, 4.2, 4.3), is based on the development of a linear elastic behaviour of the biocomposites as a first approach to the biodegradable composites modelling. In chapter seven, *Low-velocity impact behaviour of biocomposites: Numerical model considering strain rate dependence* (obj. 3.2, 4.2, 4.3), the viscoplastic behaviour is considered to model the impact behaviour of biocomposites.

Finally, the eight chapter, *Induced damage during drilling: Experimental study* (obj. 5.1) defines the biocomposites behaviour under drilling analysing the main parameters influence on the induced damage during drilling operations.

1.5 Thesis contributions

Biodegradable PLA based composites were produced by compression moulding, optimizing the method to produce a more than 100 MPa composites in a 5 minutes processing time, what make them interesting to replace fibreglass composites in most of its applications, reducing their environmental impact.

A constitutive model was successfully developed to predict the viscous and plastic behaviour found on flax, cotton and jute PLA based biocomposites. This model allows a mayor understanding of the material behaviour, as the fact that the viscous and plastic effects can be mainly attributed to fibre behaviour. The development of this model establish the base for a FEM simulation tool for biocomposites components in industry, meaning a high costs reduction in the design process.

The PLA based biocomposites were characterized under low-velocity impact test, following by compression after impact tests, revealing a high energy absorption, above the carbon fibre composites in the range of energies analysed. Moreover, no delaminations were found leading to higher values of normalized residual strength than carbon fibre reinforced composites.

Biocomposites impact modelling was successfully performed for first time, assuming a linear behaviour for ACC as a first approach to explore the limits of this assumption.

The viscoplastic behaviour of PLA based composites was considered to model its impact behaviour for first time, opening the doors to a further integration in FEM.

A study on drilling study performedon biocomposites was reported, revealing promising properties as no delaminations were found and the increment of feed rate implies damage reductions.

These contributions were published in the next papers:

Rubio-López A, Olmedo A, Díaz-Álvarez A, Santiuste C. Manufacture of compression moulded PLA based biocomposites: a parametric study. Compos Struct 2015; 131:995–1000

Rubio-López A, Hoang T, Santiuste C. Constitutive model to predict the viscoplastic behaviour of natural fibres based composites. Compos Struct 2016; 155: 8-18

A. Rubio-López, J. Artero-Guerrero, J. Pernas-Sánchez, C. Santiuste. Compression after impact of flax/PLA biodegradable composites. Under review.

Rubio-López A, Olmedo A, Santiuste C. Modelling impact behavior of allcellulose composite plates. Comp Struct 2015; 122: 139–43

Hoang T, Rubio-López A, Santiuste C. Viscoplastic FEM model to predict the impact behaviour of flax/PLA composites. Under review.

Díaz-Álvarez A, Rubio-López A, Santiuste C, Miguélez MH. Experimental analysis of drilling induced damage in biocomposites. Under review

References

[1] European Union. (2000). The Directive 2000/53/EC of the European Parliament and of the Council of 18 September 2000 on end-of-life vehicles. OJ L, 269 (34-49).

[2] European Union. (2005). The Directive 2005/64/EC of the European Parliament and of the Council of 26 October 2005 on the type-approval of motor vehicles with regard to their reusability, recyclability and recoverability. OJ L, 310 (10–27).

[3] Faruk, O., Bledzki, A. K., Fink, H. P., & Sain, M. (2012). Biocomposites reinforced with natural fibers: 2000–2010. Progress in Polymer Science, 37(11), 1552-1596.

[4] Plant/Crop-based renewable resources 2020, a Vision to Enhance U.S. Economic Security Through Renewable Plant/Crop-based Resource Use (1998), www nrel.gov/docs/legosti/fy98/24216.pdf

[5] Bodros, E., Pillin, I., Montrelay, N., & Baley, C. (2007). Could biopolymers reinforced by randomly scattered flax fibre be used in structural applications?.Composites Science and Technology, 67(3), 462-470.

[6] Le Duigou, A., Pillin, I., Bourmaud, A., Davies, P., & Baley, C. (2008). Effect of recycling on mechanical behaviour of biocompostable flax/poly (l-lactide) composites. Composites Part A: Applied Science and Manufacturing, 39(9), 1471-1478.

[7] Mohanty, A. K., Misra, M., & Hinrichsen, G. (2000). Biofibres, biodegradable polymers and biocomposites: an overview. Macromolecular materials and engineering, 276(1), 1-24.

[8] Satyanarayana, K. G., Arizaga, G. G., & Wypych, F. (2009). Biodegradable composites based on lignocellulosic fibers—An overview. Progress in polymer science, 34(9), 982-1021.

[9] Koronis, G., Silva, A., & Fontul, M. (2013). Green composites: a review of adequate materials for automotive applications. Composites Part B: Engineering, 44(1), 120-127.

[10] Gurunathan, T., Mohanty, S., & Nayak, S. K. (2015). A review of the recent developments in biocomposites based on natural fibres and their application perspectives. Composites Part A: Applied Science and Manufacturing, 77, 1-25.

[11] Pickering, K. L., Efendy, M. A., & Le, T. M. (2015). A review of recent developments in natural fibre composites and their mechanical performance. Composites Part A: Applied Science and Manufacturing.

[12] Steel mechanical properties. 20/04/2016 <http://www.steelconstruction.info/Steel_material_properties>

[13] Aramid (Kevlar) market price. 20/04/2016 <http://www.alibaba.com/product-detail/kevlar-fabric-price-of-kevlar-per_60373750766.html?spm=a2700.7724857.29.12.jhF0QT>

[14] Aramid (Kevlar) market price. 20/04/2016 <http://www.clipcarbono.com/es/59-tejido-de-fibra-de-kevlar-1200-x-1000-mm html>

[15] Carbon fibre market price. 20/04/2016 <http://www.build-on-prince.com/carbon-fiber.html#sthash.Ab1zqtdw.dpbs>

[16] Be. E – Electric Bio-Scooter. 19/04/2016 <http://www.vaneko.com/the-be-e/>

[17] Artengo TR890. 19/04/2016 <http://www.decathlon.es/raqueta-de-tenis-artengo-890-flax-fiber-id_8297316 html>

[18] Blackbird El Capitan Guitar. 19/04/2016 <https://www.blackbirdguitar.com/products/el-capitan>

[19] In'bô. Le Ventoux Bike. 20/04/2016 <http://inbo fr/en/wood-and-bamboo-bikes/9-le-ventoux.html>

[20] Caperlan. CAPERLAN BLYSS DEEP TEAM 5" FLAX Jig Fishing Rod. 19/04/2016 <https://www.decathlon.co.uk/blyss-deep-team-5-flax-fibre-id_8164177 html>

[21] Pil, L., Bensadoun, F., Pariset, J., & Verpoest, I. (2015). Why are designers fascinated by flax and hemp fibre composites?. Composites Part A: Applied Science and Manufacturing.

[22] Poilâne, C., Cherif, Z. E., Richard, F., Vivet, A., Doudou, B. B., & Chen, J. (2014). Polymer reinforced by flax fibres as a viscoelastoplastic material.Composite Structures, 112, 100-112.

[23] Huber T, Bickerton S, Müssig J, Pang S, Staiger MP. Flexural and impact properties of all-cellulose composite laminates. Compos Sci Technol 2013;88:92–98.

Chapter 2
State of the Art

In this Chapter the information regarding different natural fibres, biopolymers, manufacturing methods and biocomposites properties found in the bibliography are summarized. The goal of this section is to show a brief introduction to the advances in this research field and to provide a vision of the future challenges.

2.1 Natural fibres and biopolymers

By biocomposite term are defined those composites having high biodegradability as they are composed of natural organic materials, not mineral or synthetic. In this section biocomposites are defined within the global scale of composites, introducing the characteristics of its components.

First of all, it worth defining the biodegradability of a material, differentiating them by the time it may take for its decomposition. For this purpose, Table 2.1 has been drawn, in which is possible to realize how biocomposites can drastically reduce environmental impact, without considering the energy consumption during the materials production.

Material	Time to degrade
Conventional copy paper	1 month
PHB (polyhydroxybutyrate)	1 month
Cotton	1–5 months
Starch	2 months
Wool stocking	1 year
Bamboo stick	1–3 years
Chewing gum	5 years
Plastic	450 years
Glasses and tyres	Uncertain time

Table 2.1. Time to degrade in the environment of some materials [1].

Every composite is formed by two or more components. One of them is a matrix, which is reinforced by other materials. Such a combination is present in nature and in human body itself, as for example, wood is made of cellulose fibres that reinforce a matrix of lignin, pectin and other substances, while the muscles are composed of fibres formed by proteins that surrounds myoglobin among other components. Such combinations are those which similarly generate composites, whose main property is a high strength and stiffness combined with a low density. Also they offer dimensional stability and high capacity of cohesion of its parts. These characteristics are achieved

by combining different materials while the best of each is obtained. So that, not only is possible to obtain excellent mechanical properties, but also to get very valid materials for a huge range of applications where mechanical requirements are not demanding and the goal is a reduced cost.

There are different configuration of reinforcement, either by fibres, long or short, or by particles. For the present work, long or short fibres where studied, which can be woven or simply bonded by the matrix. The fibres themselves have excellent mechanical properties. But to be used in macroscopic applications, these fibres have to be combined in yarns, when its outstanding mechanical behaviour is reduced. Table 2.2 compares properties of different fibres, natural and industrially processed, compared with steel. In Table 2.2 shows how carbon fibre properties are outstanding, but it high costs of production makes it not employed except in cases where the purpose justifies it, as in aerospace or competitions sports. The high cost of carbon fibres and Kevlar, makes glass fibre the most widely used as it is appropriate for many low cost applications.

	Fibre /Material	Density (g/cm3)	Diameter (μm)	Tensile Strength (MPa)	Tensile Modulus (GPa)	Max. Strain (%)	Ref.
Natural fibres	Flax	1.38-1.5	20-600	345-1830	27-65	2.7-3.2	[2]
	Hemp	1.47	25-250	550-1100	38-70	1.6-4	[2, 3]
	Jute	1.3-1.49	25-250	393-800	13-26.5	1.16-1.5	[2]
	Kenaf	1.5-1.6	2.6-4	350-930	40-53	1.6	[2]
	Ramie	1.5-1.6	0.049	400-938	61.4-128	1.2-3.8	[2]
	Sisal	1.45	50-200	468-700	9.4-22	3-7	[2]
	Curaua	1.4	7-10	500-1100	11.8-30	3.7-4.3	[2]
	Abaca	1.5	7-30	430-813	31.1-33.6	2.9	[2]
	Cotton	1.5-1.6	-	287-597	5.5-12.6	3-10	[4]
	Nettle	1.51	20	650-1594	38-87	1.7-2.1	[2, 3]
	PALF*	1.5	20-80	413-1627	24.5-82.5	1.6	[5]
	Banana	1.35	115-126	542-914	20-32	5-6	[3]
	Coconut	1.15-1.46	100-460	131-220	4-6	15-40	[5]
	Bamboo	0.6-1.1	5-7	140-441	11-36	-	[6]
	Sugarcane	1.25	-	290	17	-	[6]
	Pineapple	0.7-1.55	-	400-627	1.44	14.5	[6]
	Palm	0.7-1.55	150-500	248	3.2	25	[5]
Synthetic	Lyocell	-	11.4	1019.8	8.94	12.5	[7]
	Cordenka	-	12	830	20	13	[8]
	E-glass	2.55	15-25	2000-3500	70-85	2.5-3.7	[2]
	Carbon	1.78	5-7	3400-4800	240-425	1.4-1.8	[5]
	Kevlar	1.44	-	2500-3600	60-112	2.5-3.7	[5]
	Steel	7.85	-	215-830	210-235	10-30	[9]

Table 2.2. Natural fibres properties compared to synthetic fibres and steel. *PALF = Pineapple leaf fibres.

The properties of vegetable fibres, as every natural material, have a huge variation depending on multiple factors. The most crucial of these is the growing area [10], since the growth conditions of the plant determine the strength of the fibres. And it is not only the growing area, but all the factors that influence the process of obtaining the fibres that determine their ultimate strength, reason why exist such a wide variation in the values of natural fibres shown in Table 2.2. As mentioned in the motivations (section 1.1), natural fibres are comparable to fiberglass when the specific mechanical properties are considered. Taking this into consideration, Figure 2.1 shows a comparison of specific tensile strength and specific elastic modulus of natural fibres, steel, E-glass, Kevlar and carbon fibres. According to these specific properties, is visible that some natural fibres, especially Flax, are potentially applicable in substitution of glass fibre composites. It also highlights the Ramie fibre, which high specific elastic modulus, higher than Kevlar, draws its potential use armour applications [11].

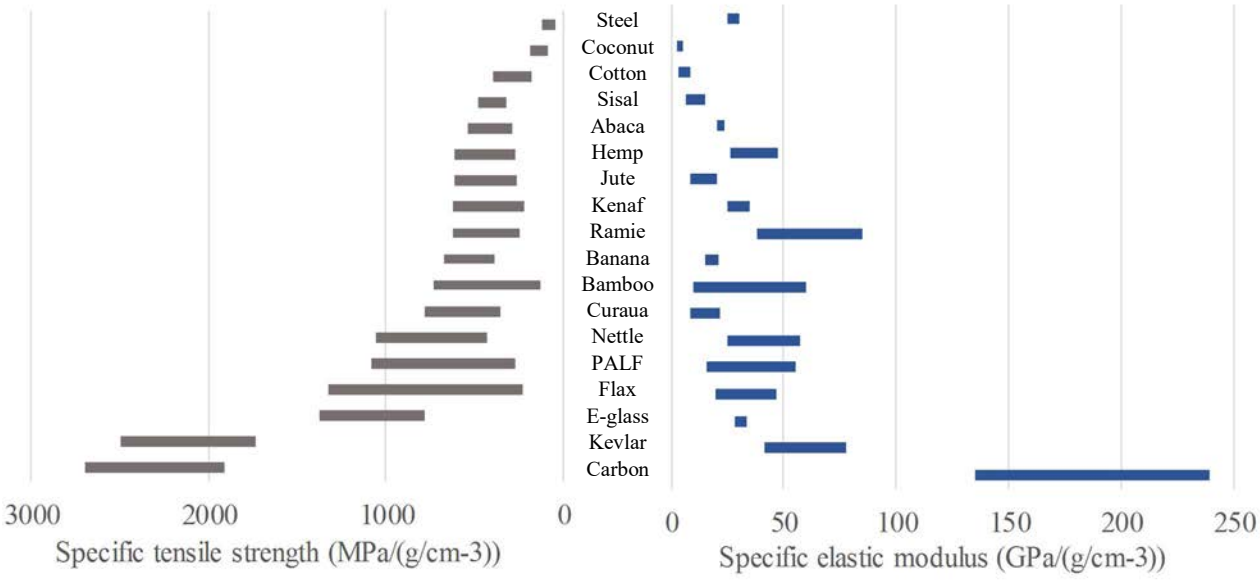

Figure 2.1. Specific tensile strength and elastic modulus of natural fibres compared to traditional fibres and steel. Data and references taken from Table 2.2.

Regarding matrixes used to bind the fibres, the most widespread are polyester, polyethylene (PE), polypropylene (PP) and epoxy resins. The use of new matrices is continuously expanding, and this is one of the fields where composite materials research is focusing on. The conventional matrices are non-biodegradable, partly because one of its functions is to protect the fibres from environmental actions. But in order to achieve a fully biodegradable material, the matrix must be non-oil based. Some of the most used bioplastics are poly-lactic acid (PLA) and poly-L-lactic acid (PLLA), which are obtained from corn, sugarcane or roots starch polymerization. PLA is widely used in 3D printing. Other bioplastics examples are Polyhydroxybutyrate (PHB), which is produced by microorganisms, and chitosan biopolymer, which is obtained from the shells of some crustaceans, therefore its origin is not plant and animal. These new arrays are beginning its journey, so improving its environmental corrosion in a composite material is under research, and is achieved by chemical or physical post treatments that affects the matrix and in some cases also the fibres, in some cases achieving improved mechanical properties. Some of the post treatments are acetylation [6], alkalinisation [4] or wave treatments [12]. In general, the properties that a matrix should present are a high shear strength, toughness and good cohesion with the fibres in addition to the aforementioned resistance to environmental aggressions. The mechanical properties of various matrices, biodegradable and traditional are presented in Table 2.3, showing that biopolymers strength and elastic modulus are similar to oil based matrixes, pointing out the great performance of PLA and PLLA. Some authors have reported a poor bonding between natural fibres and

traditional polymers [6], while mechanical properties of Natural Fibres Composites (NFC) improved when fibres are combined with biopolymers [13]. On the other hand, bioplastics use is not as extended as oil based polymers, despite they are thermoplastics. PLA costs 2.42 US$/kg [2], but its production is supposed to be increased in the next years, so its price could be expected to decrease [1]. Compared to PP, 1.65 US$/kg [2], PLA is expensive, but it also has a better mechanical behaviour (Table 3).

	Polymer	Density (g/cm3)	Melting Temperature (ºC)	Tensile Strength (MPa)	Tensile Modulus (GPa)	Max. Strain (%)	Ref.
Biodegradable	Starch	1-1.39	110-115	5-6	0.125-0.85	31-44	[2]
	PLA	1.21-1.25	150-162	21-60	0.35-3.5	2.5-6	[2]
	PLLA	1.25-1.29	170-190	15.5-65.5	0.83-2.7	3-4	[2]
	PHB	1.18-1.26	168-182	24-40	3.5-4	5-8	[2]
	PHBV	1.23-1.35	144-172	20-25	0.5-1.5	17.5-25	[2]
	Chitosan	-	180-192	12-20	0.5-0.7	17-42	[14]
Traditional	PP	0.9-1.16	161-170	30-40	1.1-1.6	20-400	[2]
	PE	0.93	120-180	23	0.14-0.9	200-600	[15]
	PVC	1.1-1.45	100-260	9-59	3.4	17	[16]
	Polyester	1.19	220-267	57-60	1.93-3	-	[17]
	Epoxy	1-1.81	120-130	45-83	10.5	0.8	[18]

Table 2.3. Mechanical properties of biodegradable and traditional matrixes used in composite materials. PLA=poly-lactic acid, PLLA=poly-L-lactic acid, PHB=polyhydroxybutyrate, PHBV=Poly(3-hydroxybutyrate-co-3-hydroxyvalerate) also produced by bacteria as PHB, PE=polyethylene, PP=polypropylene, PVC=Polyvinyl chloride.

Despite its excellent mechanical behaviour, the use of composites is not fully extended, as exists some limitations for a wider use. The main one is that there is no tradition of designing with composites comparing with the use of metals. The fact that their use has spread relatively recently (since 1938) is also significant that the calculation tools are not as widespread as those focused on metals. The damage mechanisms of a composite material are also more complex than those of more traditional materials, another barrier against its use. Moreover, composites shows a brittle behaviour and cannot be used in high temperature applications. As shown in Table 2.2 and Figure 2.1, steel properties are worst, especially taking into account the weight of the steel components, what means an increment of energy consumption when applied in transportation [2]. Despite of that, steel is still the main used material in the automotive industry [19]. Another parameter at stake is the costs of metals compared to composites, as described in Figure 2.2, where is visible how NFC could mean a turning point in the use of composites.

Figure 2.2 shows that glass fibre has a reduce cost compared with steel, Kevlar and Carbon fibre, but natural fibres could mean a high additional cost reduction, reason why is has begun its applications in some sectors. Special attention should be given to the Kenaf fibres, very common in the Asian tropics (Malaysia), and whose price is very low since it is obtained in periods of 3 months and its crops grows more than 3 m [5] and whose mechanical properties makes it valid for many applications (Table 2.2 and Figure 2.1). Flax is the strongest natural fibre and it has, in general, a lower price than E-glass, what makes it a good option (Figure 2.2). But, though the use of natural fibres is not extended in engineering design, they are widely produce for other purposes, as clothing or for the food industry, what means a good availability of the materials. The annual production volumes of the materials are also shown in Figure 4, revealing that there is a huge

background in this fibres production, what means a high reduction on the production and processing costs of NFC. For example, 54 MJ are required to produce 1 kg of glass fibre while only 15 MJ are required for the production of 1 kg of Kenaf fibres [5]. Additionally, food production generates high quantities of wastes, which could be reusable for the manufacturing of biocomposites, as in case of bagasse or corn crops, produced in sugar mills and agricultural farms in high volumes, as shown in Figure 4, and which potential use rises in insulation and building boards [1].

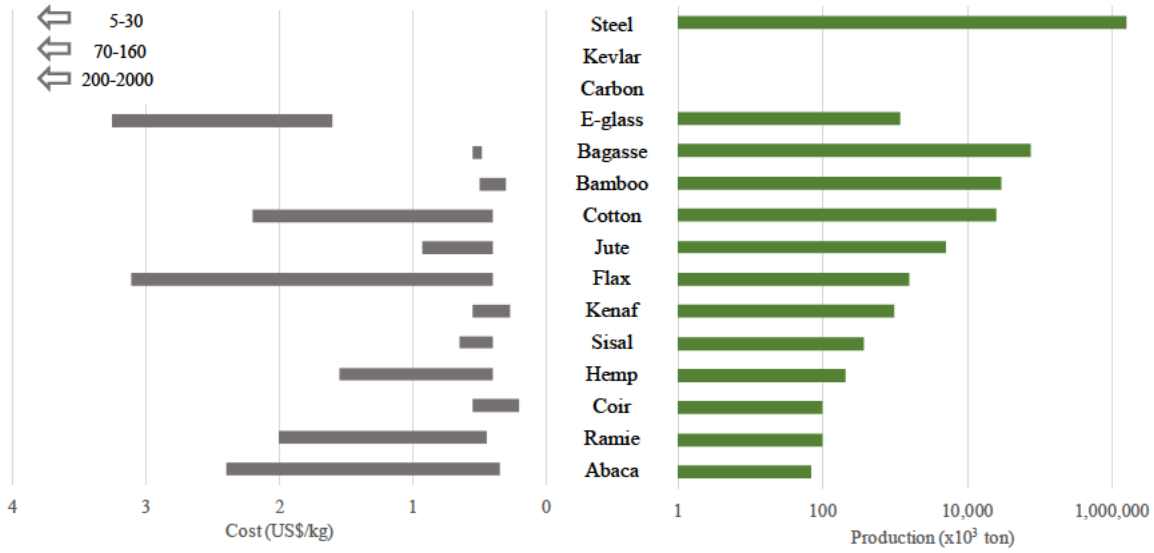

Figure 2.2. Cost and production comparative of natural fibres, traditional fibres and steel [1-3, 5-6, 20-22].

2.2. Manufacturing processes

In this section the combination of biodegradable fibres and matrices is analysed once its separated behaviour has been introduced. Some of the conventional composites fabrication techniques can be applied to manufacture biocomposites, but not all of them. For example, thermoset processes as resin transfer moulding are discarded since biopolymers are thermoplastics. One of the advantages of biocomposites is that high energy consumptions and potential respiratory problems for production workers are avoid. Finally, mechanical properties of fibres should be preserved. Thus, the most common methods which meet these requirements are injection moulding, compression moulding, extrusion and the process to obtain an All Cellulose Composites (ACC). Those methods are described above.

2.2.1. Injection moulding

The Injection moulding manufacturing process consists on injecting a fluid material into a mould, allowing to produce complex geometric components with functional elements fast and also in great numbers as moulds can have multiple cavities, so it is applied in economics of scale. It produces a minimum warping and shrinkage and no extra process is needed [6] but the cost of a mould is elevated as it is designed for a single component. This method is only possible with fibres, short or long, which are pre impregnated by the matrix. But a weave fabric or a film stacking cannot be used as the materials are forced to pass through a hopper. A scheme of the process is presented in Figure 2.3.a.

2.2.2. Compression moulding

It is based on the application of pressure and temperature to the composite, so a previous film stacking is needed. This method can be applied placing two thermoheated panels

between two compression plates of a universal testing machine, thus it is the most extended method in the manufacture of natural fibre composites in the research field [1]. It is characterized by a high reproducibility and low cycle time [6]. Woven fabrics can be used by this method, what means a better distribution of the fibres and makes possible to orient the fibres in the desired directions. After the composite production, the sample has to be cut with the desired dimensions. A scheme of this process is shown in Figure 2.3.b.

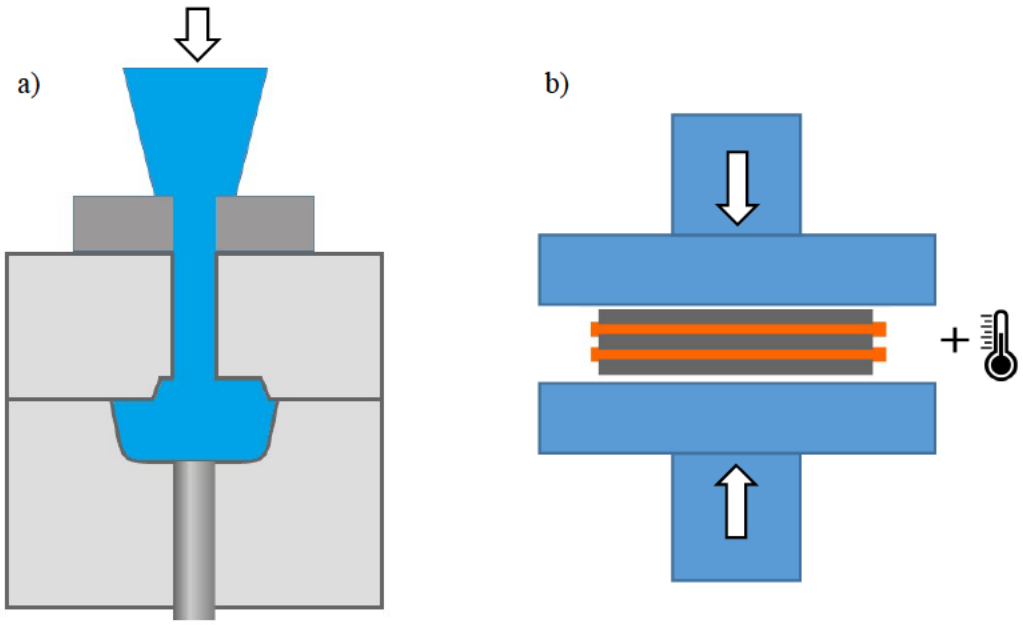

Figure 2.3. Manufacturing process scheme of a) Injection Moulding and b) Compression Moulding.

2.2.3. Extrusion process

The extrusion process is used by the plastics industry for the production of granules and also in the continuous production of semi-finished products or components. A screw extruder is used to press the passage of the components into a die. Extrusion process is usually applied to create objects of a fixed cross section, as beam profiles. Single or twin screw extruders can be used, but the single extruder do not produce a homogenous mix of the parts, so the twin-screw extruder is used for the composite materials manufacturing [6]. Only short fibres can be used with this method.

2.2.4. All Cellulose Composites (ACC)

The ACC manufacturing needs a more detailed description, as it is a novel concept based on natural fibres composition.

Besides conventional biocomposites, where the matrix is an independent material of the fibres, there exist a type of biocomposite in which cellulose extracted from the fibres acts as a matrix. As shown in Table 2.4, in which the chemical composition of different fibres is compared, the amount of each component has a large variation depending on the type of fibre, but cellulose remains in all fibres as most abundant component. The principle of ACC materials is to dilute partially or completely the abundant cellulose for binding the fibres.

ACC manufacturing can be divided into two subtypes. The first type is a two-steps process, in a first step the cellulose is completely diluted from the fibres. Then, this cellulose is added to other fibres. As an example, Nishino et al. took Kraft cellulose fibres (used for paper production) diluted in a solvent and, when mixed with Ramie fibre, cellulose was regenerated, forming the matrix [23]. In the second method, ACC are formed by a one-step process, also called partial dissolution, which is based on the application of a solvent directly to the fibres for a short time (usually less than 30 minutes), diluting the surface cellulose fibres. Though a washing bath, the solvent is removed and the diluted cellulose is regenerated, making a perfect composite adhesion because fibres and matrix chemical composition is similar. An additional pressing under heating process is needed to dry the composite. The partial dissolution process results are better than the total dissolution one in terms of mechanical properties, as the longitudinal tensile strength of cellulose decreases with increasing dissolution time [8]. A scheme of this process is presented in Figure 2.4.

Fibre	Cellulose (%)	Hemicellulose (%)	Lignin (wt.%)	Pectin (wt.%)	Moisture (wt.%)	Waxes (%)
Flax	71	18.6–20.6	2.2	2.3	8–12	1.7
Hemp	70–74	17.9–22.4	3.7–5.7	0.9	6.2–12	0.8
Jute	61–71.5	13.6–20.4	12–13	0.2	12.5–13.7	0.5
Kenaf	45–57	21.5	8–13	3–5	-	-
Ramie	68.6–76.2	13.1–16.7	0.6–0.7	1.9	7.5–17	0.3
Nettle	86	-	-	-	11–17	-
Sisal	66–78	10–14	10–14	10	10–22	2
Henequen	77.6	4–8	13.1	-	-	-
PALF	70–82	-	5–12.7	-	11.8	-
Banana	63–64	10	5	-	10–12	-
Abaca	56–63	-	12–131	1	5–10	-
Palm	60	-	11	-	-	-
Cotton	85–90	5.7	-	0–1	7.85–8.5	0.6
Coir	32–43	0.15–0.25	40–45	3–4	8	-
Cereal straw	38–45	15–31	12–20	8	-	-

Table 2.4. Natural fibres main components [5].

For the production of ACC, it is interesting to have as much cellulose fibre composition as possible, reason why synthetic 100% cellulose fibres are commonly used for this purpose instead of plant fibres, also composed by lignin, pectin and other substances (Table 2.4), which deteriorate the final adhesion between the fibres. Some of these synthetic fibres are Lyocell, Bocell, Viscose, Rayon or Cordenka. Mechanical properties of Lyocell and Cordenka were shown in Table 2.2, and their mechanical properties are better than many plant fibres due to cellulose fibres can be oriented in the longitudinal direction.

To achieve partial dissolution, only some certain solvents must be used as the green concept implies not damaging the environment. Thus, green solvents are characterized by having a very low volatility, which generates few gases into the atmosphere. They are very chemically stable and its solubility is very high for many substances. Solvents most commonly used in the literature are ionic liquids (AmimCl or BmimCl among many others), NMMO, LiCl/DMAc or NaOH-urea [8]. The disadvantage of these solvents is their high cost compared to the traditional (methanol or acetone), for example, BmimCl price is 1270 €/kg while Methanol costs 32.75 €/kg. But, after the dissolution and the regeneration

process, the solvents are recoverable, characteristic which makes ionic liquids more affordable, as they present a high recycling rate. Ionic liquids consist of salts whose melting temperature is lower than 100ºC. The NMMO bio solvent has the advantage that is miscible in water and has a very high polarity. LiCl/DMAc requires activation of the cellulose, so the DMAc is added first, after which the LiCl is added to dilute the cellulose. Meanwhile, the NaOH is the most environmentally friendly solvent, and usually accompanied by urea, which increases the power of dissolution [8].

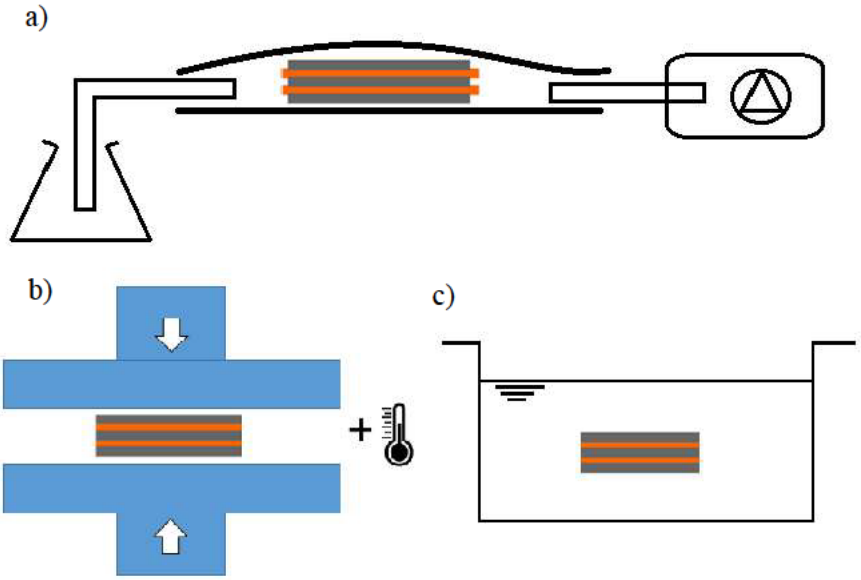

Figure 2.4. All Cellulose Composites manufacturing process stages; a) vacuum bagging solvent infusion, b) dissolution and c) ACC washing and solvent recovery.

Once the different manufacturing processes used by other authors are introduced, the resulting mechanical properties are analysed. Table 2.5 presents different cases from the literature where the mechanical behaviour of the final composites is shown, considering the manufacturing process used by each author. The properties are studied and compared in terms of their tensile strength. To compare the various results of the literature it should be noted that each material was obtained from different fibres, and even comparing the same type of fibre, the origin or high of the crop can determine a different mechanical behaviour [10]. To improve the mechanical behaviour, authors generally perform a pre drying of the components to minimize the moisture content. This drying of fibres and matrix is especially sensible when using 100% cellulose fibres as Cordenka, Bocell or Lyocell, as the water absorption reduces the binding after the dissolution process to obtain ACC [8] in a much more markedly way than using plant fibres and conventional manufacturing methods.

Composite	Max. Strain (%)	Tensile strength (MPa)	Tensile Modulus (GPa)	Manufacturing process	Ref.
Starch + 30% Jute	2 ± 0.2	26.3 ± 0.55	2.5 ± 0.23	IM	[2]
PLA + 30% Ramie	4.8 ± 0.2	66.8 ± 1.7	-	CM	[2]
PLA + 30% Jute	1.8 ± 0	81.9 ± 2.9	9.6 ± 0.36	IM	[2]
PTP + 25% Hemp	-	62 ± 2	7.2 ± 0.3	CM	[2]
PHBV + 30% Jute	0.8 ± 0	35.2 ± 1.3	7 ± 0.26	IM	[2]
PLLA + 30% Flax	2.3 ± 0.2	98 ± 12	9.5 ± 0.5	CM	[2]
PHB + 30% Flax	7 ± 1.5	40 ± 2.5	4.7 ± 0.3	CM	[2]
PLA + 30% Flax	1 ± 0.2	53 ± 3.1	8.3 ± 0.6	Extrusion + CM	[2]
PP + 30% Flax	2.7 ± 1.5	29.1 ± 4.2	5 ± 0.4	Extrusion + CM	[2]
PP + 30% Jute	1.4 ± 0.1	47.9 ± 2.7	5.8 ± 0.47	IM	[2]
PP + 30% E-glass	3.01 ± 0.22	82.8 ± 4.0	4.62 ± 0.11	CM	[2]
PLA + 70% Kenaf	53.7	223.3	30	Prepeg + CM	[10]
PLA + 30% Flax	-	54.15 ±4.57	6.13 ±0.12	CM	[24]
PLA + 30% Cordenka	-	57.97 ±5.08	4.85 ±0.03	CM	[24]
PLA + 10% Coconut	1± 0.2	67 ± 1	3.3 ± 0.1	CM	[25]
PLA + 20% Hemp	-	70 ± 3	3.5 ± 0.2	CM	[26]
PLA + 51% Bamboo	14.59 ± 1.62	77.58 ± 6.83	1.75 ± 0.19	CM	[27]
PLA + 60% Cotton	3.04 ± 0.5	41.2 ± 2	4.24 ± 0.64	CM	[7]
PLA + 60% Kenaf	1.05 ± 0.1	52.9 ± 4.5	7.14 ± 1.39	CM	[7]
PLA + 60% Hemp	1.24 ± 0.1	57.5 ± 3.6	8.06 ± 1.13	CM	[7]
PLA + 60% Lyocell	4.09 ± 0.8	81.8 ± 6.6	6.78 ± 0.52	CM	[7]
PLA + 40% Jute	1.6 ± 0.1	100.5 ± 0.4	9.4 ± 0.2	CM	[28]
PLA + 30% Abaca	-	74 ± 1.2	8 ± 0.5	Extrusion + CM	[13]
Lyocell + LiCl/DMAc	77.1 ± 5.4	169 ±8.3	4 ± 0.3	ACC	[29]
Bocell + LiCl/DMAc	64.2 ± 3.2	150 ± 1.6	4 ± 0.3	ACC	[29]
Ramie + LiCl/DMAc	8	450	27	ACC	[30]
Cellulose + LiCl/DMAc	-	211	8.2	ACC	[31]
Flax + LiCl/DMAc	0.8 ±0.1	34 ± 2	4.6 ±0.5	ACC	[32]
Lyocell + LiCl/DMAc	5.2 ± 2.6	78 ± 4	7.2 ±1	ACC	[32]
Cotton + BimimCl	20	22	0.134	ACC	[33]
Hemp + NMMO	20.8 ± 4.66	28.9 ± 3.63	1.33	ACC	[34]
80%Cellulose+20%Rice+BimimCl	11.1 ±1.5	89 ± 18	1.7 ± 0.18	ACC	[35]
Microcellulose + BimimCl	3.1 ± 1.5	120 ± 10	11 ± 2.5	ACC	[36]
Microcellulose + BimimCl	2.8 ± 0.2	100 ± 10	9 ± 2.5	ACC	[36]
Cordenka + BimimAc	-	91.2	3.72	ACC	[37]

Table 2.5. Overview of Biocomposites mechanical properties comparing the manufacturing processes. IM= Injection Moulding, CM=Compression Moulding, ACC= All Cellulose Composite.

A great dispersion can be observed in the comparison of the different manufacturing results. For example, Ochi [10] produced a 223.3 MPa PLA+70%Kenaf composite while Graupner et al. [7] reported a 52.9 MPa tensile strength of a PLA+60%Kenaf biocomposite. Nevertheless, it can

be concluded that manufacturing methods which produce more resistant specimens are compression moulding and the ACC production method.

2.3. Conclusions

Considering that the main objective of this work is the development of a constitutive model to understand the biocomposites mechanical behaviour, some conclusions can be taken from the state of the art study.

Most of fibres and matrixes can be applied to form a biocomposite, but Flax, Cotton and Jute fibres were chosen to cover high, medium and low mechanical specifications (Table 2.2 and Figure 2.1), representing a good natural fibres sample to be covered by the constitutive model.

Two manufacturing methods were chosen to obtain the better mechanical properties of the biocomposites; compression moulding and the ACC manufacturing procedure. For the compression moulding method an external matrix is needed. Therefore, PLA was acquired due to its low price and good mechanical behaviour (Figure 2.2). But two types of PLA had been used in order to accomplish the objective of compare different materials. For the ACC production an ionic liquid was selected as it can be recovered after its use, while BmimCl was chosen due to its reduced cost when comparing with other ionic liquids.

The machinery necessary for the manufacturing processes, as a thermoheated plates to heat the materials, a universal testing machine to compress or a pump for the vacuum bagging were provided by the Department of Continuum Mechanics and Structural Analysis of the University Carlos III of Madrid.

References

[1] Satyanarayana, K. G., Arizaga, G. G., & Wypych, F. (2009). Biodegradable composites based on lignocellulosic fibers—An overview. Progress in polymer science, 34(9), 982-1021.

[2] Koronis, G., Silva, A., & Fontul, M. (2013). Green composites: a review of adequate materials for automotive applications. Composites Part B: Engineering, 44(1), 120-127.

[4] Melo, J. D. D., Carvalho, L. F. M., Medeiros, A. M., Souto, C. R. O., & Paskocimas, C. A. (2012). A biodegradable composite material based on polyhydroxybutyrate (PHB) and carnauba fibers. Composites Part B: Engineering, 43(7), 2827-2835.

[5] Gurunathan, T., Mohanty, S., & Nayak, S. K. (2015). A review of the recent developments in biocomposites based on natural fibres and their application perspectives. Composites Part A: Applied Science and Manufacturing, 77, 1-25.

[6] Faruk, O., Bledzki, A. K., Fink, H. P., & Sain, M. (2012). Biocomposites reinforced with natural fibers: 2000–2010. Progress in Polymer Science, 37(11), 1552-1596.

[7] Graupner, N., Herrmann, A. S., & Müssig, J. (2009). Natural and man-made cellulose fibre-reinforced poly (lactic acid)(PLA) composites: An overview about mechanical characteristics and application areas. Composites Part A: Applied Science and Manufacturing, 40(6), 810-821.

[8] Huber, T., Müssig, J., Curnow, O., Pang, S., Bickerton, S., & Staiger, M. P. (2012). A critical review of all-cellulose composites. Journal of Materials Science, 47(3), 1171-1186.

[9] SteelConstruction.info. Steel properties 27/04/2016 <http://www.steelconstruction.info/Steel_material_properties#Other_mechanical_properties_of_steel>

[10] Ochi, S. (2008). Mechanical properties of kenaf fibers and kenaf/PLA composites. Mechanics of materials, 40(4), 446-452.

[11] Marsyahyo, E., & Rochardjo, H. S. B. (2009). Preliminary Investigation on Bulletproof Panels Made from Ramie Fiber Reinforced Composites for NIJ Level II, IIA, and IV. Journal of Industrial Textiles.

[12] Arbelaiz A, Orue A, Jauregi A, Mongragon G, Peña C, Eceiza A. Composites basados en fibras de sisal y matriz de poli(ácido láctico). Materiales Compuestos 2013;13:347-352.

[13] Bledzki, A. K., & Jaszkiewicz, A. (2010). Mechanical performance of biocomposites based on PLA and PHBV reinforced with natural fibres–A comparative study to PP. Composites science and technology, 70(12), 1687-1696.

[14] Kim KM, Son JH, Kim SH, Weller CL, Hanna M. Properties of Chitosan Films as a Function of pH and Solvent Type. Biological Systems Engineering: Papers and Publications 2006; Paper 111.

[15] WS Hampshire Inc. Mechanical properties of Polyethylene. 27/04/2016 <http://www.wshampshire.com/pdf/psg_uhmw_polyethylene.pdf>

[16] Charles, E. W., Charles, A. D., James, W. S., & Mark, T. B. (2005). PVC handbook.

[17] Efunda. Mechanical properties of Polyester. 27/04/2016 <https://www.efunda.com/materials/polymers/properties/polymer_datasheet.cfm?MajorID=P-TP&MinorID=1>

[18] Epoxy work tops. Epoxy Resin Mechanical properties. 27/04/2016 <http://plastics.ulprospector.com/generics/13/c/t/epoxy-properties-processing>

[19] Davies, G. (2003). Future trends in automotive body materials. Mater Automob Bodies, 8, 252-269.

[20] Dittenber, D. B., & GangaRao, H. V. (2012). Critical review of recent publications on use of natural composites in infrastructure. Composites Part A: Applied Science and Manufacturing, 43(8), 1419-1429.

[21] Mohanty, A. K., Misra, M., & Hinrichsen, G. (2000). Biofibres, biodegradable polymers and biocomposites: an overview. Macromolecular materials and engineering, 276(1), 1-24.

[22] Alibaba.com. Kevlar fabric price. 27/04/2016 <http://www.alibaba.com/product-detail/kevlar-fabric-price-of-kevlar-per_60373750766 html?spm=a2700.7724857.29.12.jhF0QT&smToken=49e884b2c2294ceb83904e936ca53e03&smSign=uJPT9xmHBhkwT5TFiTD3HQ%3D%3D>

[23] Nishino, T., Matsuda, I., & Hirao, K. (2004). All-cellulose composite.Macromolecules, 37(20), 7683-7687.

[24] Bax, B., & Müssig, J. (2008). Impact and tensile properties of PLA/Cordenka and PLA/flax composites. Composites Science and Technology, 68(7), 1601-1607.

[25] Jang, J. Y., Jeong, T. K., Oh, H. J., Youn, J. R., & Song, Y. S. (2012). Thermal stability and flammability of coconut fiber reinforced poly (lactic acid) composites. Composites Part B: Engineering, 43(5), 2434-2438.

[26] Song, Y. S., Lee, J. T., Ji, D. S., Kim, M. W., Lee, S. H., & Youn, J. R. (2012). Viscoelastic and thermal behavior of woven hemp fiber reinforced poly (lactic acid) composites. Composites Part B: Engineering, 43(3), 856-860.

[27] Porras, A., & Maranon, A. (2012). Development and characterization of a laminate composite material from polylactic acid (PLA) and woven bamboo fabric. Composites Part B: Engineering, 43(7), 2782-2788.

[28] Plackett, D., Andersen, T. L., Pedersen, W. B., & Nielsen, L. (2003). Biodegradable composites based on L-polylactide and jute fibres. Composites Science and Technology, 63(9), 1287-1296.

[29] Soykeabkaew, N., Nishino, T., & Peijs, T. (2009). All-cellulose composites of regenerated cellulose fibres by surface selective dissolution. Composites Part A: Applied Science and Manufacturing, 40(4), 321-328.

[30] Soykeabkaew, N., Arimoto, N., Nishino, T., & Peijs, T. (2008). All-cellulose composites by surface selective dissolution of aligned ligno-cellulosic fibres.Composites Science and Technology, 68(10), 2201-2207.

[31] Nishino, T., & Arimoto, N. (2007). All-cellulose composite prepared by selective dissolving of fiber surface. Biomacromolecules, 8(9), 2712-2716.

[32] Gindl-Altmutter, W., Keckes, J., Plackner, J., Liebner, F., Englund, K., & Laborie, M. P. (2012). All-cellulose composites prepared from flax and lyocell fibres compared to epoxy–matrix composites. Composites Science and Technology, 72(11), 1304-1309.

[33] Shibata, M., Teramoto, N., Nakamura, T., & Saitoh, Y. (2013). All-cellulose and all-wood composites by partial dissolution of cotton fabric and wood in ionic liquid. Carbohydrate polymers, 98(2), 1532-1539.

[34] Ouajai, S., & Shanks, R. A. (2009). Preparation, structure and mechanical properties of all-hemp cellulose biocomposites. Composites Science and Technology, 69(13), 2119-2126.

[35] Zhao, Q., Yam, R. C., Zhang, B., Yang, Y., Cheng, X., & Li, R. K. (2009). Novel all-cellulose ecocomposites prepared in ionic liquids. Cellulose, 16(2), 217-226.

[36] Duchemin, B. J., Mathew, A. P., & Oksman, K. (2009). All-cellulose composites by partial dissolution in the ionic liquid 1-butyl-3-methylimidazolium chloride. Composites Part A: Applied Science and Manufacturing, 40(12), 2031-2037.

[37] Huber, T., Bickerton, S., Müssig, J., Pang, S., & Staiger, M. P. (2012). Solvent infusion processing of all-cellulose composite materials. Carbohydrate polymers, 90(1), 730-733.

Chapter 3

Parametric analysis of compression moulding manufacturing conditions

The objective of this Chapter is to present an analysis of the fabrication parameters that influence on the strength of biodegradable composites manufactured through compression moulding. The effect of heating temperature, pressure, number of plies, fibre, and matrix on the tensile strength was studied. Biodegradable composites were manufactured using film stacking and compression moulding process. The strengths of biocomposite based on two different poly-lactic acid (PLA) matrix, and reinforced with four different woven fibres of Jute, Flax and Cotton were compared. The aim of this work is the development of an optimized manufacture process to reduce costs and production time of high strength biocomposites. The present manufacture method allows producing a biocomposite with tensile strength higher than 100 MPa in 5 minutes, meaning a significant reduction of production time.

3.1 Introduction

Composite materials combine lightweight and high specific stiffness and strength, these properties make composites suitable for a wide range of applications in industry [1-3]. During the last years, several researchers have introduced natural fibres as reinforcements and natural plastics as matrix to develop fully biodegradable composite materials [4], as introduced in Chapter 2, State of Art.

The use of biocomposites can lead to a reduction of the environment impact. Their lower price and the prevision of a higher production stablish a present alternative to traditional composites materials. Their low resistance to high temperatures is a limitation for some applications [5], but the flammability can be reduced [6]. Another problem reported in biocomposites is the poor bonding between the natural fibres and the biopolymer matrix [7]. Thus, numerous researchers are trying to improve manufacture processes to improve the performance of biocomposites to reducing production costs.

There is a wide range of applications for biocomposites, from the automotive sector [8] to boats [9] or electronics [10]. Their mechanical properties call biocomposites to replace most of non-renewable materials as traditional fibre glass composites [5, 7, 11-20]. For example, Bledzki et al. [21] and Müssig et al. [8] have proved the viability to use natural fibres in car panels. Present industrial applications generally combine natural fibres with petrochemical plastics as PP (polypropylene) [11]. There are also works showing that biocomposites are recyclable after it use on all this applications [22]. Recently, some authors have presented predictive models that can be used in the design of biocomposite structures [23].

Some of the conventional composites fabrication techniques can be applied to manufacture biocomposites. Thermoplastic injection moulding uses a screw-type plunger to force the plastic material into a mould [7]. All Cellulose-Composites (ACC) are obtained by the solution of the superficial cellulose of the fibres, and this cellulose acts as matrix of the fibres when dried. ACC are characterised by a total cohesion between matrix and reinforcement [12]. Other fabrication procedures are heating under vacuum [13], RTM (resin transfer moulding) [24-25], pultrusion [25] or electrospinning for bio-nanocomposites [11]. However, compression moulding after a film stacking of fibre and matrix plies is one of the most popular processes to manufacture biocomposites [5, 15-18].

Compression moulding is characterised by its high reproducibility and low cycle time [25]. Satyanarayana et al. [26] found compression moulding as the better option to obtain a composite based on natural fibres in terms of mechanical properties. This method also uses small amounts of energy, so the green concept is reinforced. The main parameters that influence on the mechanical properties of biocomposites manufactured using compression moulding are fibre material, matrix type, fibre quantity, heating temperature, and pressure and time.

Numerous vegetal fibres have been used as reinforcement; jute, flax, and kenaf can be considered the most popular fibres. Different fully biodegradable bioplastics derived from the biomass and processed to a final plastic as PLA (poly-lactic acid) [Ochi], PHA (Polyhydroxyanoates) [26] or chitosan [27] can be used as matrix. The maximum processing temperature ranges between 180ºC and 200ºC because of the natural fibres damaging, while the melting point of natural matrix usually is around 130ºC – 230ºC [28]. Consequently, temperatures between 130ºC and 200ºC are compatible.

Therefore, numerous parameters influence on the compression moulding method, and many researchers have manufactured biocomposites using different values of these parameters. For example, Ochi [15] manufactured a PLA composite reinforced with a 70% of kenaf fibres by compression moulding with a previous prepreg of the fibres. Temperature was 160ºC with a 5 minutes preheating and a hot pressing during 10 minutes with 10 MPa pressure, obtaining 223 MPa tensile strength. Jang et al. [5] used a 10% coconut fibres and PLA to produce a biocomposite at 200ºC, obtaining 65 MPa of tensile strength. Song et al. [16] kept at 170ºC during 5 min and applied 2.45 MPa pressure to obtain a 65 MPa tensile strength biocomposite made of 20% hemp, 80% PLA. Porras and Maranon [17] manufactured a 51% bamboo and 49% PLA composite by compression moulding after an extrusion of the matrix with a temperature of 160ºC and a pressure of 556.7 MPa resulting 77.55 MPa tensile strength. Graupner et al. [18] tested mixtures of different fibres and PLA, obtaining a 81.8 MPa tensile strength with a 60% Lyocell and 40% PLA biocomposite, applying 4.2 MPa of pressure during 20 min at 180ºC. Bodros et al. [19] followed a compression moulding after film stacking, using flax, glass fibre, hemp and sisal, applying different conditions depending on the fibre and the matrix.

However, very few studies have analysed the influence of the main manufacture parameters on biocomposites strength. Ochi [15] realized a parametric analysis of kenaf fibre strength, with heating times from 15 to 60 min, varying heating temperatures from 25ºC to 200ºC, determining that at 180 ºC with times of 15 and 30 minutes, the strength does not decrease, but it does with times of 60 min and with temperatures of 200ºC. Ochi also studied the influence of kenaf reinforcement quantity, determining optimum strength of biocomposites with around a 70% of reinforcement. Jang et al. [5] have studied the reinforcement quantity parameter applying different treatments to the fibres, but with a maximum reinforcement of 10%. Song et al. [16] tested different woven architectures of hemp, one twill and the other plain, and determined that the best one is the twill. Bodros et al. [19] compared biocomposites reinforced with flax fibres and manufactured with different matrixes: PHB (Polyhydroxybutyrate), PBS (Polybutylene succinate), PLA, PLLA (poly-

L-lactide), and PP. PLA and PLLA provided the better mechanical properties in terms of stiffness and strength. In addition, they showed that flax/PLLA biocomposites can be competitive with the glass-fibre/polyester composite.

Therefore, there is a need of parametric studies to optimize the results of compression moulding manufacturing process. In this work, two different PLA matrixes were reinforced with jute, flax, and cotton fibres to analyse the influence of temperature, number of plies, and pressure. As a result, a tensile strength higher than 100 MPa was obtained with a preheating time of 2 minutes and 3 minutes of heating under pressure. This result means a significant reduction of production time that can lead to reduce the manufacture cost of these materials.

3.2 Experimental

Biocomposites were manufactured using jute, cotton and flax fibres as reinforcement of PLA matrix applying compression moulding method.

3.2.1 Materials

Four woven fibres were used as reinforcement: plain weave jute (J); basket weave cotton (C), basket weave flax (BF); and plain weave flax (PF). No chemical pre-treatment was applied to woven fibres. Table 3.1 shows the mechanical properties of the fibres. Tensile strength ranges from 116.5 MPa of cotton fibres to 271.62 MPa of basket weave flax.

PLA is a thermoplastic resin that was acquired in pellets form. Two kinds of PLA polymer were used: 3260HP and 10361D, booth provided by Natureworks LLC. 3260HP PLA is aimed to an extrusion process; its typical application is to obtain final products as cups, plates or cutlery. 10361D PLA is specifically aimed as a binder of natural fibres. PLA properties were obtained from [17]. The PLA density is 1.24 g/cm3 and the melt temperature is 145-170ºC. Mechanical properties of PLA are shown in Table 1.

Material	*Tensile strength (MPa)*	*Young modulus (GPa)*
BF fibres	271.62	7.84
PF fibres	225.39	8.5
J fibres	136.18	7.385
C fibres	116.5	12.34
PLA [17]	54.27	3.18

Table 3.1. Mechanical properties for natural fibres woven plies and PLA matrix.

3.2.2 Compression moulding method

Compression moulding method is schematically showed in Figure 3.1. First, the PLA pellets are placed between two thermoheated plates at a temperature of 185ºC to obtain a uniform film. Then, the matrix films are stacked alternatively with woven plies. The stacked plies are placed between the thermoheated plates. After a pre-heating time, pressure was applied using a universal test machine Servosis ME-404/100 + PCD-1065 with a limit load of 900 kN. Finally, the biocomposite panels were dried at room temperature.

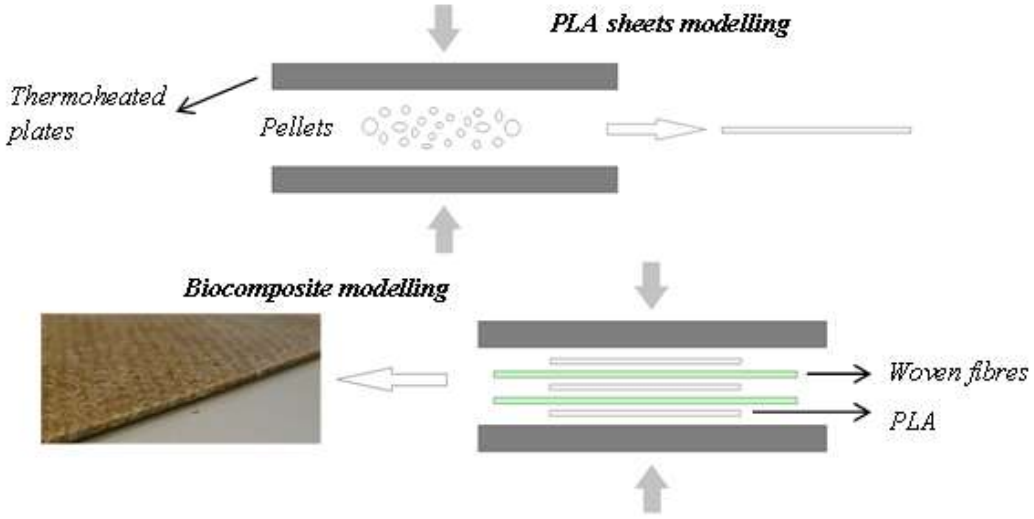

Figure 3.1. Scheme of the manufacturing process to obtain the biocomposite from natural fibres woven plies and PLA in pellets.

The values of temperature, pressure, number of plies were modified to analyse their influence on the biocomposite tensile strength. Temperature of compression ranged between 175ºC and 200ºC, pressure from 0.8 MPa and 40 MPa, and number of plies from 2 to 4.

The quantity of reinforcement was stated in a weight ratio of 65%, this parameter was not analysed in this work because Ochi [15] studied its influence on biocomposite strength founding that this is the optimum value for compression moulding procedures.

As commented before, natural fibres can be degraded at temperatures higher than 180ºC, but if this temperature is applied during a short time period, fibres do not present damage. In this work, preheating time is set in 2 minutes, heating under pressure time in 3 minutes. These are the minimum times to assure PLA melting, its homogenous distribution in the laminate, and a slowly application of pressure to avoid fibre misalignment.

3.2.3 Mechanical testing

Tensile tests were performed in a universal test machine Instron 8516. The cross-head speed was set in 0.5 mm/min. Samples were cut in rectangular specimens of 120 x 30 mm. The thicknesses of the samples depend on the number of plies and the type of woven fibre. Tensile strength was determined with the peak force of the force-displacement curve.

3.3 Results and Discussion

The results of the tensile tests are shown in Table 3.2. The modification of the different parameters leaded to 21 different configurations, four specimens were tested for each configuration. The influence of the main parameters is analysed in the next sections.

Test no.	*Temperature (ºC)*	*Pressure (MPa)*	*PLA*	*Fibre*	*Plies*	*Tensile strength (MPa)*	*Desv. (MPa)*
1	185	16	10361D	BF	2	105.95	4.54
2	185	16	10361D	BF	4	102.00	4.55
3	185	16	10361D	PF	2	98.93	1.58
4	185	16	10361D	PF	4	94.83	4.48
5	185	16	10361D	J	2	73.30	3.86
6	185	16	10361D	J	4	64.43	2.44
7	185	16	10361D	C	2	58.28	0.29
8	185	16	10361D	C	4	59.93	4.84
9	185	32	3260HP	BF	2	116.33	2.42
10	185	32	10361D	BF	2	104.70	4.44
11	175	32	10361D	BF	2	102.76	0.88
12	180	32	10361D	BF	2	110.92	6.32
13	190	32	10361D	BF	2	95.32	4.69
14	195	32	10361D	BF	2	96.80	4.52
15	200	32	10361D	BF	2	99.13	7.32
16	185	0.8	10361D	BF	2	83.75	1.91
17	185	4	10361D	BF	2	95.73	5.31
18	185	8	10361D	BF	2	106.94	4.47
19	185	16	10361D	BF	2	105.95	4.54
20	185	24	10361D	BF	2	103.55	4.51
21	185	40	10361D	BF	2	90.42	3.76

Table 3.2. Tensile strength of biocomposite manufactured with different fibres, matrix, temperature, pressure, and number of plies.

3.3.1 Type of fibre and number of plies

The comparison of the tests no. 1-8 can illustrate the influence of fibre and number of plies on tensile strength. These specimens were manufactured at the same heating temperature (185ºC) and pressure (32 MPa), and PLA matrix was 10361D.

Figure 3.2 shows a graphical representation of the results. The best results were obtained with the basket weave flax (BF), following by plain weave flax (PF), jute (J), and cotton (C). These results are in agreement with the fibre strengths shown in Table 3.1. Thus, the biocomposite tensile strength is directly related to the fibre strength.

The analysis of the influence of number of plies shows that there is more cohesion in bilayer biocomposites than the four layers ones, with the exception of cotton. This is consistent with the cohesion problems in composite materials. However, the difference between two and four layers is smaller than standard variation for flax woven biocomposites. Consequently, basket weave flax seemed to be the best option to reinforce biocomposites independently of the number of layers.

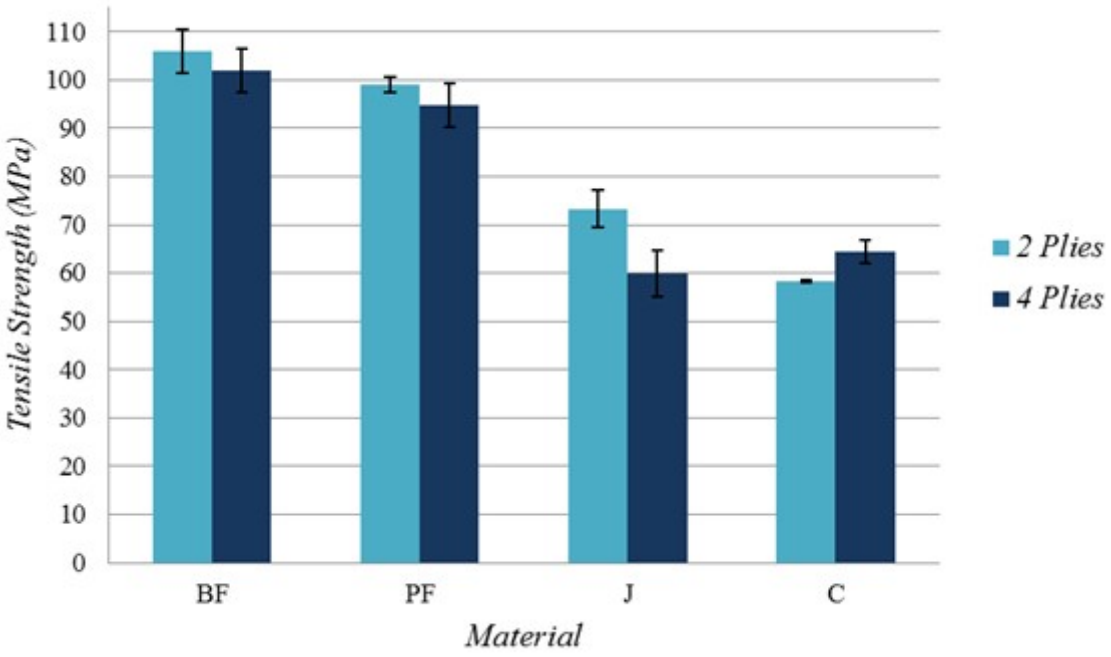

Figure 3.2. Tensile strength obtained for different number of plies and fibres: basket weave flax (BF), plain weave flax, plain weave jute (J), and basket weave cotton (C).

3.3.2 Type of PLA matrix

The two PLA matrix (3260HP and 10361D) were compared in tests no. 9 and 10. These specimens were manufactured with basket weave flax plies at the same conditions of pressure (32 MPa) and temperature (185ºC).

Results show that 3260HP PLA matrix lead to a higher tensile strength, 116.33 MPa, than PLA 10361D matrix, 104.70 MPa. These results are in contradiction with the supplier recommendations because 10361D is specifically designed for natural fibres binder, while 3260HP is make for extrusion processes. However, the higher properties obtained with 3260HP matrix are only valid for two layers laminates, it was not able to spread into the inner layers when it was applied to a four layer biocomposite. Thus, 10361D PLA was selected as the best option to be used as matrix in compression moulding process.

3.3.3 Heating temperature

The influence of heating temperature, from 175ºC to 200ºC, was analysed through comparison of tests no. 10-15. These results are represented in Figure 3.3. These specimens were manufactured from 10361D PLA matrix reinforced with basket weave flax woven plies, and the applied pressure was 32 MPa.

Heating temperatures over 200ºC produced fibre damage due to overheating. On the other hand, the matrix was not completely melted for heating temperatures below 175ºC. Thus, the temperature must be high enough for matrix melting, but no so high to produce fibres damage. As Figure 3.3 shows, specimens manufactured with heating temperatures between 180ºC and 185ºC presented the maximum tensile strength. However, some of the specimens produced at 175ºC and 180ºC were discarded because of the

presence of delaminations. The tensile strength corresponding to 180ºC heating temperature shown in Figure 3.3, 110.92 MPa, was obtained as the average of intact specimens, however many other specimens were manufactured but not tested due to delaminations. Consequently, 185ºC was chosen as the optimum heating temperature.

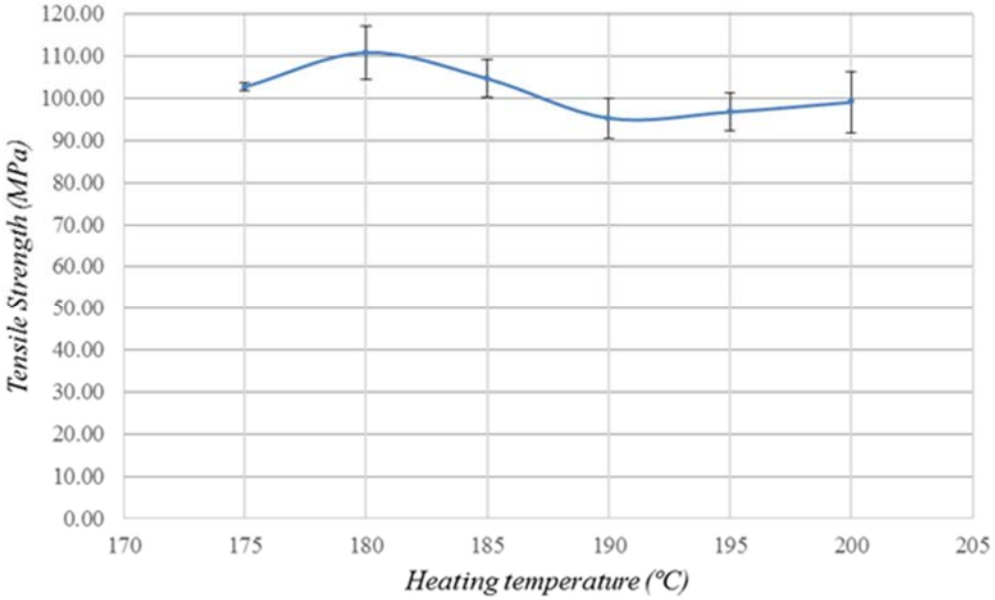

Figure 3.3. Tensile strength as a function of heating temperature.

3.3.4 Pressure

The effect of pressure was studied comparing the tests no. 10, 16-21. The heating temperature was stated at 185ºC to manufacture 10361D PLA based biocomposite reinforced with basted weave flax fibres. Results are graphically represented in Figure 3.4. Tensile strength increases with manufacture pressure until 8 MPa, then there is plateau until a manufacture pressure of 32 MPa, finally tensile strength decreases with pressure. Pressure over 32 MPa produced fibre breakage, while pressure under 8 MPa mean lack of cohesion in the biocomposite. Thus, there is a wide range of pressure, between 8 MPa and 32 MPa that can be used to produce biocomposites with similar mechanical properties.

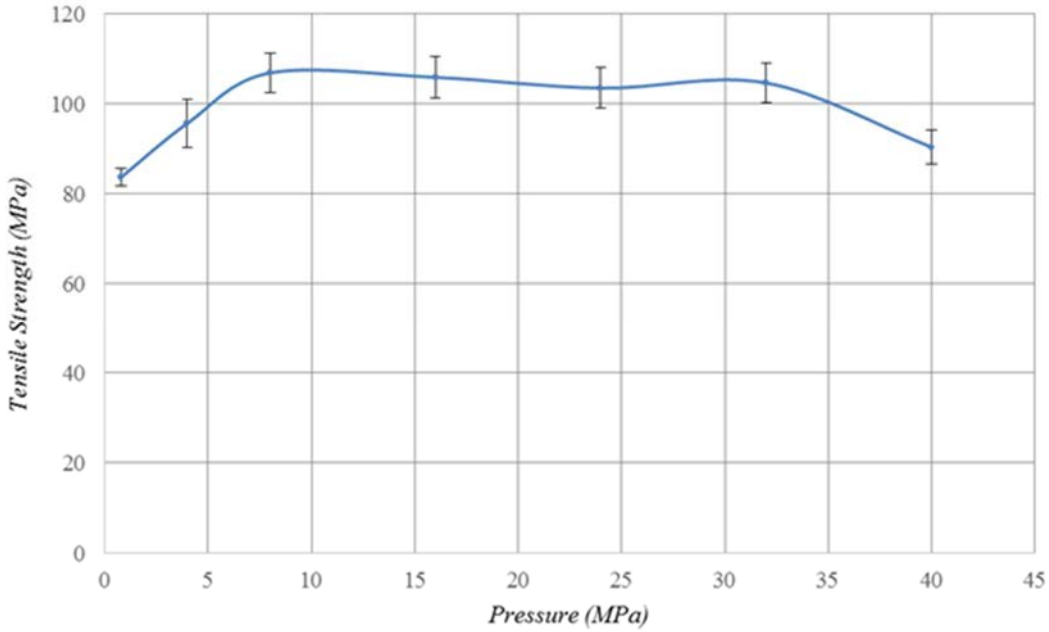

Figure 3.4. Tensile strength as a function of the pressure applied in compression moulding method.

3.4 Conclusions

The influence of heating temperature, pressure, type of fibre and matrix, and number of plies is studied in this work. The results of 21 tests configurations are analysed, leading to the next conclusions:

Biocomposite strength is directly related to fibre strength. This conclusion is not obvious because implies similar adhesion between the matrix and the different fibres. Thus, biocomposites manufactured with basket weave flax fibres presented the higher tensile strength.

The influence of matrix is related to the number of plies. For two-plies biocomposites the higher strength was obtained with 3260HP PLA matrix. However, this matrix presented spreading problems for higher number of plies. Thus, 10361D PLA matrix was selected as the best option.

A heating temperature of 185ºC was found as the optimum value. Higher heating temperatures produce less-strength biocomposites because fibres are damaged due to overheating. While, matrix melting is not complete for lower heating temperatures.

A wide range of pressure during compression moulding, from 8 MPa to 32 MPa, leaded to similar values of tensile strength. Lower pressure implies lack of cohesion in the biocomposite, and higher pressure produce fibre breakage.

The present method can produce a biocomposite with a tensile strength higher than 100 MPa in a production time of 5 minutes, 2 minutes of preheating and 3 minutes of heating under pressure. This result implies a significant reduction of production time leading to a reduction of the manufacture cost of biocomposites.

However, more studies must be carried out to improve this method. The conclusions are stated only from the tensile strength point of view. There are other mechanical and physical

properties, as biodegradability, which should be studied to verify the quality of biocomposite manufactured with the present method.

References

[1] Santiuste C, Soldani X, Miguélez MH. Machining FEM model of long fiber composites for aeronautical components. Compos Struct 2010;92(3):691-8.

[2] Santiuste C, Barbero E, Miguélez MH. Computational analysis of temperature effect in composite bolted joints for aeronautical applications. J Reinf Plast Compos 2001;30(1):3-11.

[3] Olmedo A, Santiuste C, Barbero E. An analytical model for predicting the stiffness and strength of pinned-joint composite laminates. Compos Sci Tech 2014;90:67-73.

[4] Mantia FPL, Morreale M. Green composites: A brief review. Compos Part A: Appl S 2011;42(6):579-88.

[5] Jang JY, Jeong TK, Oh HJ, Youn JR, Song YS. Thermal stability and flammability of coconut fiber reinforced poly (lactic acid) composites. Compos Part B: Eng 2012;43(5):2434-8.

[6] Bocz K, Szolnoki B, Marosi A, Tábi T, Wladyka-Przybylak M, Marosi G. Flax fibre reinforced PLA/TPS biocomposites flame retarded with multifunctional additive system. Polym Degrad Stab 2013;106:63-73.

[7] Bledzki AK, Jaszkiewicz A, Scherzer D. Mechanical properties of PLA composites with man-made cellulose and abaca fibres. Compos Part A: Appl S 2009;40(4):404-12.

[8] Müssig J, Schmehl M, von Buttlar HB, Schönfeld U, Arndt K. Exterior components based on renewable resources produced with SMC technology—Considering a bus component as example. Ind crop Prod 2006;24(2):132-45.

[9] Brouwer WD. Natural Fiber Composites, Saving Weight and Cost with Renewable Materials Thirteenth International Conference on Composite Materials. 2001.

[10] Serizawa S, Inoue K, Iji M. Kenaf fiber reinforced poly (lactic acid) used for electronic products. J Appl Polym Sci 2006;100(1):618-24.

[11] John MJ, Thomas S. Biofibres and biocomposites. Carbohydr polym 2008;71(3):343-64.

[12] Huber T, Pang S, Staiger MP. All-cellulose composite laminates. Compos Part A: Appl S 2012;43(10):1738-45.

[13] Summerscales J, Dissanayake N, Virk A, Hall W. A review of bast fibres and their composites. Part 2–Composites. Compos Part A: Appl S 2010;41(10):1336-44.

[14] Voorn BV, Smit HHG, Sinke RJ, Klerk BD. Natural fibre reinforced sheet moulding compound. Compos Part A: Appl S 2001;32(9):1271-9.

[15] Ochi S. Mechanical properties of kenaf fibers and kenaf/PLA composites. Mech mater 2008;40(4):446-52.

[16] Song YS, Lee JT, Ji DS, Kim MW, Lee SH, Youn JR. Viscoelastic and thermal behavior of woven hemp fiber reinforced poly(lactic acid) Composites. Compos Part B: Eng 2012;43:856–60.

[17] Porras A, Maranon A. Development and characterization of a laminate composite material from polylactic acid (PLA) and woven bamboo fabric. Compos Part B: Eng 2012;43(7):2782-8.

[18] Graupner N, Herrmann AS, Müssig J. Natural and man-made cellulose fibre-reinforced poly (lactic acid)(PLA) composites: An overview about mechanical characteristics and application areas. Compos Part A: Appl S 2009;40(6):810-21.

[19] Bodros E, Pillin I, Montrelay N, Baley C. Could biopolymers reinforced by randomly scattered flax fibre be used in structural applications?. Compos Sci Technol 2007;67(3):462-70.

[20] Ochi S. Development of high strength biodegradable composites using Manila hemp fiber and starch-based biodegradable resin. Compos Part A: Appl S 2006;37(11):1879-83.

[21] Bledzki AK, Faruk O, Sperber VE. Cars from BioFibres. Macromol Mater Eng 2006;291(5):449-57.

[22] Duigou AL, Pillin I, Bourmaud A, Davies P, Baley C. Effect of recycling on mechanical behaviour of biocompostable flax/poly (l-lactide) composites. Compos Part A: Appl S 2008;39(9):1471-8.

[23] Rubio-López A, Olmedo A, Santiuste C. Modelling impact behaviour of all-cellulose composite plates. Compos Struct 2015;122:139-43.

[24] Oksman K. High quality flax fibre composites manufactured by the resin transfer moulding process. J Reinf Plast Compos 2001;20(7):621-7.

[25] Faruk O, Bledzki AK, Fink HP, Sain M. Biocomposites reinforced with natural fibers: 2000–2010. Prog Polym Sci 2012;37(11):1552–96.

[26] Satyanarayana KG, Arizaga GG, Wypych F. Biodegradable composites based on lignocellulosic fibers—an overview. Prog Polym Sci 2009;34(9):982-1021.

[27] Julkapli NM, Akil HM. Thermal properties of kenaf-filled chitosan biocomposites. Polym-Plast Tech Eng 2010;49(2):147-53.

[28] Dittenber DB, GangaRao HV. Critical review of recent publications on use of natural composites in infrastructure. Compos Part A: Appl S 2010;43(8):1419-29.

Chapter 4

Constitutive model to predict the dynamic behaviour of biocomposites

The mechanical behaviour of traditional composites is usually assumed as linear-elastic up to failure. However, composites based on natural fibres are characterized by non-linear elasticity, viscous effects and plastic strains before failure. This chapter presents a rheological model to predict the viscoplastic behaviour of natural fibres based composites. The model was calibrated using a stress-strain curve and two relaxation tests for three different composites reinforced with flax, jute and cotton fibres. The model predicted successfully the behaviour of biocomposites loaded at different strain rates.

4.1 Introduction

Traditional composites consist on the combination of synthetic fibres from mineral origin as glass or carbon fibres with oil-based polymer matrices as epoxy, polyethylene or polypropylene. In the last years, natural fibres (flax, cotton, sisal, jute, etc.) were introduced as potential substitutes of synthetic fibres in order to reduce the environmental impact of composites [1]. Few years ago, also vegetal origin polymers as polyhidroxybutyrate (PHB) or poly-lactic acid (PLA) were studied for their application as matrices to obtain a fully biodegradable composite, recyclable and with competitive mechanical properties [2]. The high specific mechanical strength of some fibres as well as their reduced costs make biocomposites suitable to preplace traditional composites for numerous applications [3].

Natural fibres as reinforcement of non-biodegradable plastics have already been used in automotive industry [4] and numerous publications studying these materials can be found [3-5]. However, the interest on fully biodegradable composites is growing as the authorities require ever more the use of recyclable materials due to environmental social concerns [6].

The disposal of theoretical models to predict the mechanical behaviour of biodegradable composites can help to get a better understanding of their performance and their use in industrial applications can increase. The mechanical behaviour of traditional composites has been widely studied [7-9]. Their behaviour can be usually assumed as linear-elastic up to failure [7], and the main objective in the development of predictive models is the implementation of accurate failure criteria [8] and the prediction of their energy absorption capability [9]. However, the development of constitutive models to predict the mechanical behaviour of biocomposites is an almost unexplored field. The results of experimental studies have shown viscoelastic and viscoplastic effects [10], thus traditional composites models assuming linear-elastic behaviour can be implemented in biocomposites only as a first approach [11].

The preliminary studies that have been initiated to predict the mechanical behaviour of natural fibres based composites can be divided into three different categories. The first category includes models for the prediction of the elastic properties and they are based on the rule of mixtures. The next step is the development of micromechanical models based on the reproducibility of a unit cell with FEM (finite element modelling), these models can be grouped in the second category. Finally, the third category includes constitutive models developed to consider the viscoplastic behaviour of biocomposites in a simplified mathematical formulation.

Numerous publications can be found in the first category, for example, Ihueza et al. [12] simulated the behaviour of polyester and natural fibre composites under multiaxial stress state. Facca et al. [13] developed a model to predict the elastic modulus of natural fibres reinforced thermoplastics. Virk et al. modelled the tensile properties of jute fibres [14] and predicted the elastic modulus and strength of natural fibre composites [15]. These models are based in the prediction of the elastic properties, but they cannot include the strain rate dependency or the presence of permanent strains.

Regarding the micromechanical models, Andersons and Modniks [16] reproduced the tensile stress/strain behaviour of short fibre flax/epoxy composites. Sliseris et al. [17] also developed a micromechanical model based on the generation of fibres, bundles and fibre defects randomly with FEM to consider the fibre orientation, reproducing the stress/strain behaviour of short fibre and woven fabrics of flax reinforcing an epoxy matrix. Muttrand et al. [18] created a numerical model to reproduce randomly the cross-section geometry of flax fibres inside a flax/epoxy composite. Beakou and Charlet [19] simulated a flax bundle through a numerical model. These models are based on the definition of the fibre configuration, what means an overly high computational cost when implementing this in a macro mechanical FEM model.

Very few works can be found in the third category. Andersons et al. [20] developed a semiempirical tensor-linear model in order to predict the non-linear stress/strain behaviour of unidirectional flax/epoxy composites. Only the model proposed by Poilane et al. [10] can be considered a constitutive model considering the viscoelastic behaviour present in natural fibre composites. They developed a non-linear phenomenological model for flax/epoxy composites, based on rheological elements with eight parameters. The repetitive loading and unloading tensile tests on flax/epoxy composites with different yarn configurations were successfully predicted. However, this model was applied only to flax/epoxy composites, thus none model has been able to predict the viscoplastic behaviour of fully-biodegradable composites

In this chapter, a rheological model is introduced to define the viscoplastic behaviour of biocomposites. The model predicted accurately the viscoplastic behaviour of PLA based composites reinforced with three different woven fibres (flax, jute and cotton). One of the main goals of the present model is that it can be calibrated using only quasi-static tests; the influence of strain rate can be obtained from relaxation tests. Once the model is calibrated, it predicts the stress-strain curves obtained at different strain rates.

4.2 Experimental procedure

4.2.1 Materials

Two types of biocomposites have been subject of study in this work; PLA based composites manufactured by compression moulding and All-Cellulose Composites (ACC) manufactured through solvent infusion.

Three different woven fibres (flax, jute and cotton) with no chemical pre-treatments were acquired to verify the capability of the model to predict the mechanical behaviour of different PLA based biocomposites. Cotton and flax have 2x1 basket weave configuration while jute fabric configuration is plain. PLA matrix can be obtained from roots, sugarcane or corn starch polymerization [3]. For this study, PLA 10361D was acquired from Natureworks LLC, and it is defined as a biodegradable thermoplastic resin specifically aimed as a natural fibre binder. Fibres and matrix properties were studied in a previous work [21].

ACC specimens were provided by Prof. Mark Staiger's research group from the Department of Mechanical Engineering, University of Canterbury, Christchurch, New Zealand. The specimens are composed by Cordenka™ K2/2 twill weave fabric textile, while the solvent used for the composite formation was BmimAc ionic liquid, as detailed in [20].

4.2.2 Manufacturing process

PLA based biocomposites were produced by compression moulding process. First, three PLA layers and two woven fibres plies were alternatively stacked, then the laminate was place between two thermoheated plates, and pressure was applied by a universal testing machine. An optimization of the manufacturing process was performed as reported in [21], revealing that the optimum manufacturing parameters are 185ºC plates initial temperature, applying 8-16 MPa of pressure during 3 minutes after 2 minutes of preheating time. The fibre weight ratio was stated in 65% as studied by Ochi et al. [22]. The size of manufactured plates was 150x150 mm, while thicknesses were different for each raw material: 1.50±0.05 mm for cotton, 1.15±0.03 mm for jute and 1.27±0.02 mm for flax composites.

Fabric and PLA plies were maintained in an oven under 95ºC during 30 minutes before the compression moulding processing to remove water content. All the materials were stored in stable constant conditions of 46% RH and 20ºC before and after the manufacturing process to control the environmental conditions influence.

ACC specimens were produced through a solvent infusion process, in which the ionic liquid is infused by vacuum bagging into the 4 staked layers in order to solve the superficial cellulose of the fibres in a hot press. The specific values of the manufacturing parameters can be checked in [20]. After the hot pressing, the plates are washed to remove the solvent, which is regenerated.

4.2.3 Mechanical testing

An Instron 8516 universal testing machine was used to perform both tensile and relaxation tests. Manufactured plates were cut into 120x15 mm rectangular specimens. Cotton and flax 2x1 basket weave samples were oriented longitudinally.

Three different crosshead velocities were used for the tensile tests to obtain the stress-strain curves: 0.5 mm/min, 5 mm/min and 20 mm/min. The free length between clamping areas was established in 40 mm for all the tests, thus strain rates were $2.08 \cdot 10^{-4}$ s^{-1}, $2.08 \cdot 10^{-3}$ s^{-1} and $8.33 \cdot 10^{-3}$ s^{-1}.

Relaxation tests were performed imposing an initial displacement of the head with a 10 mm/s crosshead speed, leading to a strain rate equal to $2.5 \cdot 10^{-1}$ s^{-1}. This initial displacement was maintained until the recorded force was relaxed to a constant value.

4.3 Model description

Rheological models are based on the use of elastic, plastic and viscous elements [23] to determine the mechanical behaviour of a material and its temporal dependence under different loading conditions.

The model used in this work is defined with three branches in parallel, as shown in Fig. 4.1. In the first branch (a), the non-linear elastic behaviour of the material is defined through a Yeoh model [24], a phenomenological model based in rubber behaviour that defines the non-linear elastic behaviour using the strain energy density function. In the second branch (b), the viscous behaviour of the material is defined through a Maxwell model. Finally, in the third branch (c), the plasticity is introduced by a frictional analogy to the Maxwell model. Figure 4.1 represents the scheme of the whole model, defined by only five elements.

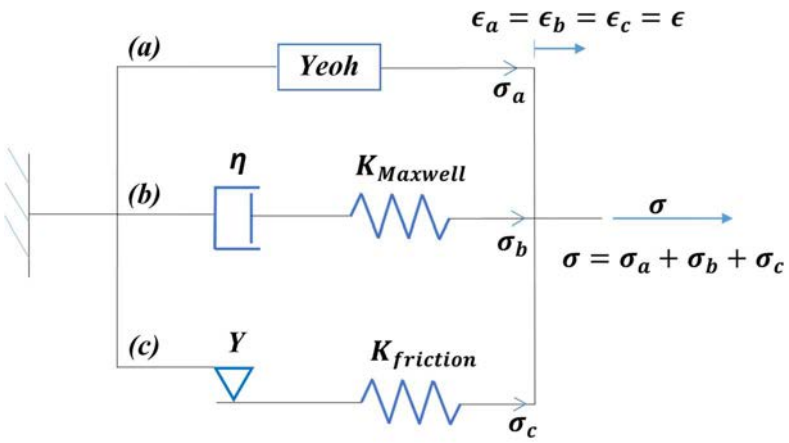

Figure 4.1. Rheological model scheme. Branch (a) describes non-linear elastic, branch (b) considers viscous effects and branch (c) includes plasticity.

4.4 Constitutive equations

Yeoh non-linear elastic model is based on incompressible materials, thus, the energy density function depends on the first invariant of the left Cauchy-Green deformation tensor in a cubic form, as Eq. (1) shows.

$$W = \sum_{i=1}^{3} C_i (I_1 - 3)^3 \tag{1}$$

where W is the strain energy density function, C_i represents elastic constants and $I_1$is the first invariant. The first invariant is the trace of the left Cauchy-Green deformation tensor ($B=FF^T$, being F the deformation gradient tensor and B the left Cauchy-Green deformation tensor). Considering incompressibility and uniaxial extension, the stretches ($\lambda = \epsilon + 1$) in the three principal directions can be related as $\lambda_1 \cdot \lambda_2 \cdot \lambda_3 = 1$ and $\lambda_2 = \lambda_3$, thus

$$I_1 = \lambda_1^2 + \lambda_2^2 + \lambda_3^2 = \lambda^2 + \frac{2}{\lambda} \tag{2}$$

Considering the left Cauchy-Green deformation tensor expressed as $B = \lambda^2 \cdot n_1 \times n_1 + \frac{1}{\lambda} \cdot (n_2 \times n_2 + n_3 \times n_3)$ and uniaxial extension, orienting the principal stretches with the coordinated basis vectors, the stress in the principal direction results: $\sigma_{11} = -p + 2 \cdot \lambda^2 \frac{\partial W}{\partial I_1}$ and $\sigma_{22} = \sigma_{33} = -p + \frac{2}{\lambda}\frac{\partial W}{\partial I_1} = 0$, thus $p = \frac{2}{\lambda}\frac{\partial W}{\partial I_1}$ and

$$\sigma_{11} = 2 \cdot (\lambda^2 - \frac{1}{\lambda})\frac{\partial W}{\partial I_1} \tag{3}$$

The derivate of strain energy density function can be obtained from Eq. (1):

$$\frac{\partial W}{\partial I_1} = \sum_{i=1}^{3} i \cdot C_i (I_1 - 3)^{i-1} \tag{4}$$

Introducing Eq. (2) in Eq. (4) and Eq. (4) in Eq. (3), stress can be expressed as a function of strain for the non-linear Yeoh model under uniaxial extension, Eq. (5):

$$\sigma_{Yeoh} = \frac{2\epsilon(3 + \epsilon(3 + \epsilon))((1 + \epsilon)^2 C_1 + \epsilon^2(3 + \epsilon)(2(1 + \epsilon)C_2 + 3\epsilon^2(3 + \epsilon)C_3)}{(1 + \epsilon)^2} \tag{5}$$

where C_1, C_2 and C_3 are three elastic constants.

The second branch (b) function is to introduce the viscous effects, thus a Maxwell model was used, whose behaviour is described by Eq. (6). The Maxwell model behaviour is given by a spring and a dashpot in series, thus the stress is the same in both elements ($\sigma_{dashpot} = \sigma_{spring} = \sigma$) and the total strain is the sum of the spring and dashpot strains ($\epsilon_{dashpot} + \epsilon_{spring} = \epsilon$). The constitutive equation of the Maxwell model is obtained including the spring definition $\sigma = K \cdot \epsilon$ (K is the spring's constant) and the dashpot equation $\sigma = \eta \cdot \frac{d\epsilon}{dt}$ (η is the dashpot constant) in the strain-rate equation, $\dot{\epsilon}_{dashpot} + \dot{\epsilon}_{spring} = \dot{\epsilon}$, yielding:

$$\dot{\sigma}_{Maxwell} + \frac{K}{\eta} \cdot \sigma_{Maxwell} = K \cdot \dot{\epsilon} \tag{6}$$

Finally, branch (c) introduces plasticity through a spring and a frictional element in series. These two elements produce a frictional analogy to the Maxwell model to define a plastic behaviour. The model stiffness is dominated by the spring element until the frictional element is activated, the role of the frictional element is to stablish a limit for the stress. Thus, the definition of the stress/strain relationship for the frictional branch is given in two sections as shown in Eq. (7), before and after the yield strain is reached ($\varepsilon_y = Y/K_{Friction}$).

$$\begin{aligned} if\ \varepsilon < \varepsilon_y \quad &\rightarrow \quad \sigma_{Friction} = K_{friction} \cdot \epsilon \\ if\ \varepsilon \geq \varepsilon_y \quad &\rightarrow \quad \sigma_{Friction} = Y \end{aligned} \tag{7}$$

Being defined the constitutive equation of each branch, the constitutive equation of the global model is given by Eq. (8).

$$\sigma = \sigma_{Yeoh} + \sigma_{Maxwell} + \sigma_{Friction} \tag{8}$$

4.5 Stress-strain response

The solution of the constitutive equations for the tensile test is presented in this section. The three branched can be solved separately imposing initial conditions: $\epsilon(0) = 0$ and $\sigma(0) = 0$, and imposing a constant strain rate. The solution of the Maxwell model differential equation is:

$$\sigma_{Maxwell-Tensile} = \dot{\epsilon} \cdot \eta \cdot \left(1 + e^{-\frac{K_{Maxwell}}{\eta} t}\right) \tag{9}$$

The solution for the Yeoh and the friction branches are independent of the strain rate, thus the solution can be found replacing $\epsilon = \dot{\epsilon} \cdot t$ in Eq. (5) and Eq. (7). The solution of the global model, Eq. (8), for different strain rates is shown in Figure 4.2.

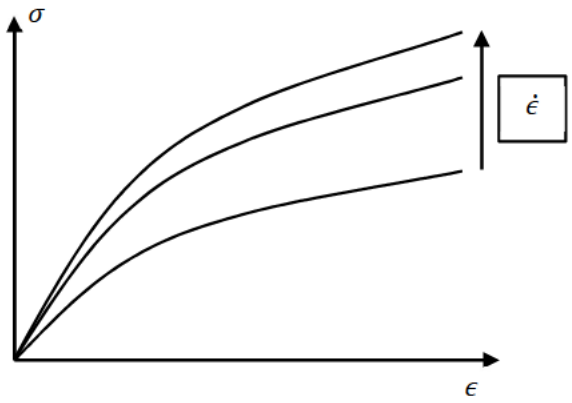

Figure 4.2. Tensile tests strain rate dependence. Stress-strain curves obtained for different strain rates.

4.6 Relaxation response

In relaxation tests an initial strain is imposed and maintained with time ($\epsilon = \epsilon_0$ and $\dot{\epsilon} = 0$). The initial strain is considered to be applied instantaneously, thus infinity strain rate can be assumed, see Figure 4.3a. Therefore, the dashpot of the Maxwell model can be considered initially blocked and the first value of the stress is controlled by the spring $\sigma(0) = K_{Maxwell} \cdot \epsilon_0$. On the other hand, the dashpot will be relaxed during the test and the final value of the stress in the Maxwell model is zero. The solution of ODE Eq. (6) is:

$$\sigma_{Maxwell-Relaxation} = K_{Maxwell} \cdot \epsilon_0 \cdot e^{-\frac{K_{Maxwell}}{\eta} t} \tag{10}$$

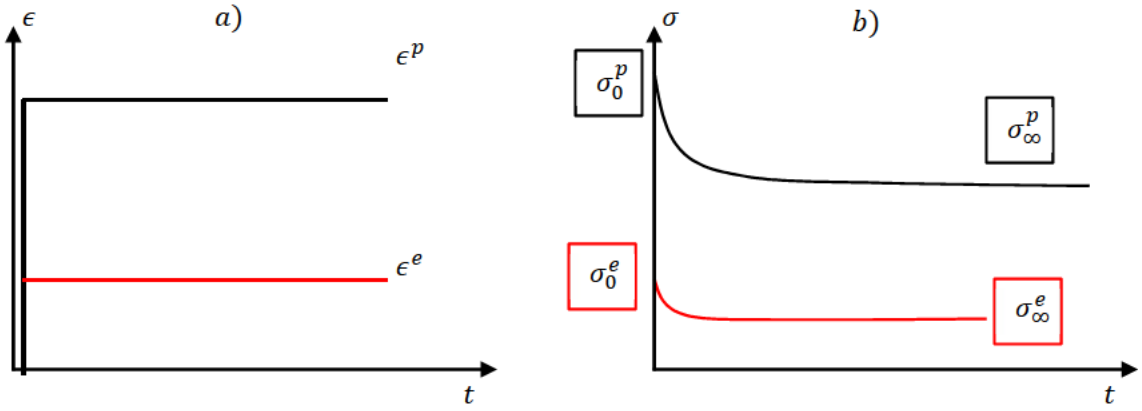

Figure 4.3. Relaxation test description. a) Strain vs. Time curves. b) Stress vs. Time curves.

The solutions of the Yeoh and the frictional elements are time independent. Thus solution can be obtained introducing $\epsilon = \epsilon_0$ in Eq. (5) and Eq. (7), respectively. The stress remains constant in these two elements as the strain does. The global response of the model in the relaxation tests is shown in Figure 4.3b. Two different tests are shown in Figure 4.3, viscoelastic and viscoplastic, denominated by superindexes "e" and "p" respectively. The strain imposed in the viscoelastic relaxation test is lower than the yield strain while the strain imposed in the viscoplastic relaxation test is higher.

4.7 Model calibration and validation

Seven parameters are used to define the present model: C_1, C_2, and C_3 are the elastic constant of the Yeoh model, $K_{Maxwell}$ and η are the spring and dashpot constants of the Maxwell model, and $K_{friction}$ and Y are the friction model parameters. Three different tests were conducted to calibrate these parameters for each material: viscoelastic and viscoplastic relaxation tests (Figures 4.3a and 4.3b) and a quasi-static tensile test (Figure 4.2). Two tensile tests were conducted at higher strain rates to validate the ability of the model to predict the viscoplastic behaviour of biocomposites.

Four values can be obtained from relaxation tests to calibrate the model. The initial stress of the viscoelastic test (σ_0^e) is defined by Eq. (11) while the final stress (σ_∞^e) is given by Eq. (12), being ϵ^e the imposed strain. The initial and final stresses of the viscoelastic relaxation test are shown in Eq. (13) and Eq. (14) respectively, being ϵ^p the imposed strain.

$$\sigma_0^e = \sigma_{Yeoh}(\epsilon^e) + (K_{friction} + K_{Maxwell}) \cdot \epsilon^e, \tag{11}$$

$$\sigma_\infty^e = \sigma_{Yeoh}(\epsilon^e) + K_{friction} \cdot \epsilon^e \tag{12}$$

$$\sigma_0^p = \sigma_{Yeoh}(\epsilon^p) + Y + K_{Maxwell} \cdot \epsilon^e \tag{13}$$

$$\sigma_\infty^p = \sigma_{Yeoh}(\epsilon^p) + Y. \tag{14}$$

The values of $K_{friction}$, $K_{Maxwell}$, and Y can be obtained as a function of Yeoh parameters using Eq.(11), Eq. (12) and Eq.(13). Yeoh parameters, C_1, C_2, C_3, were fitted through an adjustment with least squared applied to a quasi-static tensile tests to obtain the stress-strain curve. Finally, dashpot parameter (η) was calibrated with the relaxation tests by least squared fit considering the viscoelastic and viscoplastic tests curvatures.

Eq. (14) was not used for the model calibration, for this reason σ_{∞}^{p} was used for validation. Additionally, two stress-strain curves obtained at higher strain rates were used to validate the model. Therefore, a great coherence is obtained as the model parameters were calibrated with a set of tests and different tests were used for validation.

4.8 Results and discussion

4.8.1 Experimental results

The results of the tensile tests conducted to obtain three stress-strain curves at different strain rates are shown in Figure 4.4. The stiffness and the strength of flax composites are much higher than that of jute and cotton composites. The nonlinearity of cotton composites is clearer than in the other materials, there is a great difference between the slope of the stress-strain curves after and before the yield point.

The viscous effects can be observed in the three materials because the stiffness increases with strain rate, but the influence of strain rate is lower in jute composites. In flax and cotton composites the stresses always increase with strain rate. However, in jute composites stresses increase when strain rate rise from $2.08\text{x}10^{-4}$ s^{-1} to $2.08\text{x}10^{-3}$ s^{-1}, but the curves for strain rates of $2.08\text{x}10^{-3}$ s^{-1} and $8.33\text{x}10^{-3}$ s^{-1} are overlapped. The stiffness increment observed in flax/PLA composites in similar to that reported by Polilâne et al. [10] in flax/epoxy composites, thus the viscous effects can probably be attribute to the mechanical behaviour of fibres.

The values of the imposed strains of the relaxation tests were selected from the stress-strain curves shown in Figure 4.4. The elastic and plastic strains were chosen to conduct relaxation tests before and after the yield point, the values of the strains are shown in Table 4.1. Figure 4.5 shows the relaxation results for each material, comparing viscoelastic with viscoplastic behaviour. In the three materials, viscoplastic tests needed more time to get a stable value of the final stress than viscoelastic tests. Cotton and ACC needed more time to get stable than flax while flax needed more time than jute. The initial and final stresses of each test are summarized in Table 4.1.

	Flax/PLA	Cotton/PLA	Jute/PLA	ACC
Elastic strain. (-)	0.0025	0.0025	0.00175	0.0025
Plastic strain (-)	0.025	0.025	0.0125	0.025
σ_0^e(MPa)	14.2±0.3	8.9±0.1	9.3±0.4	5.6±0.3
σ_{∞}^{e} (MPa)	11.7±0.4	7.2±0.2	8.2±0.2	4.7±0.1
σ_0^p (MPa)	81.1±2.2	42.0±1.5	41.9±0.5	87.4±1.5
σ_{∞}^{p} (MPa)	52.6±1.5	24.5±0.7	32.3±1.0	39.1±0.7

Table 4.1. Relaxation tests results: initial and final stresses.

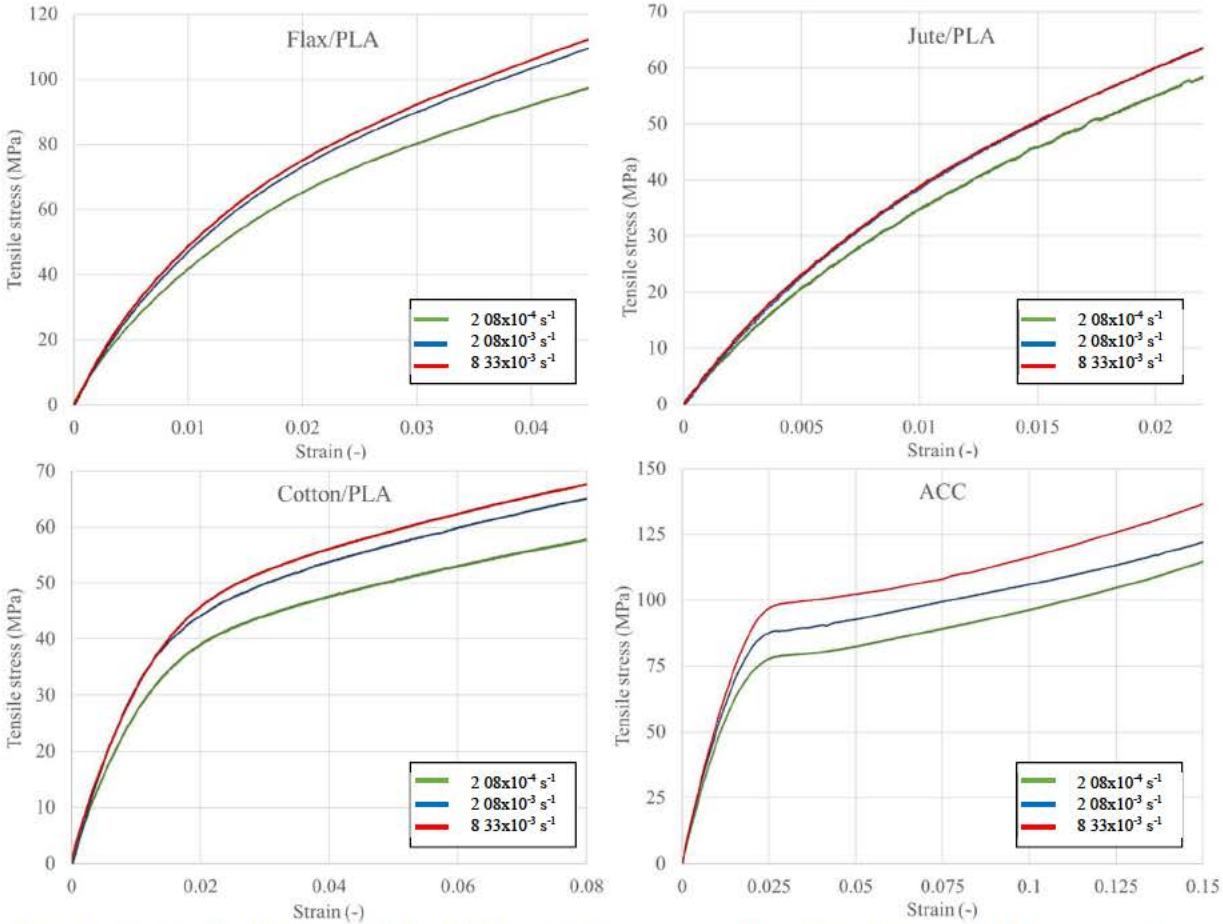

Figure 4.4. Tensile tests conducted at different strain rates in flax, jute, cotton and ACC composites.

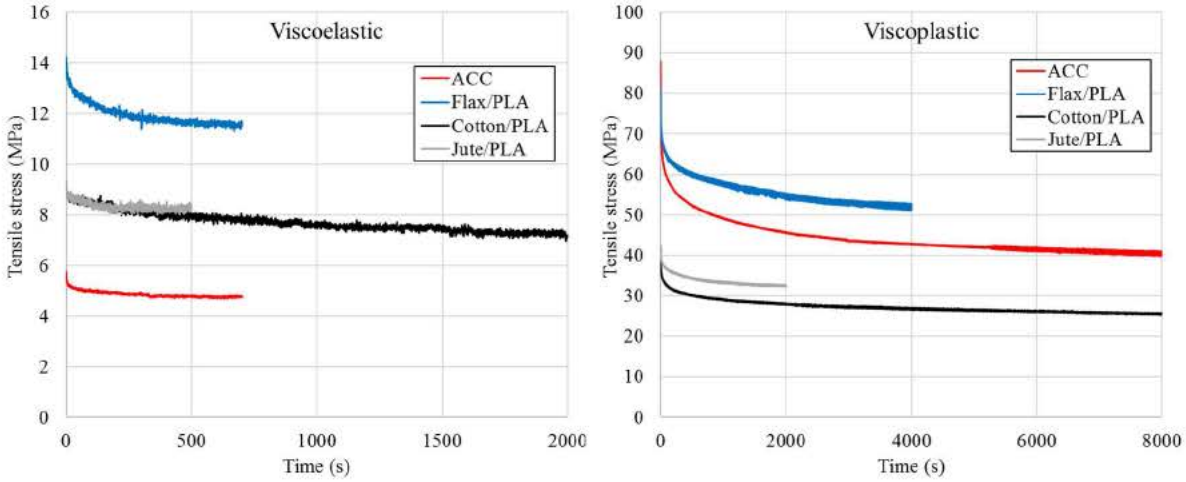

Figure 4.5. Viscoelastic and viscoplastic relaxation tests results for flax/PLA, cotton/PLA, jute/PLA and ACC composites.

4.8.2 Model calibration

The results of relaxation tests and the stress-strain curves obtained at a strain rate of 2.08×10^{-4} s^{-1} were used to calibrate the model for the three materials. The values of the parameters calibrated are summarized in Table 4.2. ACC parameters are not involved as was not possible to simulate its behaviour with the present model.

Parameter	Flax/PLA	Jute/PLA	Cotton/PLA
$K_{Maxwell}$ (Pa)	1.08 x10^9	6.86 x10^8	6.40 x10^8
$K_{friction}$ (Pa)	2.58 x10^9	2.15 x10^9	2.71 x10^9
η (Pa s)	2.30 x10^{11}	6.14 x10^{10}	5.19 x10^{11}
Y (Pa)	1.23 x10^7	4.87 x10^6	2.36 x10^7
C_1 (-)	3.38 x10^8	4.14 x10^8	2.16 x10^7
C_2 (-)	-1.81 x10^{10}	-2.76 x10^{10}	-1.63 x10^9
C_3 (-)	6.56 x10^{11}	1	2.15 x10^{10}

Table 4.2. Model parameters for flax/PLA, jute/PLA and cotton/PLA composites.

A comparison between the experimental data and the model predictions with the fitted parameters is shown in Figures. 4.6, 4.7 and 4.8 for flax, jute and cotton composites respectively. In each figure, the *a* and *b* graphs represents the viscoelastic and viscoplastic relaxation tests, where $K_{friction}$, $K_{Maxwell}$, η and Y were fitted, while *c* graph shows the stress/strain test where C_1, C_2 and C_3 parameters were calibrated through a least squares fitting.

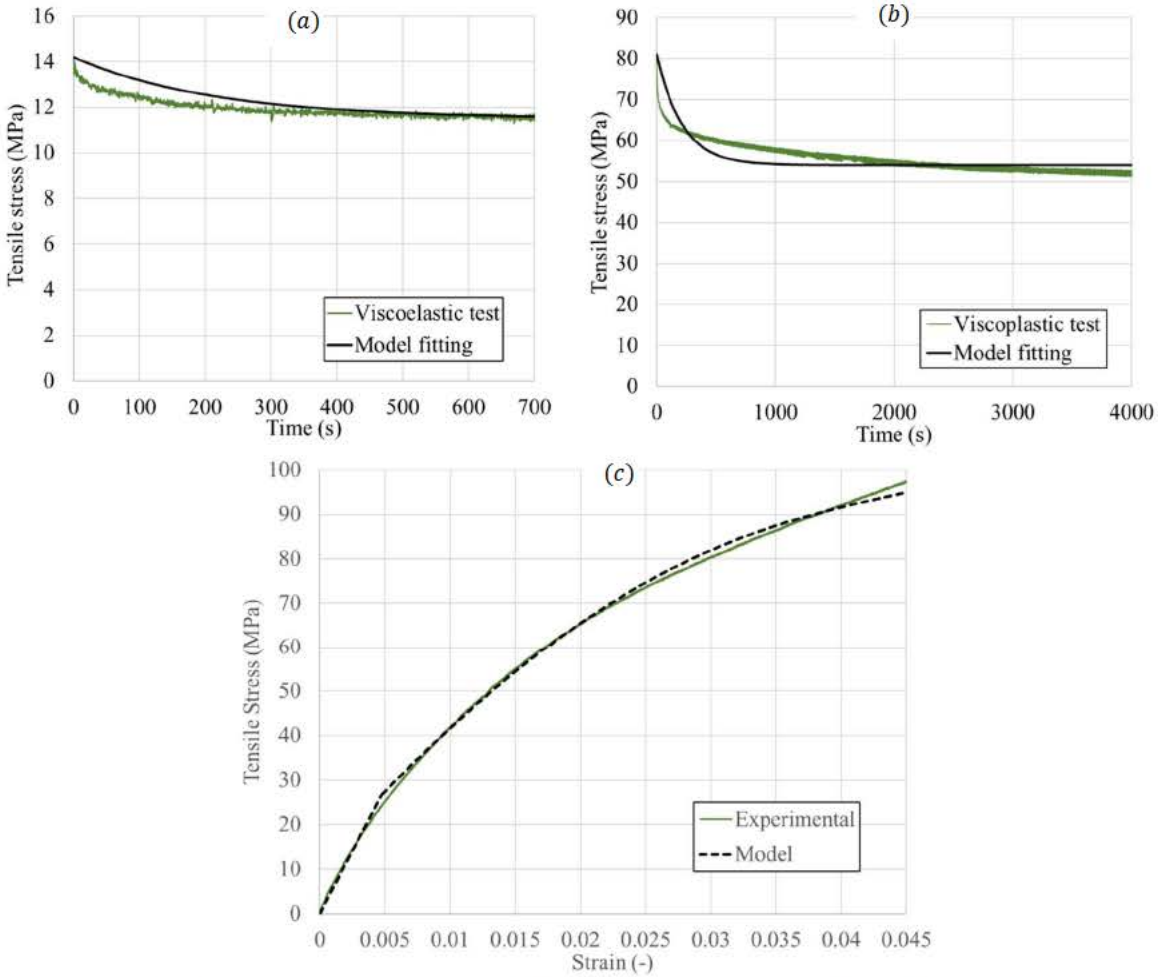

Figure 4.6. Model parameters calibration of flax/PLA composites. (a) Viscoelastic relaxation test. (b) Viscoplastic relaxation test. (c) Stress-strain curve.

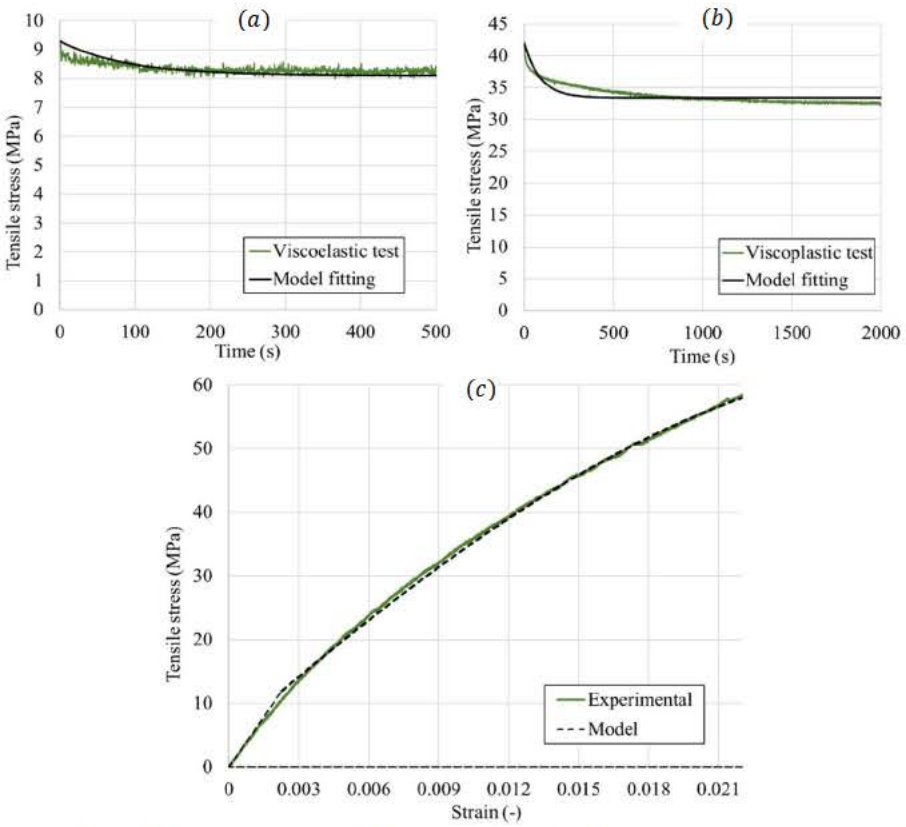

Figure 4.7. Model parameters calibration of jute/PLA composites. (a) Viscoelastic relaxation test. (b) Viscoplastic relaxation test. (c) Stress-strain curve.

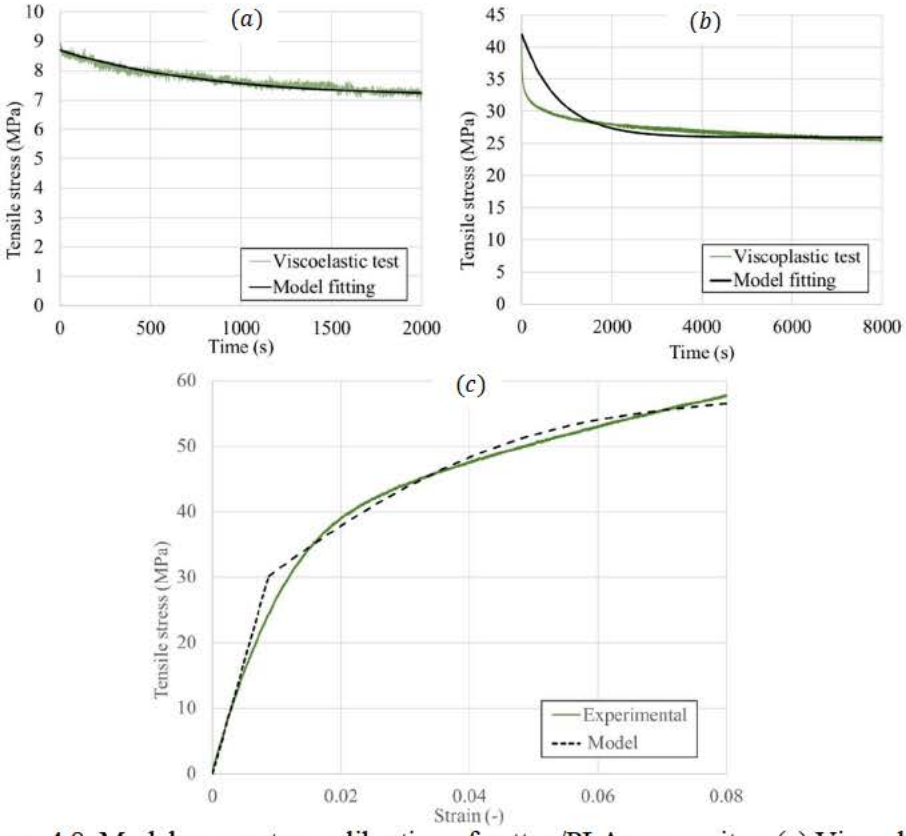

Figure 4.8. Model parameters calibration of cotton/PLA composites. (a) Viscoelastic relaxation test. (b) Viscoplastic relaxation test. (c) Stress-strain curve.

ACC calibration results are shown in Figure 4.9, were is shown how the viscoplastic correlation do not fulfill the equations (13) and (14), conditions used for the validation. As the model do not fulfill the imposed conditions, the material was discarded and a different model should be developed for the ACC biocomposites.

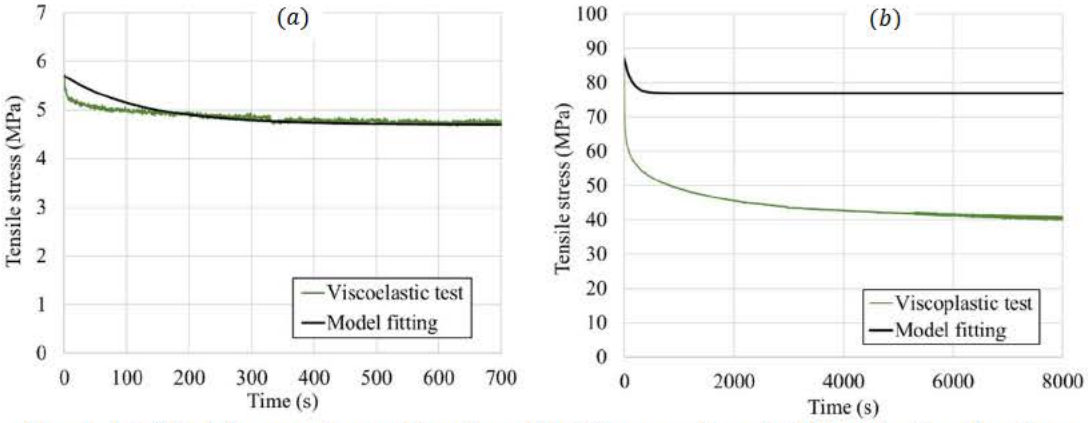

Figure 4.9. Model parameters calibration of ACC composites. (a) Viscoelastic relaxation test. (b) Viscoplastic relaxation test.

4.8.3 Model validation

The first data used to validate the model were the final stress obtained in the viscoplastic relaxation tests (σ_∞^p). Table 4.3 includes the experimental data and the model predictions for the three materials. An excellent agreement between predictions and experiments can be observed, being the maximum error lower than 6%.

Moreover, the tensile tests conducted at strain rates of $2.08 \cdot 10^{-3}$ s^{-1} and $8.33 \cdot 10^{-3}$ s^{-1} were used to validate the accuracy of the model in the prediction of the strain rate influence on stress-strain curves. Figures 4.10, 4.11 and 4.12 show the comparison between experimental data and predicted stress-strain curves for flax, jute and cotton composites. A reasonable agreement between the predictions and the experiments obtained, thus the model can be considered validated. The model predicts the influence of strain rate leading to an increase of the stiffness according to experimental results. It should be noticed that the model was calibrated using a single tensile test at a single strain rate, moreover the influence of strain rate is different in each material as it was explained before.

Nevertheless, the model accuracy is not perfect. The results with flax and jute composites show a better prediction capacity than with cotton. One of the reasons is that the friction branch controls the predicted yield strain, thus it is independent on strain rate. This hypothesis can be assumed for flax and jute composites according to experimental results. However, the yield strain in cotton composites experiences a slightly increase with strain rate as it was observed in experimental tests. The ACC's were discarded, as mentioned in the calibration section, due to its high error.

	Flax/PLA	Cotton/PLA	Jute/PLA	ACC
σ_∞^p Experimental(Mpa)	52.6	24.5	32.3	39.1
σ_∞^p Model, eq.(13) (Mpa)	54	26	34	77
Error (%)	2.6	5.8	5.0	49.3%

Table 4.3. Comparison between experimental and predicted final stress in viscoplastic relaxation tests (σ_∞^p).

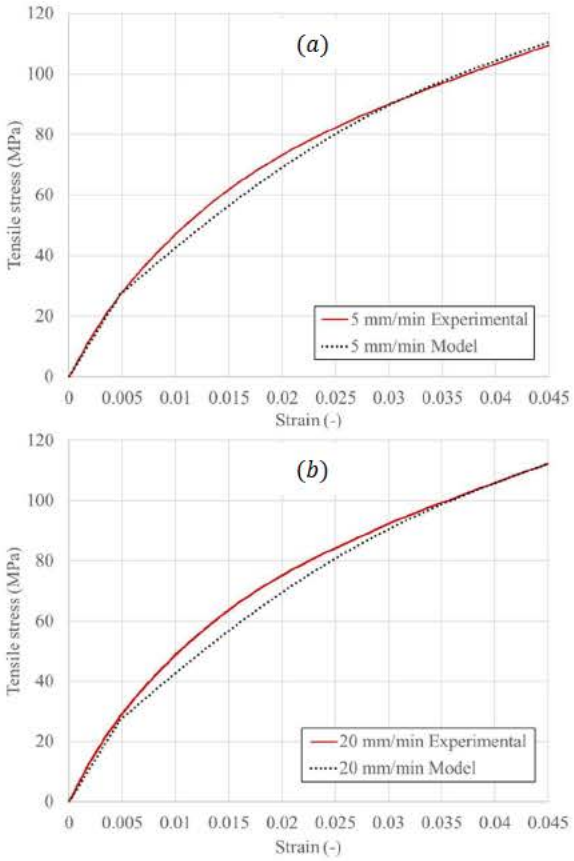

Figure 4.10. Tensile tests conducted on flax/PLA composites at strain rates of (a) $2.08x10^{-3}s^{-1}$ and (b) $8.33x10^{-3}s^{-1}$. Experimental results and model predictions.

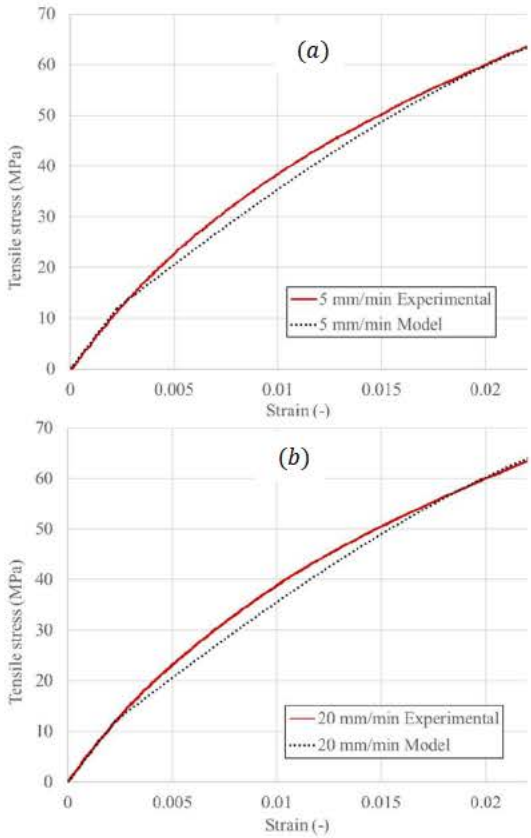

Figure 4.11. Tensile tests conducted on jute/PLA composites at strain rates of (a) $2.08x10^{-3}s^{-1}$ and (b) $8.33x10^{-3}s^{-1}$. Experimental results and model predictions.

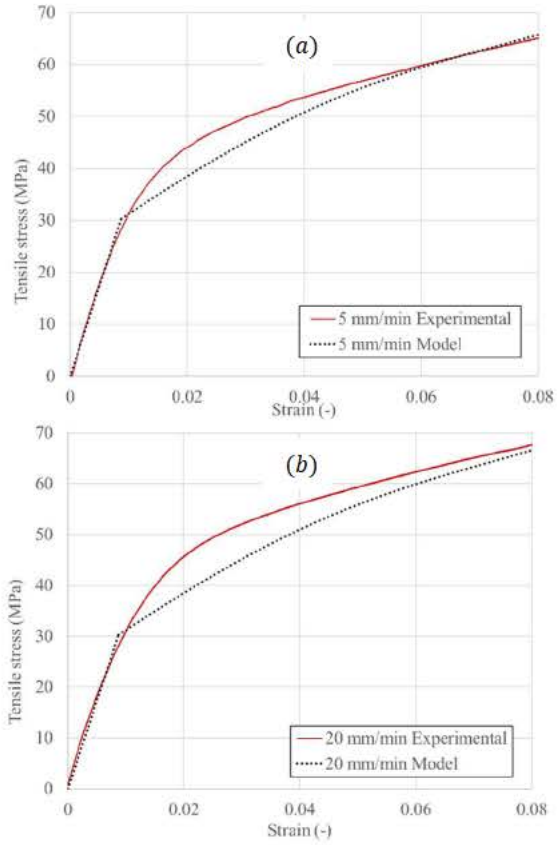

Figure 4.12. Tensile tests conducted on cotton/PLA composites at strain rates of (a) $2.08x10^{-3}s^{-1}$ and (b) $8.33x10^{-3}s^{-1}$. Experimental results and model predictions.

4.9 Conclusions

A constitutive model for fully biodegradable composites was developed for the first time. The model, based on rheological elements, includes the consideration of non-linear elastic behaviour, viscous effects and plastic strains. The model was successfully validated for three different biocomposites: flax/PLA, jute/PLA, and cotton/PLA woven laminates.

It should be noticed that the model was calibrated for each material using two relaxation tests and the stress-strain curve obtained at a single strain rate. The model predicted with a reasonable accuracy the influence of strain rate, the predicted stress-strain curves at higher strain rates were in agreement with experimental results. All the materials experience an increment in the stiffness with strain rate, but this effect was higher in flax and jute composites than in cotton laminates. The model predicted this difference between materials even when it was calibrated using only relaxation tests.

One of the main goals of the present model is that the model was validated for three different materials, what means that the model can help to bring some light to the physics behind the viscoplastic behaviour of biocomposites. This is only the first attempt to develop a constitutive model for fully-biodegradable material but some hypotheses are proposed:

1- The plastic strains can be accurately predicted with a single friction element. This means that the yield point can be associated to a value of strain that initiates the plastic behaviour. One of the most probable reasons is the friction between fibres inside the yarns. The plastic behaviour of the matrix is an alternative explanation but it can be neglected due to the great differences in the values of yield strain for composites reinforced with different fibres.
2- The viscous effects can be attributed to fibres behaviour. The influence of matrix can be neglected again because the viscous effects are higher in the composites reinforced with stiffer fibres. Moreover, the influence of strain rate on the stiffness of flax/PLA composites is similar to that reported by other authors in flax/epoxy composites.
3- The non-linear elastic behaviour can be probably explained by a combination of woven fibres and matrix.

These hypotheses can be considered the starting point for future research in this field. The present promising results can lead to get a better understanding of the mechanical behaviour of biocomposites and to increase their use in industrial applications to replace mineral fibres and oil-based polymer matrices.

References

[1] Mohanty AK, Misra M, Drzal LT (Eds.). Natural fibers, biopolymers, and biocomposites. CRC Press, 2005

[2] Wambua P, Ivens J, Verpoest I. Natural fibres: can they replace glass in fibre reinforced plastics? Compos Sci Technol 2003; 63(9):1259–64.

[3] Satyanarayana KG, Arizaga GGC, Wypych F. Biodegradable composites based on lignocellulosic fibers-An overview. Prog Polym Sci 2009; 34(9): 982-1021

[4] Koronis G., Silva A., Fontul M. Green composites: a review of adequate materials for automotive applications. Compos Part B: Eng 2013; 44(1): 120-7.

[5] John MJ, Thomas S. Biofibres and biocomposites. Carbohydr Polym 2008; 71(3):343-64

[6] European Union. The Directive 2000/53/EC of the European Parliament and of the Council of 18

September 2000 on end-of-life vehicles. OJ L 2000, 269:34-49.

[7] Santiuste C, Thomsen OT Frostig Y. Thermo-mechanical load interactions in foam cored axi-symmetric sandwich circular plates–High-order and FE models. Compos Struct 2011; 93(2): 369-76.

[8] Santiuste C, Sánchez-Sáez S, Barbero E. A comparison of progressive-failure criteria in the prediction of the dynamic bending failure of composite laminated beams. Compos Struct 2010; 92(10): 2406-14.

[9] Soldani X, Santiuste C, Muñoz-Sánchez A, Miguélez MH. Influence of tool geometry and numerical parameters when modeling orthogonal cutting of LFRP composites. Compos Part A: Appl Sci Manuf 2011: 42(9): 1205-16

[10] Poilâne C., Cherif ZE, Richard F, Vivet A, Doudou, BB, Chen J. Polymer reinforced by flax fibres as a viscoelastoplastic material. Compos Struct 2014; 112(1):100–12

[11] Rubio-López A, Olmedo A, Santiuste C. Modelling impact behaviour of all-cellulose composite plates. Compos Struct 2015; 122:139-43

[12] Ihueze CC, Okafor CE, Okoye CI. Natural fiber composite design and characterization for limit stress prediction in multiaxial stress state. J King Saud Univ-Eng Sci 2013; 27(2): 193-206

[13] Facca AG, Kortschot MT, Yan N. Predicting the elastic modulus of natural fibre reinforced thermoplastics. Compos Part A: Appl Sci Manuf 2006; 37: 1660–71.

[14] Virk AS, Hall W, Summerscales J. Modelling tensile properties of jute fibres. Mater Sci Technol 2011; 27(1): 458-60.

[15] Virk AS, Hall W, Summerscales J. Modulus and strength prediction for natural fibre composites. Mater Sci Technol 2012; 28(7): 864-71.

[16] Modniks J, Andersons J. Modeling the non-linear deformation of a short-flax-fiber-reinforced polymer composite by orientation averaging. Compos Part B: Eng 2013; 54: 188-93.

[17] Sliseris J, Yan L, Kasal B. Numerical modelling of flax short fibre reinforced and flax fibre fabric reinforced polymer composites. Compos Part B: Eng 2016; 89: 143-54.

[18] Mattrand C, Béakou A, Charlet K. Numerical modeling of the flax fiber morphology variability. Compos Part A: Appl Sci Manuf 2014; 63: 10-20.

[19] Beakou A, Charlet K. Mechanical properties of interfaces within a flax bundle-Part II: Numerical analysis. Int J Adhes Adhes 2013; 43: 54–9

[20] Andersons J, Modniks J, Spārniņš E. Modeling the nonlinear deformation of flax-fiber-reinforced polymer matrix laminates in active loading. J Reinf Plast Compos 2015; 34(3): 248-56

[21] Rubio-López A, Olmedo A, Diaz-Alvarez A, Santiuste C. Manufacture of compression moulded PLA based biocomposites: A parametric study. Compos Struct 2015; 131: 995-1000.

[22] Ochi S. Mechanical properties of kenaf fibers and kenaf/PLA composites. Mech mater 2008; 40(4): 446-52.

[23] Persson A, Karlsson F. Modelling non-linear dynamics of rubber bushings-parameter identification and validation. PhD thesis, Lund University 2003.

[24] Yeoh OH. Some forms of the strain energy function for rubber. Rubber Chem technol 1993; 66(5): 754-71

Chapter 5

Low velocity impact behaviour of biocomposites: Experimental study

The study of the impact behaviour and the post-impact residual strength of fully biodegradable composites is presented in this Chapter. To this end, low-velocity impact tests and compressive residual strength tests were carried out on flax/PLA laminates. The main failure mode was fibre failure, while delaminations were not found, thus energy absorption mechanisms in flax/PLA laminates are different to those found in traditional composites. Additionally, flax/PLA composites were compared with carbon/epoxy laminates showing that biocomposites present some important advantages in terms of absorbed energy and normalized residual strength.

5.1 Introduction

Natural fibres are a promising option to substitute traditional composites reinforced by synthetic fibres in industrial applications as automotive or aeronautics in terms of sustainability [1]. In addition, natural polymers can be used as matrix reinforced with natural fibres to obtain a fully biodegradable composite material, which could contribute to fulfil the environmental objectives specified by the European legislation [2]. Biocomposites can compete in terms of strength per weight with traditional composites but also in terms of costs [1, 3]. One of the main potential applications of biocomposites is automotive industry due to their energy absorption capability [4]. Vehicle components manufactured with natural fibres can be subjected to crash impacts or stone strikes during its service live. Thus, there is a need to understand the impact and post-impact behaviour of biocomposites laminates.

Energy absorption capability and residual strength are the main variables analysed in impact testing. However, absorbed energy depends on test configuration. Charpy and Izod are the most popular impact tests on biocomposites [5-6]. These tests were originally designed to determinate ductile-brittle transition of materials, therefore they are usually conducted on metals, most often assuming a pre-existing notch, which is not suitable for testing composites. An alternative method is drop-weight test, in which a known mass is dropped from a given height onto a flat, un-notched sample. Drop-weight tests have proven to be valuable source of information about the impact and post-impact behaviour of traditional composites [7-12].

There are some works about low-velocity impact behaviour and residual strength of composites manufactured with natural fibres and non-biodegradable matrices [13-17]. Liang et al. [13] studied flax/epoxy composites, finding delamination combined with transverse cracking, and matrix cracking in the resin-rich zones as the main energy absorption mechanisms during impacts. Residual compressive strength dropped by 30% and 15% (depending on stacking sequence) for specimens impacted at 10J.

Dhakal and his colleagues published several works [14-16] analysing the impact behaviour of hemp/polyester and jute/polyester laminates. They found matrix cracking, delamination and fibre breakage as the predominant failure modes. Post-impact behaviour was studied through flexural after impact (FAI) tests performed on impacted jute/polyester specimens showing a great influence of temperature on residual strength. Petrucci et al. [17] found a significant reduction of flexural strength, about 90%, when the specimens were impacted at 12J for flax/epoxy laminates and 6J for hemp/epoxy laminates.

However, only one experimental study about low-velocity impact on fully biodegradable composites has been published [18], and post-impact behaviour of biocomposites is an almost unexplored field. Huber et al. [18] developed low-velocity impact on All-Cellulose-Composites (ACC) manufactured from Cordenka fibres. ACC laminates showed a combination of high flexural strength and interfacial adhesion leading to a great energy absorption capability under low-velocity impacts. Rubio-López et al. [19] completed the work of Huber et al. [18] with a numerical analysis of the aforementioned low-velocity impacts on ACC laminates. They developed a numerical model to predict the main failure mechanisms. However, no study about post-impact behaviour of fully biodegradable composites was found.

In an attempt to study the impact behaviour and the after-impact residual strength of fully biodegradable composites, this work presents the analysis of low-velocity impact tests and compressive residual strength of flax/PLA laminates. The study of the impact behaviour includes the analysis of contact forces, absorbed energy, coefficient of restitution, failure mechanisms, permanent deflections, and damaged area. The influence of hemispherical impactor nose diameter is also analysed. Additionally, results were compared with carbon/epoxy laminates showing that biocomposites present some important advantages in terms of absorbed energy and normalized residual strength.

5.2 Experimental

5.2.1 Manufacturing

PLA matrix was reinforced with flax woven fibres to manufacture fully biodegradable composites. Flax fibres without chemical pre-treatment were used in a 2x1 basket weave configuration. The matrix was 10361D PLA, a biodegradable thermoplastic resin provided by Natureworks LLC in pellets form. The 10361D PLA is specifically aimed as a binder of natural fibres. The PLA density is 1.24 g/cm3 and its melting temperature is 145-170ºC.

Composites were manufactured by compression moulding after ply stacking. First, the PLA pellets were placed between two thermoheated plates at a temperature of 185ºC to obtain a uniform film. Then, 5 matrix films were stacked alternatively with the 4 woven plies of 200 mm x 200 mm. The stacked plies were placed between the thermoheated plates. After a 2 minutes pre-heating at 185ºC, 16 MPa pressure was applied during 3 minutes using a universal test machine Servosis ME-404/100. Finally, the biocomposite panels were dried at room temperature. A thickness of 2.64±0.11 mm resulted after the compression moulding. The quantity of reinforcement was fixed in a weight ratio of 65%, as Ochi [20] stated as the optimum value for compression moulding procedures with natural fibres. Composites, fibres and PLA were stored at constant conditions before manufacturing and testing (23ºC, 50% RH). The tensile strength of the resulting biocomposite laminate is 100 MPa. This manufacturing procedure is described in detail in Rubio et al. [21].

5.2.2 Low velocity impact tests

Low-velocity impact tests on manufactured panels were performed by means of an INSTRON-CEAST Fractovis 6875 drop weight tower. The specimens were hit orthogonally with an impactor bar which is free fall accelerated through a guide. At the end of the bar two different diameter of hemispherical nose were placed (12.7 and 20 mm) with different masses of 3.76 kg and 3.815 kg respectively; the impactor bar is instrumented, registering the contact force during the impact. After the impact, an anti-rebound system held the impactor to avoid multi hits on the specimen. Eight impact energies were chosen for each impactor diameter to study the damage threshold energy in the biocomposite laminates and the perforation energy, resulting in 16 test configuration. For each combination of impactor diameter and impact energy two different panels were tested, allowing to ensure the repeatability. Moreover, for each impact energy one of the panels was chosen for destructive analysis and the other one for compression after impact test.

The aforementioned manufactured biocomposite panels were cut in square specimens of 80 x 80 mm, they were placed on a steel support and clamped along their outer border in such a way that a circular laminate area of 55 mm in diameter was the effective free span. The specimens were tested at constant conditions of 23ºC and 50% RH.

5.2.3 Evaluation for analysis of damage mechanisms

Several techniques were employed to evaluate damage induced by low-velocity impacts: visual inspection, destructive analysis and permanent deflection measurements. Visual inspection was used to identify external damage mechanisms, while destructive analysis was performed to analyse internal damage. The specimens were cut along two perpendicular paths using a diamond saw (Well 3242). Special caution has been taken to avoid any interference in the intra or interlaminar damage for its later analysis, which it has been accomplished using a proper water refrigeration system. Since no delamination was observed in the impacted specimens, damaged area was defined using the permanent deflection. The damage area is defined as the points with a permanent deflection higher than 1mm. This area was assumed elliptical, thus two perpendicular axes were measured to calculate damaged area. The permanent deflection in the impacted face was measured by means of a laser extensometer MEL M27L/50. The laser was attached to an automatic positioning system to measure not only the maximum permanent deflection, but also the deflection along a path in the specimen.

5.2.4 Compression after impact (CAI)

Compression after impact tests were carried out with an Instron 8500 universal testing machine. CAI tests must be carried out in a device that avoids global buckling of the impacted specimens, so that failure is induced by the damage generated during impact Figure 5.1c. The CAI device consist in four anti-buckling plates as shown in the scheme of Figure 5.1a. The device have a rectangular opening in the middle that left the central surface of the specimen free and did not modify the surfaces damaged by the impact [12]. The dimensions of the set-up were adapted to the geometry of the specimens (80 × 80 mm), Figure 5.1b. The two rear plates were welded to the loading plates, the specimens were placed in the set-up and each of the front anti-buckling plates was screwed to the rear plates. A free zone of 4 mm is left between the upper and lower anti-buckling plates.

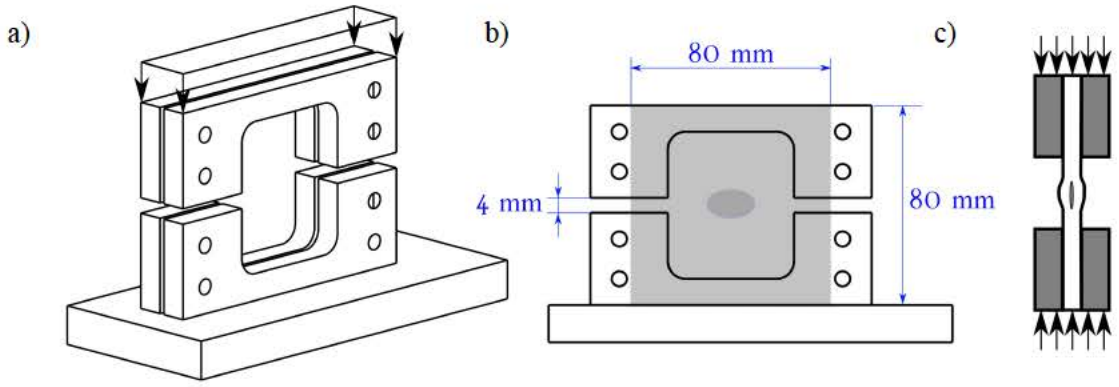

Figure 5.1. Compression after impact device. a) Three dimensional sketch. b) Front view. c) Failure mode scheme.

5.3 Results and discussion

Impact energy ranged from 3.8 J to 20.0 J. Figures 5.2 and 5.3 show the force-displacement curves obtained with 12.7 mm and 20 mm diameters respectively. Three impact energies were selected to illustrate the most representative impact tests. The force-displacement curve for the lower impact energy showed a linear elastic behaviour until damage onset. The initiation of damage produced some small force drops until peak force is reached; finally, the impactor bounces back and contact force drops to zero. A similar curve is obtained for intermediate impact energy but with higher values of peak force and maximum displacements. The specimen was penetrated when it was impacted with the maximum energy, thus impactor does not bounce back and the displacement increases until contact force drops to zero.

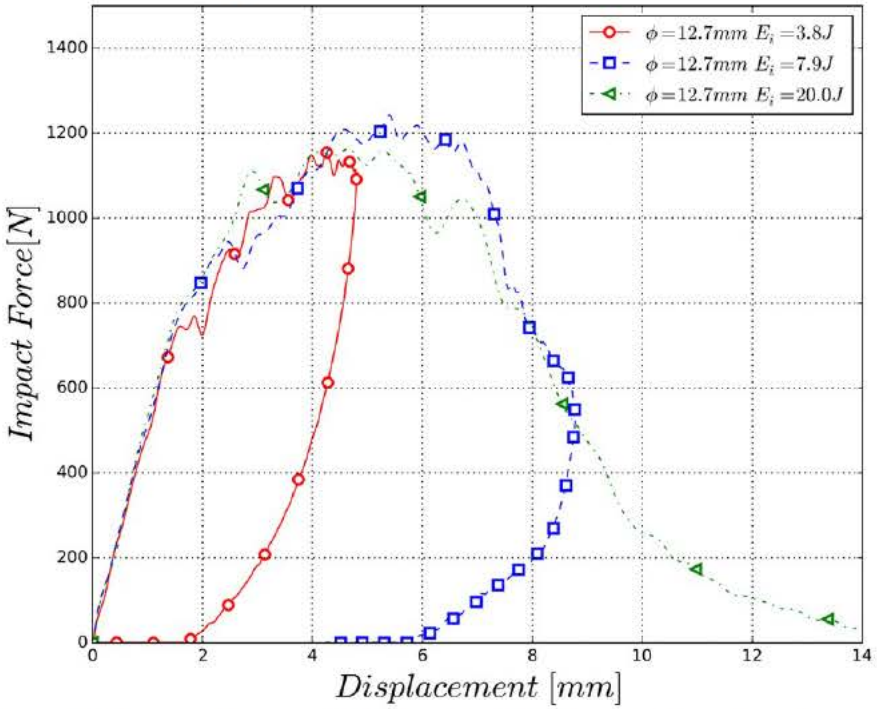

Figure 5.2. Force-displacement curves, 12.7 mm diameter impactor. Impact energies = 3.8 J, 7.9 J and 20.0 J.

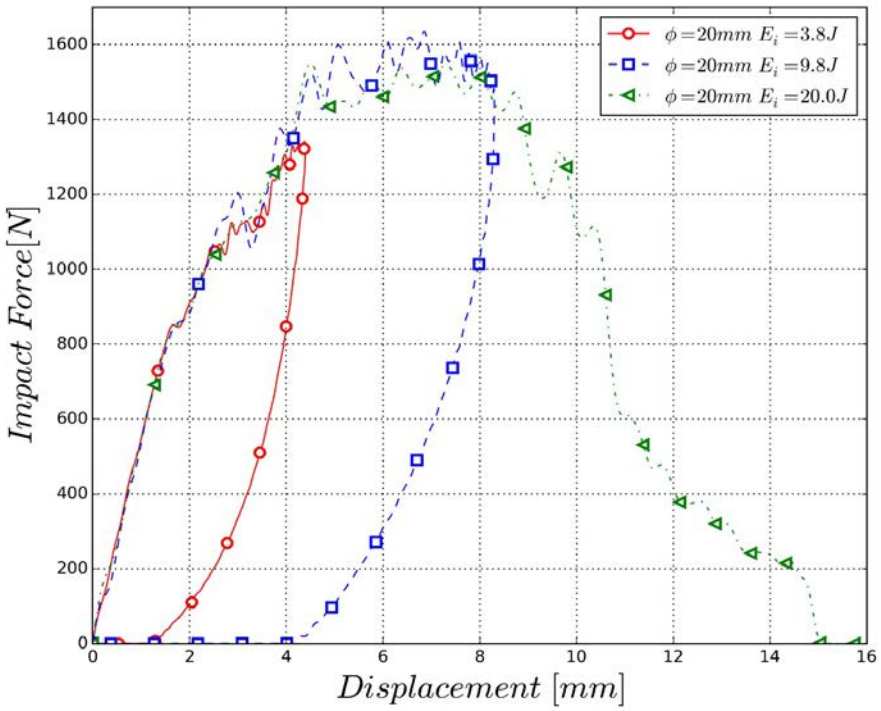

Figure 5.3. Force-displacement curves, 20 mm diameter impactor. Impact energies = 3.8 J, 9.8 J and 20.0 J.

The evolution of peak force with impact energy showed two trends, Figure 5.4. First, peak force increased with impact energy until 4.7 J using the 12.7 mm nose diameter and 7.9 J with the 20 mm nose diameter. Then, there is a plateau with a peak force of 1200 N for the 12.7 mm nose diameter, and 1600 N for the 20 mm nose diameter. The impact energies that divided these two trends corresponded to the onset of a visible crack reducing plate stiffness and, consequently, limiting contact force. Peak forces obtained with 12.7 mm nose diameter were lower than those produced with 20 mm nose diameter due to the stress concentration in the contact area.

Figure 5.5 shows the evolution of absorbed energy with impact energy, two clear stages can be observed. First, there is a linear relationship between impact and absorbed energy. In this first stage, the specimen was damaged but not penetrated by the impactor, thus impactor bounced back after the impact. The second trend is characterized by the full penetration of the specimen, thus penetration energy was defined as the minimum impact energy that produced the penetration. The lower impact energy that produced specimen full penetration were 10 J and 15 J for the 12.7 mm and 20 mm nose diameters respectively. In the second stage, absorbed energy was stabilized when increasing impact energy as the energy absorbing capability of the laminate was raised. The smaller impactor nose leaded to a higher stress concentration, thus penetration was produced for lower impact energy.

In addition, Figure 5.5 shows the evolution of absorbed energy with impact energy obtained with woven carbon/epoxy laminates [10]. These results were selected because the geometry of plates and impactor was the same that those used in the present work. The energy absorbed by the carbon/epoxy laminates was lower than by flax/PLA laminates. For example, carbon/epoxy plates absorbed 7.1 J when they were impacted at 10 J, while flax/PLA specimens absorbed 7.9 J, meaning an increment of 11.3%. This result implies that, under the same impact conditions, the energy absorbed by flax/PLA laminates is higher. It should be noticed that these results applied to range of impact energies studied.

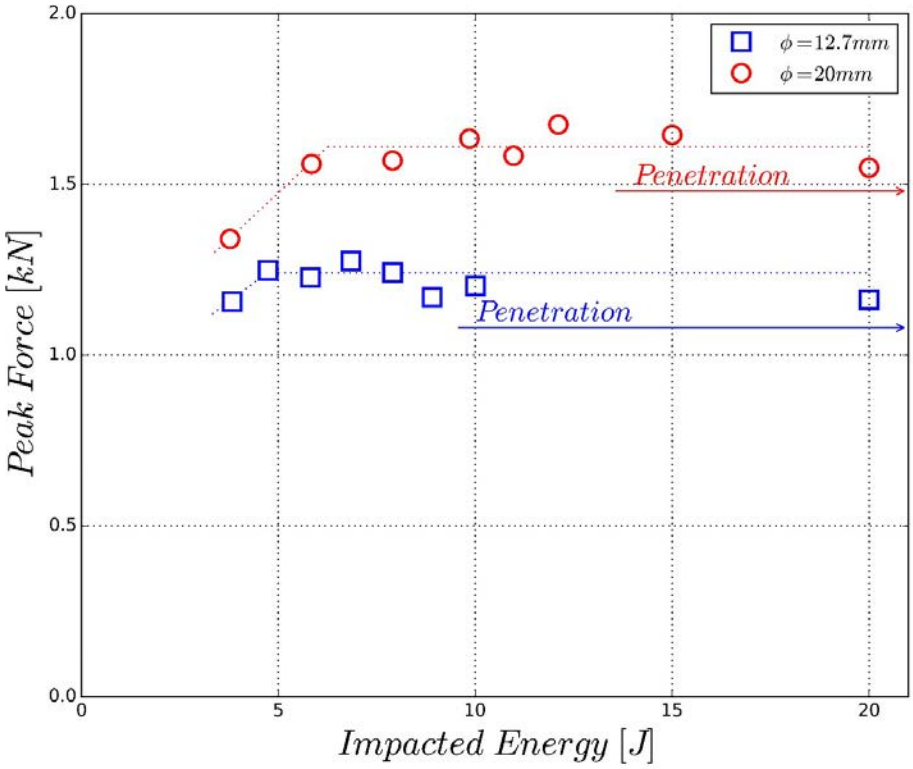

Figure 5.4. Peak-force versus impact energy for 12.7 mm and 20 mm nose diameters.

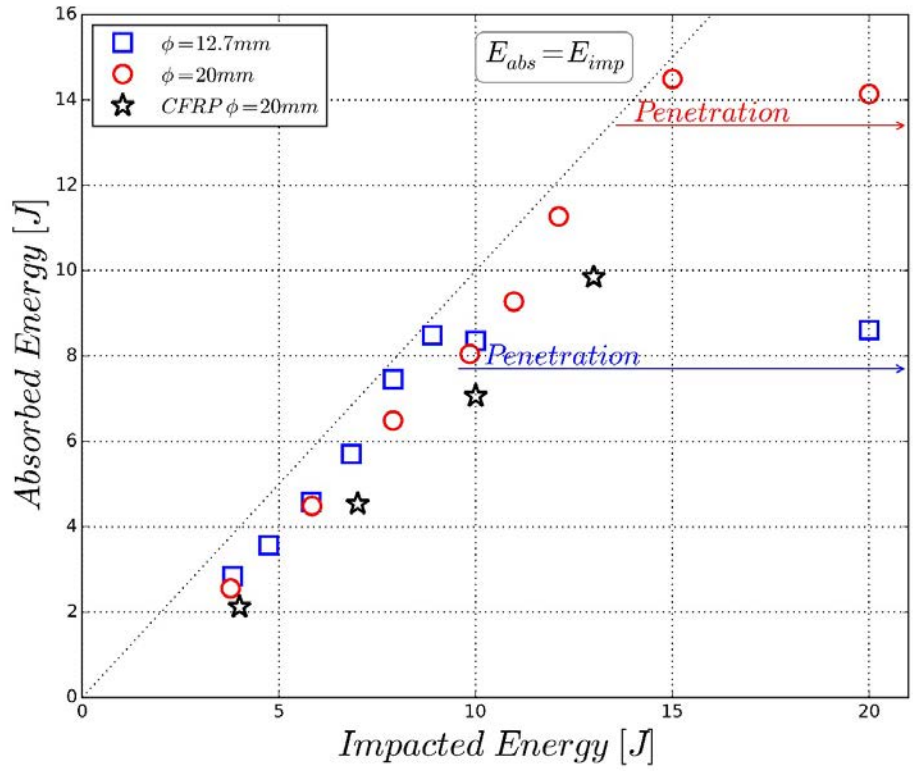

Figure 5.5. Absorbed energy versus impact energy for biocomposites using 12.7 mm and 20 mm nose diameters and woven carbon/epoxy composite with the 20 mm nose diameter.

To study the composite response in terms of energy COR, coefficient of restitution [11], was calculated as:

$$\text{COR} = \sqrt{\frac{E_i - E_a}{E_i}} \qquad (1)$$

where Ei is the impact energy in each case and Ea represents the absorbed energy under the impact energy. COR decreases as the impact energy increases until penetration energy is reached because more energy is dissipated due to failure mechanisms in the composite, Figure 5.6. In the case of penetration energy the COR value is zero. The values of penetration energy predicted by COR is in agreement with those showed in Figure 5.5.

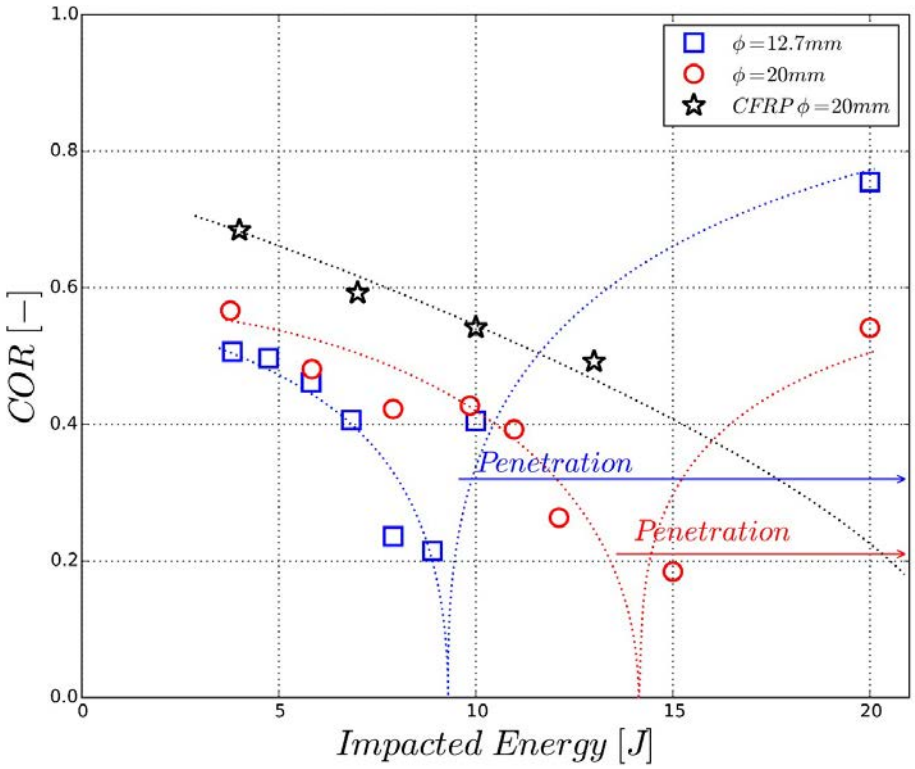

Figure 5.6. Coefficient of restitution (COR) vs impact energy.

5.4 Analysis of damage mechanisms

Figure 5.7 shows front and back faces of specimens impacted by the 12.7 mm impactor at 5.8 J, 7.9 J and 10 J. For the lower impact energy, only fibre failure in the back face in cross shape is observed; this shape is typical in woven laminates [11]. The failure appears earlier in the back face because higher strains are produced in this face due to the combined effect of the bending and membrane tensile forces. As the energy increases, the length of fibre failure in the back face increases and fibre failure appears also in front face. Finally, in the case of higher energy, fibre failure is enough to allow the full penetration of the impactor. It can be seen how the fibre failure in the front face is rounded, while in the back face has a cross shape creating a pyramidal deformation. This can be explained because in the front face appear a new failure mechanism, the shear failure, while in the back face tensile forces are the cause of the failure. This shear failure occurs only when impact energy is closed to penetration limit or above it. Same conclusions can be obtained for the failures

produced in the specimen impacted with the 20 mm impactor, but cracks are larger due to the higher diameter of the impactor and the impact energy need to perforate the specimens was higher.

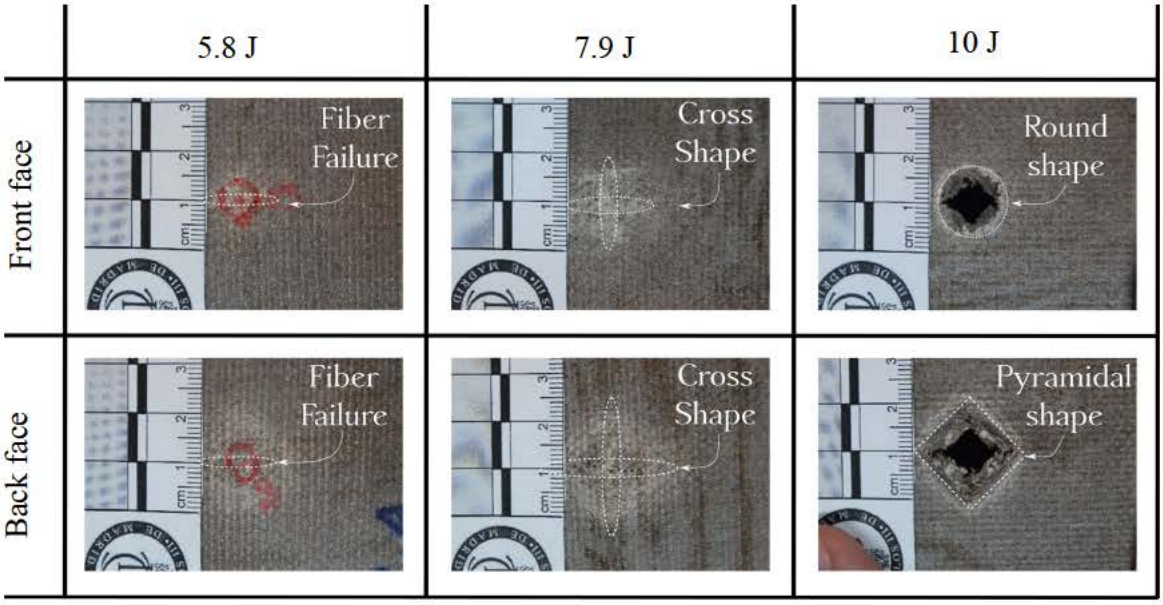

Figure 5.7. Photographs of the different failure mechanisms. Impactor nose diameter: 12.7 mm. Impact energies = 5.8 J, 7.9 J and 10 J.

Specimens were cut through its two central paths to analyse internal damage, pictures of the specimens impacted with the 12.7 mm impactor at 3.8 J, 5.8 J and 10 J are shown in Figure 5.8, where it can be observed how damage extension increases with impact energy. The main failure mechanism found is fibre failure; matrix cracking was associated with fibre failure while no transverse cracks in resin-rich zones were found; and there were no delaminations between adjacent plies. Delamination is one of the main failure mechanisms found in traditional composited subjected to low-velocity impacts, thus flax/PLA laminates show a different impact behaviour. There are four possible reasons that can be used to explain the absence of delamination: first, delamination produced in woven laminates is smaller than that produced in tape laminates, event in the case of traditional composites [12]; second, the difference between mechanical properties of fibres and matrix is lower than in traditional composites [22]; third, PLA shows a ductile failure in comparison with other matrices as epoxy [23]; finally, the rough surface of natural fibres does not promote the propagation of cracks in the matrix-fibre interface [4]. The first two reasons, woven architecture and lower differences in mechanical properties, could justify minor delaminated areas, but only the last two reasons, ductile failure of PLA and rough surface of natural fibres, can explain the complete absence of delaminations.

Permanent deflections were measured in all the impacted specimens along two perpendicular paths. Figure 5.9 shows a path for specimens impacted at different energy levels (3.8 J, 5.8 J, 7.9 J and 10.0 J) with the 12.7 mm diameter impactor. The maximum deflection corresponds to the centre of the plate, while the outer regions (from -40 to -27.5 mm and from 27.5 to 40 mm) were clamped during the test. Both maximum deflection and damaged area increase with impact energy; except in the case of 10.0 J. Damage area decreased when impact energy is higher than penetration energy because damage mechanisms, mainly fibre failure, are located in the surrounding of the contact area. Same conclusions can be obtained for the deflection registered in the specimen impacted with the 20 mm impactor.

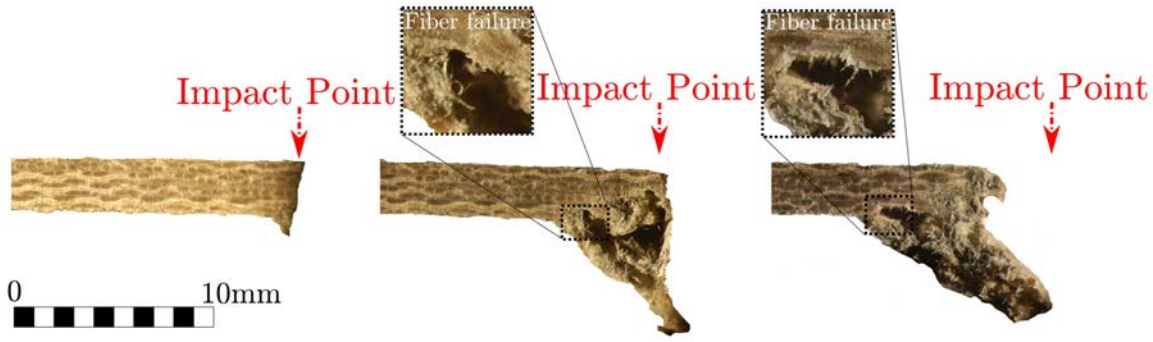

Figure 5.8. Photograph of the cut surface. Composites impacted with 12.7 mm impactor. From left to right: 3.8 J, 5.8 J and 10.0 J.

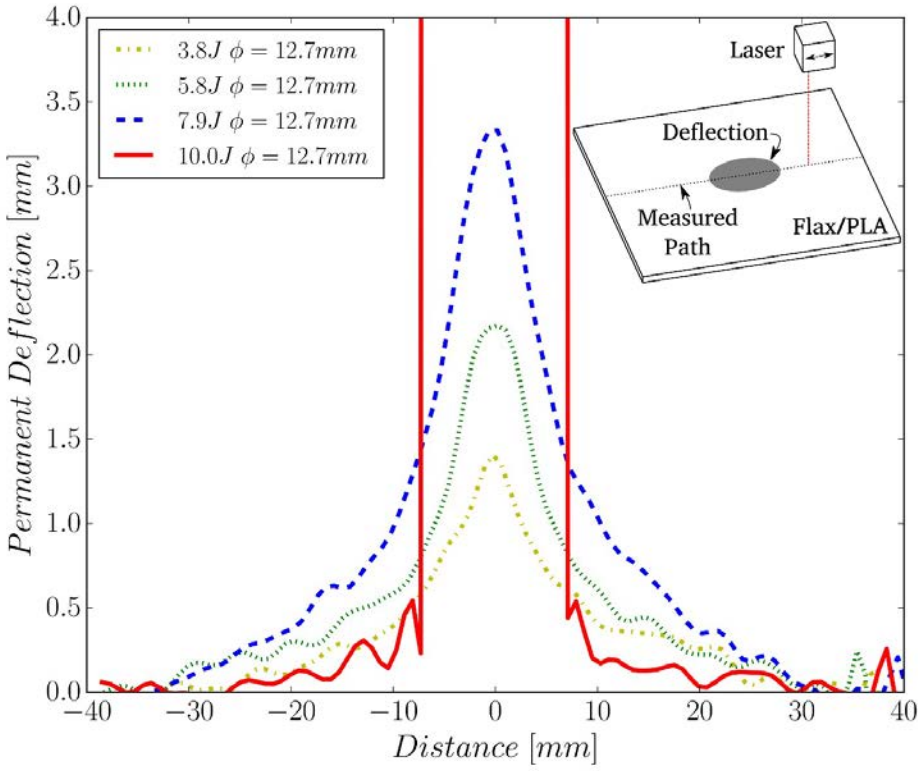

Figure 5.9. Permanent deflection vs position for different impact energy. Impactor nose diameter: 12.7 mm.

Maximum permanent deflection as a function of the impact energy is shown in Figure 5.10. For lower values of impact energy, permanent deflection increases with impact energy, and there are no significant differences between the 12.7 mm and the 20 mm nose diameters. However, when impact energy is near to the penetration energy, permanent deflections produced with the 12.7 mm impactor nose are much higher because penetration energy is lower than with the 20 mm impactor nose. The highest values of permanent deflections correspond to the pyramidal shape produced when impact energy is close to penetration limit.

Damaged area is represented as function of the impact energy in Figure 5.11. Damaged area is defined as the points with permanent deflection higher than 1mm, and it is assumed elliptical, whose axes length were obtained by two perpendicular paths. The evolution of damaged area with impact energy shows three regions. In the first region, damage area increase with impact energy

until values near to penetration energy. In the third region, when the specimen was perforated, damaged area is constant with a value slightly higher to the projected surface of the impactor nose. In the transition region, damaged area decreases with impact energy from maximum damage area to the value corresponding to penetration.

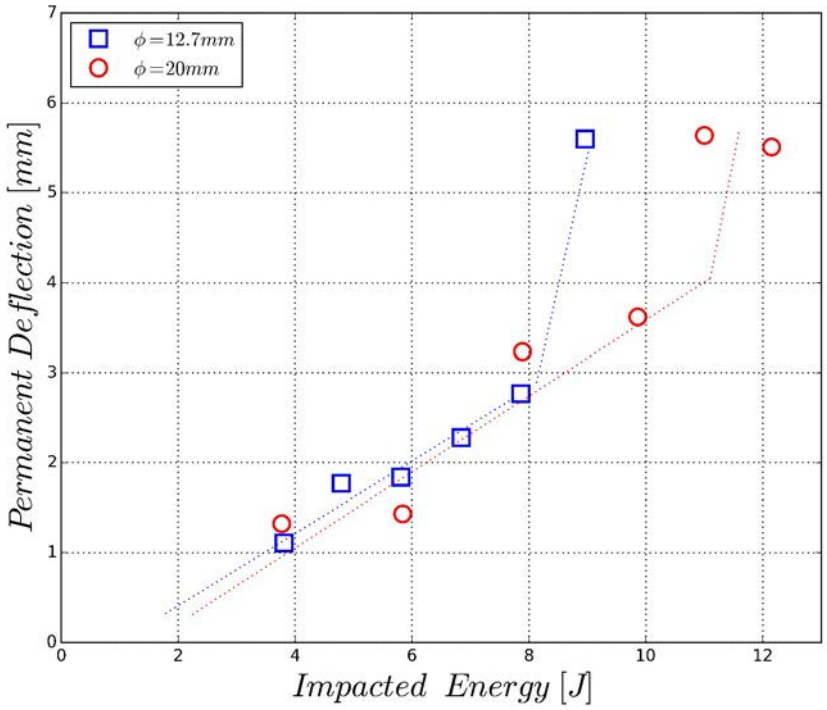

Figure 5.10. Maximum deflection vs Impact energy

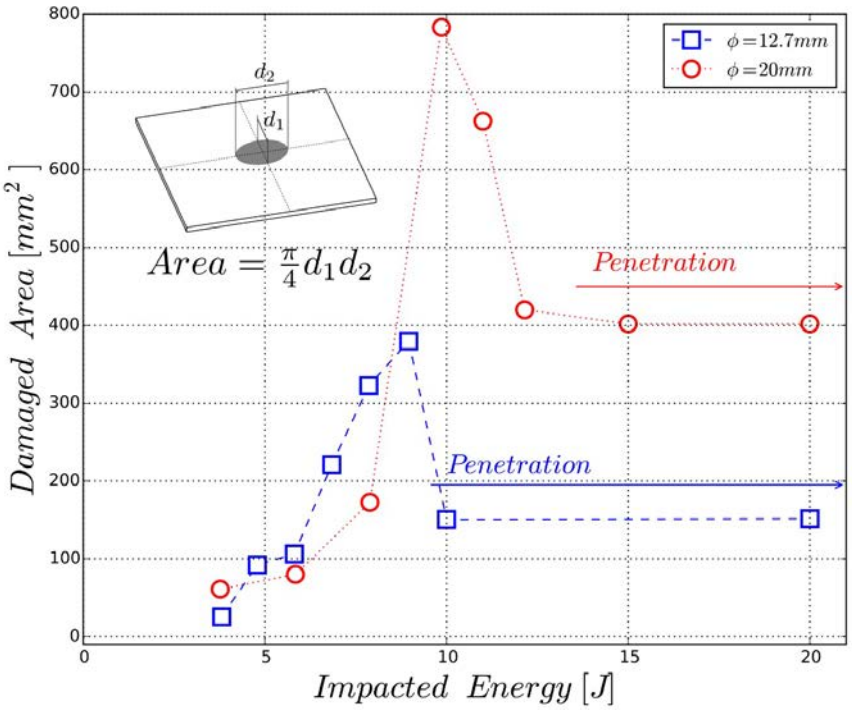

Figure 5.11. Damaged area vs impact energy

Normalized residual strength obtained in the CAI test is represented versus the impact energy in Figure 5.12. The results of carbon/epoxy woven laminates under the same conditions of impact and CAI tests reported by [12] are also included in Figure 5.12. Concerning to flax/PLA specimens, residual strength decreases with impact energy for impact energies under perforation limit. This reduction is due to the increment of damage produced in the laminate. A plateau is observed for impact energies over perforation limit, the minimum normalized residual strength of perforated laminates is 68% for specimens impacted with the 12.7 mm diameter nose, and 60% for the 20 mm diameter nose. It should be noticed that even when specimens were perforated, they exhibit a residual strength higher than carbon/epoxy laminates. Thus, under the same impact conditions, in the range of studied impact energies, absorbed energy and normalized residual strength are higher in flax/PLA woven laminates than in carbon/epoxy laminates due to different failure mechanisms. Fibre failure is the main energy absorption mechanism in flax/PLA laminates, while delamination and matrix cracking play a main role in the energy absorbed by carbon/epoxy plates. Specimens impacted with the 20 mm impactor shows a lower residual strength than the 12.7 mm impactor due to their wider damaged area.

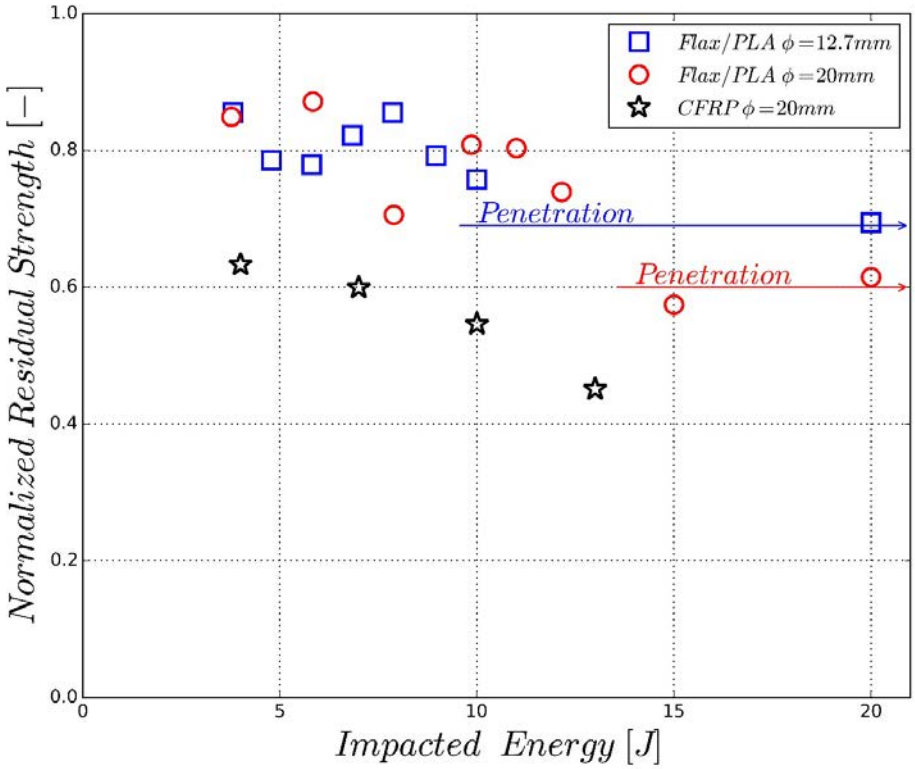

Figure 5.12. Normalized residual strength vs impact energy

5.5 Conclusions

Impact behaviour and residual strength of fully biodegradable composites have been analysed. Two hemispherical impactor noses were compared with diameters of 12.7 mm and 20 mm and impact energy ranged from barely visible damage to penetration. Contact force recorded with the 12.7 diameter nose was lower due to higher stress concentrations. The analysis of damaged area, calculated from the analysis of permanent deflection confirmed that damaged area was more reduced for the 12.7 mm diameter nose. Absorbed energy and COR were used to find the impact energy necessary to produce the full penetration of the laminates, this penetration energy was lower for the 12.7 mm diameter nose. Residual compressive strength was higher in the specimen impacted

with the 12.7 mm diameter nose because both, damaged area and absorbed energy, were lower than in specimens impacted with the 20 mm diameter nose.

The main failure mode was fibre failure, while delaminations were not found. This result implies that the energy absorption mechanisms when flax/PLA laminates are subjected to low-velocity impacts are different to those found in traditional composites and in composites manufactured with natural fibres and non-biodegradable matrices. The present results were compared with tests on carbon/epoxy woven laminates reported in [10] and [12]. These impact and CAI tests were carried out under the same conditions that present work, including specimen geometry. The results showed that fully biodegradable composites as flax/PLA composites present some advantages when they are compared with traditional composites. Due to the absence of delamination and the ductile failure of the matrix, both absorbed energy and normalized residual strength of flax/PLA composites are higher than those obtained in carbon/epoxy laminates, in the range of studied impact energies.

This is the first study of the after-impact residual strength of fully biodegradable composites, the present results show that this is a promising research field and biocomposites can be suitable for numerous industrial applications. However, more studies must be done to verify these results with other fibres and matrices.

References

[1] Milanese, AC, Cioffi MOH, Voorwald HJC. Thermal and mechanical behaviour of sisal/phenolic composites. Compos Part B: Eng 2012:43(7);2843-50.

[2] Bodros, E, Pillin, I, Montrelay, N, Baley, C, Could biopolymers reinforced by randomly scattered flax fibre be used in structural applications? Compos. Sci. Tech. 2007:67(3);462-70.

[3] Porras A, Maranon A. Development and characterization of a laminate composite material from polylactic acid (PLA) and woven bamboo fabric. Compos Part B: Eng 2012:43(7);2782-8.

[4] Melo JDD, Carvalho LFM, Medeiros AM, Souto CRO, Paskocimas CA. A biodegradable composite material based on polyhydroxybutyrate (PHB) and carnauba fibers. Compos Part B: Eng 2012:43(7);2827-35.

[5] B. Bax. J. Müssig , Impact and tensile properties of PLA/Cordenka and PLA/flax composites, Compos. Sci. Tech. 68(7) (2008) 1601-7.

[6] O. Faruk, A.K. Bledzki, H.P. Fink, M. Sain, Biocomposites reinforced with natural fibers: 2000–2010, Prog. Polym. Sci. 37(11) (2012) 1552–96.

[7] Ivañez I, Santiuste C, Sanchez-Saez S. FEM analysis of dynamic flexural behaviour of composite sandwich beams with foam core. Compos Struct 2010;92(9):2285-91.

[8] Santiuste C, Sánchez-Sáez S, Barbero E. A comparison of progressive-failure criteria in the prediction of the dynamic bending failure of composite laminated beams. Compos Struct 2010;92(10):2406-14.

[9] Santiuste C, Sánchez-Sáez S, Barbero E. Residual flexural strength after low-velocity impact in glass/polyester composite beams. Compos Struct 2010;92(1):25-30.

[10] Gómez-del Rıo T, Zaera R, Barbero E, Navarro C. Damage in CFRPs due to low velocity impact at low temperature. Compos Part B: Eng 2005;36(1):41-50.

[11] Artero-Guerrero JA, Pernas-Sánchez J, López-Puente J, Varas D. Experimental study of the impactor mass effect on the low velocity impact of carbon/epoxy woven laminates. Compos Struct 2015;133:774-81.

[12] Sánchez-Sáez S, Barbero E, Zaera R, Navarro C. Compression after impact of thin composite laminates. Compos Sci Tech 2005;65(13):1911-9.

[13] Liang S, Guillaumat L, Gning PB. Impact behaviour of flax/epoxy composite plates. Int J Impact Eng 2015;80:56-64.

[14] Dhakal HN, Zhang ZY, Richardson MOW, Errajhi OAZ. The low velocity impact response of non-woven hemp fibre reinforced unsaturated polyester composites. Compos Struct 2007;81(4):559-67.

[15] Dhakal HN, Arumugam V, Aswinraj A, Santulli C, Zhang ZY, Lopez-Arraiza A. Influence of temperature and impact velocity on the impact response of jute/UP composites. Polym Test 2014;35:10-19.

[16] Dhakal HN, Zhang ZY, Bennett N, Reis PNB. Low-velocity impact response of non-woven hemp fibre reinforced unsaturated polyester composites: Influence of impactor geometry and impact velocity. Compos Struct 2012;94(9):2756-63.

[17] Petrucci R, Santulli C, Puglia D, Nisini E, Sarasini F, Tirillò J, Kenny JM. Impact and post-impact damage characterisation of hybrid composite laminates based on basalt fibres in combination with flax, hemp and glass fibres manufactured by vacuum infusion. Compos Part B: Eng 2015;69:507-15.

[18] Huber T, Bickerton S, Müssig J, Pang S, Staiger MP. Flexural and impact properties of all-cellulose composite laminates. Compos Sci Tech 2013;88:92-98.

[19] Rubio-López A, Olmedo A, Santiuste C. Modelling impact behaviour of all-cellulose composite plates. Compos Struct 2015;122:139-43.

[20] Ochi S. Mechanical properties of kenaf fibers and kenaf/PLA composites. Mech mater 2008;40(4):446-52.

[21] Rubio-Lopez A, Olmedo A, Diaz-Alvarez A, Santiuste C. Manufacture of compression moulded PLA based biocomposites: A parametric study. Compos Struct 2015;131:995-1000.

[22] Koronis G, Silva A, Fontul M. Green composites: a review of adequate materials for automotive applications. Compos Part B: Eng 2013:44(1);120-7.

[23] Graupner N, Herrmann AS, Müssig J. Natural and man-made cellulose fibre-reinforced poly (lactic acid)(PLA) composites: An overview about mechanical characteristics and application areas. Compos Part A 2009;40(6):810-21.

Chapter 6

Low velocity impact behaviour of biocomposites: Numerical model

All-Cellulose Composites (ACC) are almost entirely manufactured from cellulose, resulting a fully biodegradable material with perfect compatibility between matrix and reinforcement. In this study, a finite element numerical model to predict the low-velocity impact behaviour of ACC laminates is reported. The model was validated through comparison with experimental data from scientific literature conducted on ACC plates made from Cordenka woven plies. In addition, the model was applied to the analysis of failure modes and influence of impact energy.

6.1 Introduction

Composite material are characterised by the combination of at least two materials, usually polymer matrix reinforced with carbon of glass fibres, with the intention to get properties that cannot be achieved using the constituent materials separately. In the last years, numerous researchers have introduced natural fibres as reinforcement to increase the biodegradability of composites. The works that have studied biocomposites made of natural fibres as jute, hemp, linen or cotton have shown promising results related with their mechanical properties [1-6]. However, the high properties of natural fibres cannot be fully exploited in many biocomposites due to poor bonding between natural fibres and polymer matrix [7].

In recent years, a new class of monocomponent composites based on cellulosic materials, so-called all-cellulose composites (ACCs) have emerged. In ACCs, both the matrix and reinforcement are cellulosic, but the first is isotropic while the latter is highly anisotropic [8]. Nishino [9] introduced the concept of ACC materials to overcome problems associated with the compatibility and interfacial adhesion of matrix and reinforcement using chemically identical materials. In addition, the fact that such materials are fully bio-based and fully biodegradable will certainly improve their relevance in future applications [10, 11]. Huber and his collaborators published an excellent review reporting the different processing routes that have been applied to the manufacture of ACCs using a broad range of different solvent systems and raw materials [12].

The most of the research done on ACCs are focused on their behaviour under quasi-static conditions. Impact properties of ACCs are extremely important to find industrial applications e.g. in automobile structures, but these properties are difficult to quantify. Impact testing of materials is performed to determine the amount of energy that can be absorbed during a suddenly applied force. Impact testing is usually performed by Charpy or Izod test machines [6]. Charpy and Izod tests, originally designed to determine ductile–brittle transitions in metals, most often assume a pre-existing notch, which is not suitable for testing composite materials [13].

An alternative method is the drop-weight test, in which a known mass is dropped from a given height onto a flat, un-notched sample. The drop-weight test is a more realistic test of what a structural component would experience in its service life. Drop-weight tests have proven to be valuable source of information about the impact behaviour of woven composites [14], tape laminates [15], and sandwich structures [16]. However, the use of these tests on biocomposites has not received comparable attention in scientific literature. Only a recent work published by Huber and his co-workers [17] has studied the impact behaviour of ACC plates subjected to low-velocity impact produced by a drop-weight test.

The development of theoretical models to predict the impact behaviour of composites has shown to be useful tool to get a better understanding the failure modes and the energy absorption mechanisms [15, 16, 18, 19]. However, the modelling of ACCs structures is an almost unexplored field. This work is focussed on the development of the first numerical model to predict the low-velocity impact behaviour of ACC plates using finite element method (FEM). The numerical model was validated with experimental data published in [17]. Moreover, the FEM model was used to analyse the influence of impact energy on the peak force and absorbed energy during impact. The threshold energy that produced the striker penetration was also estimated.

6.2 Model description

A FEM model reproducing low-velocity impact tests on ACCs was developed using ABAQUS/Explicit code.

6.2.1 Material modelling

Two solids are involved in the impact test, striker and ACC plate. The striker was modelled using a linear elastic behaviour (E = 210 GPa, $\upsilon = 0.3$). The ACC plate was modelled using a modification of the Hashin failure criteria [20] implemented in a VUMAT user subroutine. The model was modified because Hashin criteria was developed for tape plies, while the ACC plates analysed in this work were manufactured from woven plies. These modifications for woven laminates were similar to those developed by Lopez-Puente et al. to modify Hou criteria for tape laminates [21].

Fibre failure. This damage criterion considers tensile and compressive fibre breakage in directions 1 and 2. Thus two different equations were used, Equation (1) for fibres at 0º and Equation (2) for fibres at 90º:

$$d_{f1} = \left(\frac{\sigma_{11}}{X_T}\right)^2 + \left(\frac{\tau_{12}}{S_f}\right)^2 \qquad (1)$$

$$d_{f2} = \left(\frac{\sigma_{22}}{Y_T}\right)^2 + \left(\frac{\tau_{12}}{S_f}\right)^2 \qquad (2)$$

where XT and TY are tensile strength in 1 and 2 directions respectively, and they have the same value for this material; Sf is the shear strength; σ_{11} and σ_{22} are the normal stress in directions 1 and 2; and τ_{12} the shear stress. When one of these damage variables equals one, all the stress components are set to zero.

Matrix failure was predicted using the next equation:

$$d_d = \left(\frac{\sigma_{33}}{Z_r}\right)^2 + \left(\frac{\tau_{13}}{S_f}\right)^2 + \left(\frac{\tau_{23}}{S_f}\right)^2 \qquad (3)$$

where Z_r is the interlaminar strength; and τ_{13} and τ_{23} are the corresponding out-of plane shear stresses. Equation (3) is applied only to out-of-plane tensile stresses ($\sigma_{33} > 0$). When this damage variable equals one, all the stress components that appear in the equation are set to zero.

To avoid sudden changes in the stiffness of the finite elements when damage occurs leading to instability problems and lack of convergence during the simulation, the stress components were corrected using a smooth transition, Equation (4).

$$\sigma_{ij}^{cor} = \sigma_{ij} \cdot \left(1 - \frac{2 - e^{s(d_i - 1/2)}}{2 - e^{s/2}}\right) \qquad (4)$$

where σ_{ij} and σ_{ij}^{cor} are the stress before and after the correction, di is the corresponding damage parameter, and s is the variable that controls the slope of the stress decay when the damage is close to 1. The value s = 30 was adopted according to [21].

Moreover, the simulation of the impact involves the perforation of the plate, thus a finite element erosion criterion is required. When damage occurs in an element, the stresses on it drop to zero and large deformations appear. A maximum strain criterion was adopted to remove the distorted elements: after each time increment the longitudinal strains (ε_1, ε_2 and ε_3) are calculated; if one of them reaches a critical value (ε_i= 1) the element is removed. Thus, erosion criterion only affects to elements that have been already degraded.

It should be noticed that this model is based on the assumption of the hypothesis of linear-elastic behaviour up to failure. Moreover, the mechanical behaviour of ACCs is considered strain rate independent. These hypotheses have been widely used in the modelling of carbon and glass fibre composite [15, 16, 18, 19]. However, more experimental works and impact tests are required to prove these hypotheses in biodegradable composite. Since this is the first attempt to model the impact behaviour of ACCs, these assumptions are provisionally considered to explore the model accuracy to reproduce the behaviour of ACC plates.

6.2.2 Geometry and boundary conditions

The geometry of the model reproduced the experimental tests reported in [17]. The plate consisted on a circular plate of diameter (D_p) 40mm and thickness (t_p) 2mm composed of five Cordenka layers. The striker was modelled as a hemispherical solid of diameter (D_s) 20mm with a mass of 9.54kg, as shown in Figure 6.1.

The ACC plate was made of Cordenka fibres using ionic liquid BimimAc as solvent. The mechanical properties of Cordenka ACC plates were reported by Huber´s research group in [17] and [22]. The density, elastic modulus, and tensile strength are 450 g/m2, 3.72 GPa, and 91.2 MPa respectively. The shear strength (Sf) was set in 52.65 Mpa using Equation (5) proposed by Bledzki et al. [6].

$$S_{12} = \frac{X_T}{\sqrt{3}} \qquad (5)$$

The external surface of the plate was clamped to reproduce the experimental tests boundary conditions. An initial velocity of 4.17m/s (v_{imp}) was imposed to the striker leading to impact energy of 83.71 J. Figure 6.1 shows the geometry and boundary condition.

Moreover, an interaction contact was defined between the striker surface and a node region that included all the plies of the plate. The interaction contact was modelled using the algorithm surface-node surface contact available in ABAQUS/Explicit.

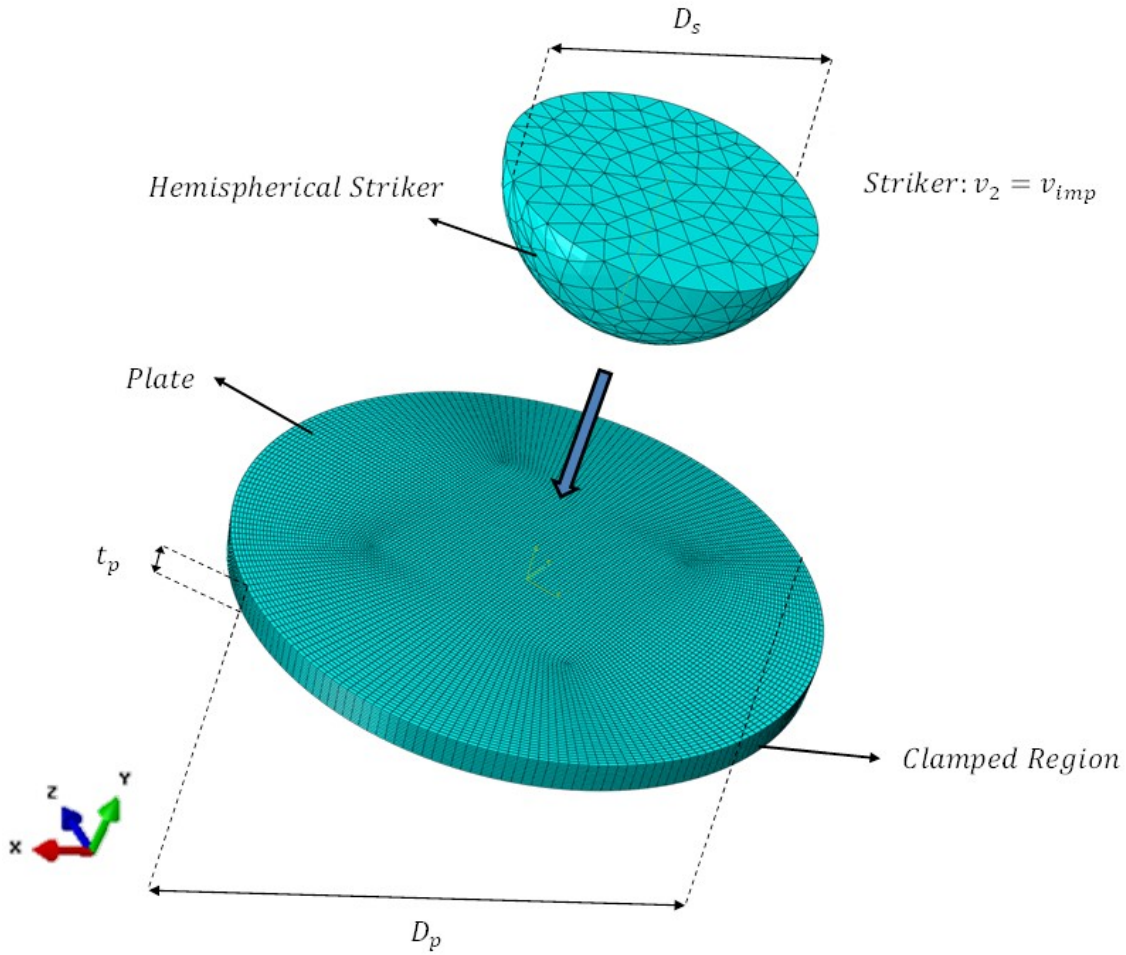

Figure 6.1. Finite element model. Geometry and boundary conditions.

6.2.3 Finite element mesh

The sensitivity of the mesh was analysed with successive space discretization. The selected mesh for the plate had 134784 linear brick elements, with reduced integration (C3D8R). The striker was modelled with 5890 quadratic tetrahedral elements (C3D10M). The three dimensional non-homogeneous mesh, with smaller elements in the contact area is shown in Figure 6.1.

6.3 Results and discussion

6.3.1 Model validation.

To validate the FEM model the numerical results were compared with the experimental data from [17] in terms of force-displacement curve and absorbed energy. Figure 6.2 shows the comparison between experimental and numerical force-displacement curves. An excellent agreement between numerical prediction and experimental data was found. The model showed an accurate prediction of stiffness, peak force and force drop after damage. The numerical and experimental peak forces were 3.87kN and 3.68kN respectively, with an error of 5.16%.

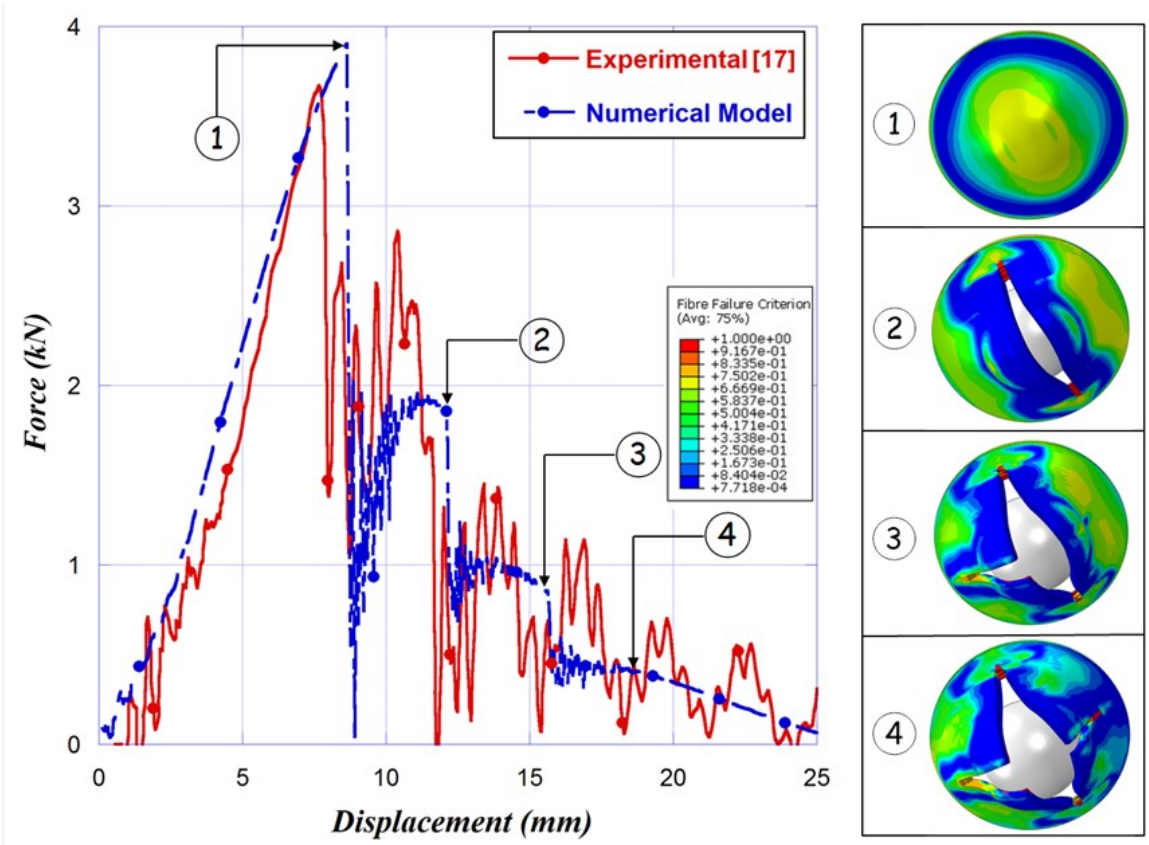

Figure 6.2. Force-displacement curve (numerical and experimental results) and damage evolution.

The force displacement curves were integrated to calculate the energy absorbed by the ACC plate during the impact process. The evolution of the absorbed energy is shown in Figure 6.3. The numerical model overestimated the absorbed energy but the evolution of the numerical predictions agreed with the experimental results. The total absorbed energy according to numerical and experimental results are 28.27 J and 26.04 J respectively, resulting in an error of 8.56%.

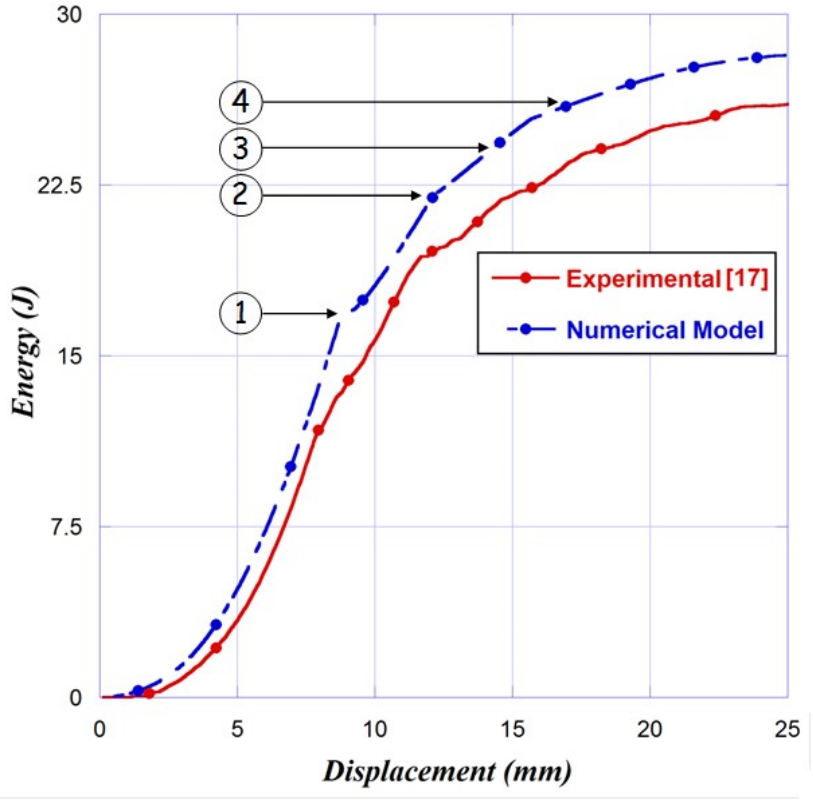

Figure 6.3. Absorbed energy versus striker displacement. Comparison between numerical and experimental results.

6.3.2 Damage mechanisms.

FE model results were used to analyse the damage mechanisms that produced the failure of the ACC plate. The deformed shape of the plate at some relevant points of the force-displacement curve is shown in Figure 6.2. The main failure criterion according to the simulations was fibre breakage in agreement with the results reported in [17], thus Figure 6.2 represents the field of the fibre failure criterion.

The first point corresponds to the previous moment to the force drop, the failure criterion is lower than one in all the elements thus no damage was found in the plate. The second point, after the first force drop, shows the first crack propagation produced by fibre failure due to tensile stresses. The third point, after the second force drop, shows a second crack in perpendicular direction. Finally, the fourth point corresponds to a point after the third force drop. At this point, a new crack appears leading to the pyramidal shape failure observed in the experimental tests [17]. These results show that the progressive failure of the ACC plate is a consequence of the consecutive cracks that are propagated during striker penetration. The FEM model was able to reproduce force history and damage mode observed in experimental tests.

6.3.3 Influence of impact energy

In addition, the validated FEM model was applied to analyse the influence of impact energy. The initial impact velocity of the striker was modified to study the behaviour of the ACC plate under impact energies from 0 to 83.71 J. Figure 6.4 shows the evolution of peak force and absorbed energy with the impact energy. Three stages can be observed in this curve.

The first stage corresponds to impact energy from 0 to 1.2 J. The behaviour of the plate was elastic thus the absorbed energy was zero. The peak force increased linear with impact energy. No damage was observed in the plates.

In the second stage, for impact energy from 2 J to 30 J, the value of the absorbed energy increased with increasing impact energies. In these impacts the plate was damaged but not penetrated by striker. On the other hand, the value of the peak force increased for impact energy from 2 J to 19 J. A crack was observed in the ACC plate for impact energies higher than 19 J, see Figure 6.5b, thus the peak force was stabilised at a value around 3800 N. The residual velocity of the striker for impact energy equal to 30 J was zero, thus 30 J was estimated as the impact energy perforation threshold.

In the third stage, impact energies higher than 30 J, the plate was perforated, Figures 6.5c-d. The absorbed energy was almost constant because the impact energy was higher than the energy absorbing capability of the ACC plate. Failure mode observed corresponded to fibre breakage and subsequent crack propagation in principal directions leading to a four-petal pyramid shape.

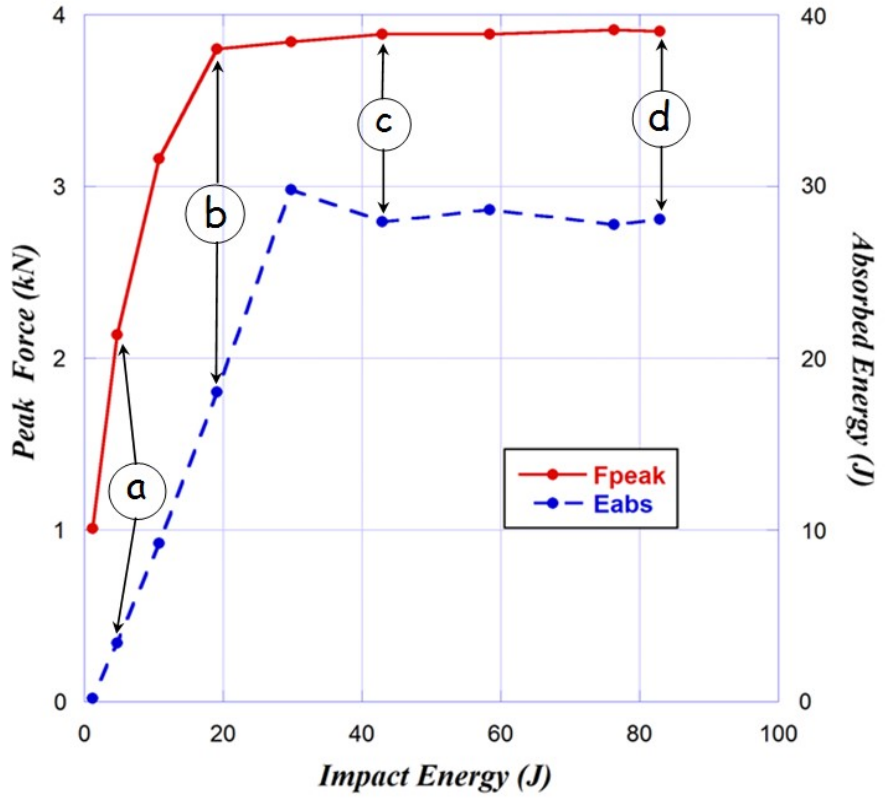

Figure 6.4. Peak force and absorbed energy versus impact energy. Numerical results.

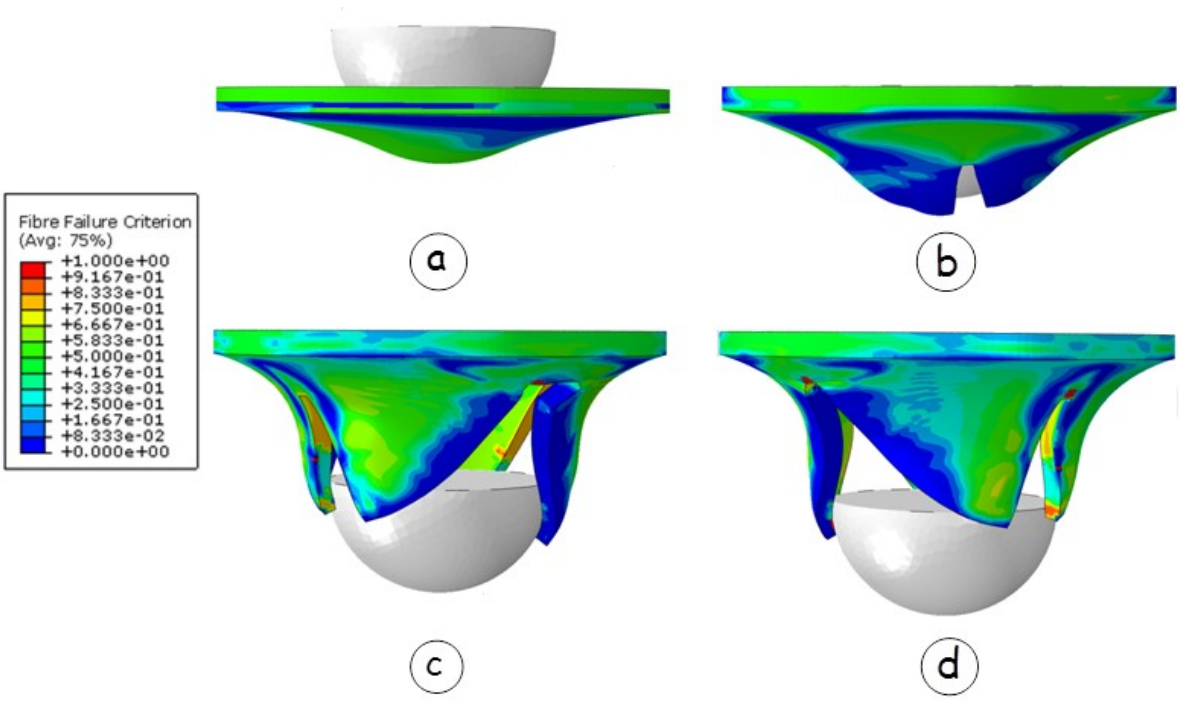

Figure 6.5. Failure modes under different impact energies. A) impact energy 4.77 J. b) impact energy 19.08 J: . c) impact energy 42.93 J. d) impact energy 83.71 J

6.4 Conclusions

A finite element numerical model to predict the behaviour of ACC plates under low-velocity impacts was presented for the first time. The model was validated through comparison with experimental results. Force-displacement curve, absorbed energy and failure modes predicted by the model were in agreement with experimental data. The results showed that the progressive failure of the ACC plate is a consequence of the consecutive cracks that appear during the striker penetration. The main failure mode was fibre breakage due to tensile stresses. Moreover, the influence of impact energy was analysed finding the impact energy threshold that produce the striker penetration.

The model presented in this work is the first step in the development of numerical models to predict the impact behaviour of biodegradable composite plates. Some of the model hypotheses, such as linear-elastic behaviour up to failure and strain-rate independence, should be analysed in future works. The promising results obtained with this model can be useful in the development of predictive tools to provide new application for biodegradable composite materials.

References

[1] Faruk O, Bledzki AK, Fink HP, Sain M. Biocomposites reinforced with natural fibers: 2000–2010. Progress in Polymer Science 2012;37(11):1552– 1596.

[2] Akil HM, Omar MF, Mazuki AAM, Safiee S, Ishak ZAM, Abu Bakar A. Kenaf fiber reinforced composites: A review. Mater Des 2011;32(8-9):4107–4121.

[3] Koronis G, Silva A, Fontul M. Green composites: A review of adequate materials for automotive applications. Compos Part B: Eng 2013;44(1):120–127.

[4] Tawakkal ISMA, Talib RA, Abdan K, Ling CN. Mechanical and physical properties of Kenaf-derived Cellulose (KDC)-filled polylactic acid (PLA) composites. Bioresources 2012;7(2):1643-4655.

[5] Xiao-Yun W, Qiu-Hong W, Gu H. Research on Mechanical Behaviors of the Flax/Polyactic Acid Composites . Journal of Reinforced Plastics and Composites 2010;29(17):2561-2567.

[6] Bledzki AK, Jaszkiewicz A. Mechanical performance of biocomposites based on PLA and PHBV reinforced with natural fibres – A comparative study to PP. Compos Sci Technol 2010;70(12):1687-1696.

[7] George J, Sreekala MS, Thomas S. A review on interface modification and characterization of natural fiber reinforced plastic composites. Polym Eng Sci. 2001;41(9):1471–85.

[8] Gindl-Altmutter W, Keckes J, Plackner J, Liebner F, Englund K, Laborie MP. All-cellulose composites prepared from flax and lyocell fibres compared to epoxy–matrix composites. Compos Sci Technol 2012(11);72:1304–1309.

[9] Nishino T, Arimoto N. All-Cellulose Composite Prepared by Selective Dissolving of Fiber Surface. Biomacromolecules 2007;8(9):2712-2716.

[10] Song YS, Lee JT, Ji DS, Kim MW, Lee SH, Youn JR. Viscoelastic and thermal behavior of woven hemp fiber reinforced poly(lactic acid) Composites. Compos Part B: Eng 2012;43:856–860.

[11] Soykeabkaew N, Arimoto N, Nishino T, Peijs T. All-cellulose composites by surface selective dissolution of aligned ligno-cellulosic fibres. Compos Sci Technol 2008;68(10-11):2201–2207.

[12] Huber T, Müssig J, Curnow O, Pang S, Bickerton S, Staiger MP. A critical review of all-cellulose composites. J Mater Sci 2012;47(3):1171–1186.

[13] Ku H, Cheng YM, Snook C, Baddeley D. Drop weight impact test fracture of vinyl ester composites: micrographs of pilot study. J Compos Mater 2005;39(18):1607-1620.

[14] Santiuste C, Sanchez-Saez S, Barbero E. Residual flexural strength after low-velocity impact in glass/polyester composite beams. Compos Struct 2010;92(1):25-30.

[15] Santiuste C, Sanchez-Saez S, Barbero E. A comparison of progressive-failure criteria in the prediction of the dynamic bending failure of composite laminated beams. Compos Struct 2010;92(10):2406-2414.

[16] Ivañez I, Santiuste C, Sanchez-Saez S. FEM analysis of dynamic flexural behavior of composite sandwich beams with foam core. Compos Struct 2010;92(9):2285-2291.

[17] Huber T, Bickerton S, Müssig J, Pang S, Staiger MP. Flexural and impact properties of all-cellulose composite laminates. Compos Sci Technol 2013;88:92–98.

[18] Buitrago BL, Santiuste C, Sánchez-Sáez S, Barbero E, Navarro C. Modelling of composite sandwich structures with honeycomb core subjected to high-velocity impact. Compos Struct 2010;92(9):2090-2096.

[19] Santiuste C, Díaz-Álvarez J, Soldani X, Miguélez H. Modelling thermal effects in machining of carbon fiber reinforced polymer composites. Journal of Reinforced Plastics and Composites 2014;33(8):758-766.

[20] Hashin Z. Failure criteria for unidirectional fiber composites. Trans ASME J Appl Mech 1980;47(2):329–34.

[21] Lopez-Puente J, Zaera R, Navarro C. An analytical model for high velocity impacts on CFRPS woven laminates. Int Solids Struct 2007;44:2837-57.

[22] Huber T, Bickerton S, Müssig J, Pang S, Staiger MP. Solvent infusion processing of all-cellulose composite materials. Carbohyd Polym 2012;90(1):730–733.

Chapter 7

Low velocity impact behaviour of biocomposites: Numerical model considering strain rate dependent properties

The mechanical behaviour of conventional composites is usually assumed as linear-elastic up to failure. However, natural fibres based composites are characterized by viscoplastic behaviour. This study presents the first FEM model that includes the plastic behaviour and the influence of strain rate to predict the impact behaviour of natural fibres based composites. The model was validated through comparison with low-velocity impact tests. Numerical predictions were in agreement with experimental results conducted with two impactor nose at different impact energies.

7.1 Introduction

During the last years, natural fibres have been introduced as reinforcements in order to develop biodegradable composites [1,2,3]. In terms of matrices, non-biodegradable polymeric materials (such as epoxy, polyethylene or polypropylene) are typically used with natural fibres [4]. However, biodegradable matrices (such as polysaccharides, proteins, polyesters, lignin, lipids, etc.) can also be used to obtain 100 % eco-sustainable composites [4-6]. The introduction of fully biodegradable composites reduces the use of non-biodegradable materials and non-renewable resources. The main advantages of biocomposites are their low cost, lightweight and less energy consumption for their production. Biodegradable composites are applied in different industrial applications and engineering fields such as packaging, biotechnology, automotive industry or environmental technology, offering significant advantages in terms of environmental impact, cost and weight [4,7-9].

One of the most relevant drawbacks of traditional composites is their sensitivity under low-velocity impacts [10]. Therefore, there are numerous studies about the low-velocity impact behaviour of traditional composites. The development of predictive FEM models has been used to get a better understanding of the impact behaviour of composites [11-14]. For instance, Antonucci et al. [11] used cohesive elements to predict delamination evolution on carbon fibres composites under multiple low-velocity impact tests. Ivañez et al. [12] studied the low-velocity impact behaviour on sandwich beam. The FEM model results were used to explain the influence of foam core on induced damage during impact. The behaviour of traditional composites reinforced with carbon or glass fibres can be usually assumed as linear elastic up to failure, and the main objective

in the development of predictive FEM models is the implementation of accurate failure criteria and the prediction of absorbed energy [14].

However, very few studies analysed the behaviour of biodegradable composites under low-velocity impacts, being most of them experimental [15,16]. Huber et al. [15] studied the behaviour of all-cellulose composites (ACCs) made from Cordenka fibres under low-velocity impact produced by a drop weight test, founding that ACC laminates exceed the impact properties of most conventional composites. Dhakal and his co-workers [16] have investigated the fibre weave architecture effect on the low-velocity impact response of jute fibre reinforced methacrylated soybean oil composite, founding that woven laminates possess better toughness properties.

The promising results of these few studies means that biodegradable composites can be competitive in terms of strength under low-velocity impacts. However, the development of numerical models to predict the impact behaviour of biodegradable composites is an almost unexplored field. The first numerical model was presented by Rubio-López et al. [17] to predict the low velocity behaviour of ACC composite plates using a FEM model. This model was based on the traditional composites hypotheses: linear-elastic behaviour up to failure and strain rate independent behaviour [12, 14].

On the other hand, different studies have proved the strong influence of the strain-rate on the behaviour of the biocomposites and their non-linear behaviour [17-19]. Therefore, traditional composite models assuming linear-elastic behaviour up-to-failure can be implemented in biocomposites only as a first approach.

This paper presents the first FEM model for biodegradable composites considering viscoplastic behaviour. The non-linear mechanical behaviour of the composites is defined as a function of the strain-rate and failure criterion based on maximum strains included to delete damaged elements. FEM model was implemented in ABAQUS/Explicit software. The results are validated through the comparison with experimental tests conducted on a drop-weight tower with different impactor nose hemispherical sizes and different impact energies. Biodegradable composite plates were manufactured from flax woven fibres and poly-lactic acid (PLA) matrix.

7.2 Experimental Set-up

Flax woven fibres were combined with PLA matrix to manufacture the specimens. PLA 10361D was acquired from Natureworks LLC, and it is defined as a biodegradable thermoplastic resin specifically aimed as a natural fibre binder. Fibres and matrix properties were studied in a previous work [20]. Biocomposites were produced by compression moulding process. First, five PLA layers and four woven fibres plies were alternatively stacked, then the laminate was place between two thermoheated plates, and pressure was applied by a universal testing machine. An optimization of the manufacturing process was performed as reported in [20], revealing that the optimum manufacturing parameters are obtained with plates at 185ºC initial temperature, applying 8-16 MPa of pressure during 3 minutes after 2 minutes of preheating time. The fibre weight ratio was stated in 65% as studied by Ochi et al. [21]. A resulting thickness of 2.64±0.11 mm were obtained. The specimens were cut into square plates of 80x80 mm.

Woven fibres and PLA plies were maintained in an oven under 95ºC during 30 minutes before the compression moulding processing to remove water content. All the materials were stored in stable constant conditions of 46% RH and 20ºC before and after the manufacturing process to control the environmental conditions influence.

A CEAST Fractovis 6875 drop weight tower was used to carry out the experimental low-velocity impact tests. The specimens were clamped at the outer region, leaving a circular area of diameter equal to 55 mm. The drop-weight tests were carried out by using an impactor with hemispherical noses of 12.7 mm and 20 mm. The impactor weights were 3.76 kg and 3.815 kg. Impact energy was modified from 3.7 J to 10 J to verify the model capacity to reproduce different damage sizes. The maximum value of impact energy was below the penetration energy, so that all the specimen was damaged but not penetrated. This range of impact energies was selected because this is the critical impact in traditional composites, low-velocity impacts that produce a barely visible damage but leading to a significant reduction in residual strength.

7.3 Model description

7.3.1 Material Model

Two solids are modelled for the impact test: the impactor and the composite plate. The impactor was modelled using a linear elastic behaviour (E=210 GPa, nu = 0.3). since no permanent deformation after impact were found.

Composite material model considers both plastic behaviour and influence of strain rate. Stress-strain curves published in a previous work [18] were used to reproduce the influence of strain rate. Figure 7.1 shows the stress-strain curves obtained at strain rates from 2.08e-4 to 8.33e-3 s^{-1}, where significant influence of strain rate can be observed. Stiffness and strength of biocomposites increase with strain rate, while ultimate strain decreases. The mechanical behaviour is clearly non-linear.

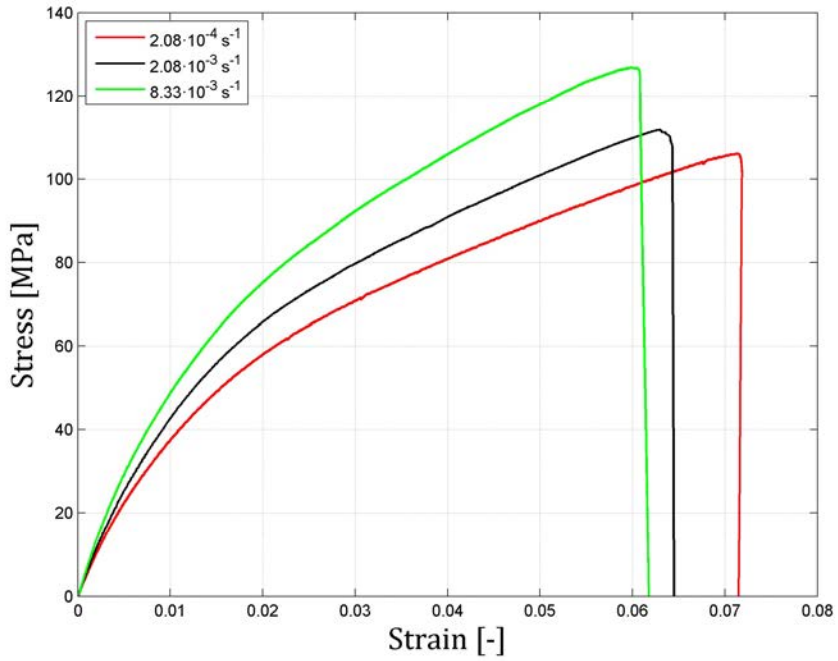

Figure 7.1. Stress-strain curves obtained experimentally under different strain rates: $2.08 \cdot 10^{-4}$ s^{-1}, $2.08 \cdot 10^{-3}$ s^{-1} and $8.33 \cdot 10^{-3}$ s^{-1} [17].

The elastic behaviour was considered strain-rate independent with a Young modulus of 5GPa. Once yield stress was reached, the plastic behaviour was determined as a function of strain rate following the corresponding stress-strain curve. An interpolation was conducted for values of strain rate different to those obtained in experimental tests. Yield stress was also defined as a function of strain rate. For instance, yield stress was equal to 23 MPa for a strain rate of 2.08e-4 s^{-1} and equal to 47.1 MPa for a strain rate of 8.33e-3 s^{-1}. Thus, a non-linear plastic behaviour considering plastic strain and strain rate dependent behaviour was implemented.

Finally, an erosion criterion was included to delete damage elements considering the influence of strain rate on the ultimate strain observed in experimental tests. A VUSDFLD user subroutine developed in ABAQUS/Explicit used to define a maximum strain criterion. This criterion allows the removal of the elements that presents strains higher than the maximum defined as a function of strain rates.

Cohesive elements were not included to predict de-bonding between plies because delamination were not observed in experimental tests. Thus, perfect bonding between plies was considered.

7.3.2 Geometry and Mesh

The geometry of the model reproduces the experimental drop-weight tests described in the previous section. The composite consisted on a circular plate of diameter (D_p) 55 mm and thickness (t_p) 2.55 mm. Two different impactors had been used to model the impactor bar. For simplicity, only the hemispherical nose of the impactors was modelled in the simulation. They were modelled as a hemispherical solid of two different diameters ($D_{s_{12.7mm}}$) 12.7mm and ($D_{s_{20mm}}$) 20mm with a mass of 3.7 and 3.815 kg, respectively, as shown in Figure 7.2.

The external surface of the plate was clamped in order to reproduce the experimental drop-weight tests boundary condition. Different initial velocities were imposed to the striker leading to different impact energies.

Moreover, an interaction contact was defined between the impactor surface and the node region of the plate to consider the contact of the impactor surface with all the composite plies. The interaction was modelled using the algorithm surface-node surface contact available in ABAQUS/Explicit.

A mesh sensitivity study was conducted to analyse the influence of mesh size. The selected mesh for the plate had 172,860 linear brick elements, with reduced integration (C3D8R). The strikers were also modelled with 2340 and 9680 brick elements (C3D8R) for the cases of 12 mm and 20 mm of diameter, respectively.

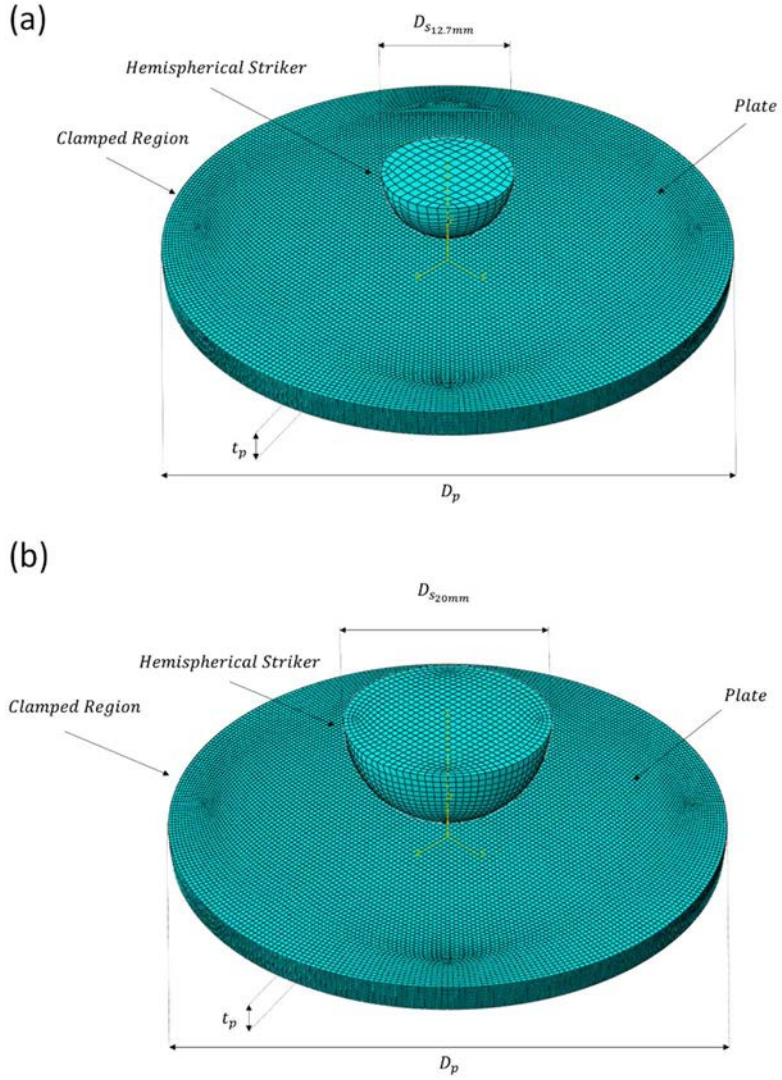

Figure 7.2. Mesh and geometry of the FEM models. a) Impactor nose with ϕ12.7 mm. b) Impactor nose with ϕ 20 mm.

7.4 Results and discussion

Numerical results were validated through comparison with experimental data obtained in drop-weight tests. Figure 7.3 shows the comparison between the experimental and numerical results in terms of contact force history with impactor nose of ϕ 12.7 mm. There is an excellent agreement between numerical and experimental curves. The evolution contact force was similar for all the impact energies. First, the impact force increased because of the contact between the impactor and the plate up to the damage onset. Then, there is a plateau while damage is progressing in the composite plate. Finally, contact force decreases up to zero as the impactor moved backwards and the plate region that was affected recovered its initial position. FEM model was able to reproduce all the stages with a reasonable accuracy.

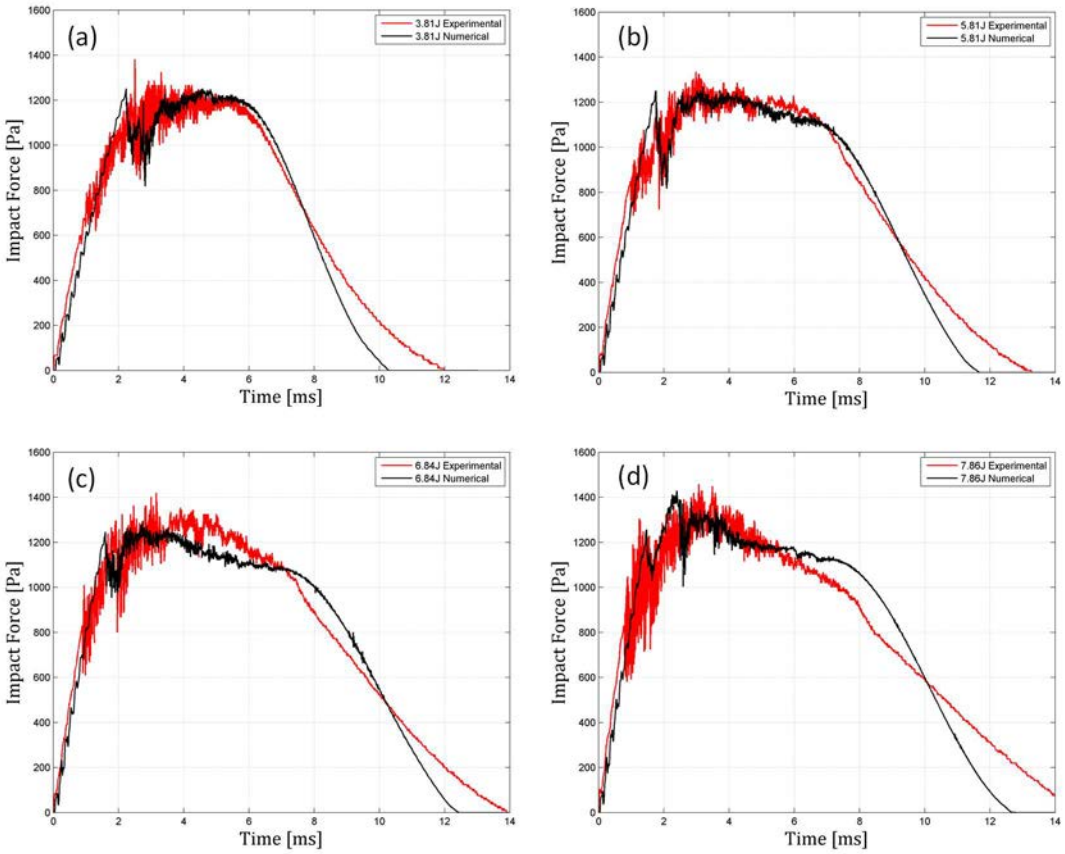

Figure 7.3. Contact force history for different impact energies. Impactor nose with ϕ 12.7 mm.

Figure 7.3 only shows the results with the impactor nose of ϕ 12.7 mm, the results with the impactor nose of ϕ 20 mm were similar. The values of peak forces for both diameters as a function of impact energy are represented in Figure 7.4. A good correlation between the experimental and numerical results were obtained. There are some discrepancies that can be attributed to the noise of experimental data. For instance, Figure 7.3c shows a good agreement between numerical and experimental contact forces, however in Figure 7.4 a difference of about 150 N in peak force can be observed due to the noise of experimental curve. This noise in experimental curves is attributed to the eigen-frequencies of the impactor, the simplified impactor geometry of the FEM model cannot reproduce this high-frequency vibrations [14].

The values of impact energies and peak forces are higher with the impactor nose of ϕ 20 mm. The force is distributed in a wider area thus a higher contact force is applied before damage initiation. Due to this phenomenon, higher values of impact energy can be applied before penetration.

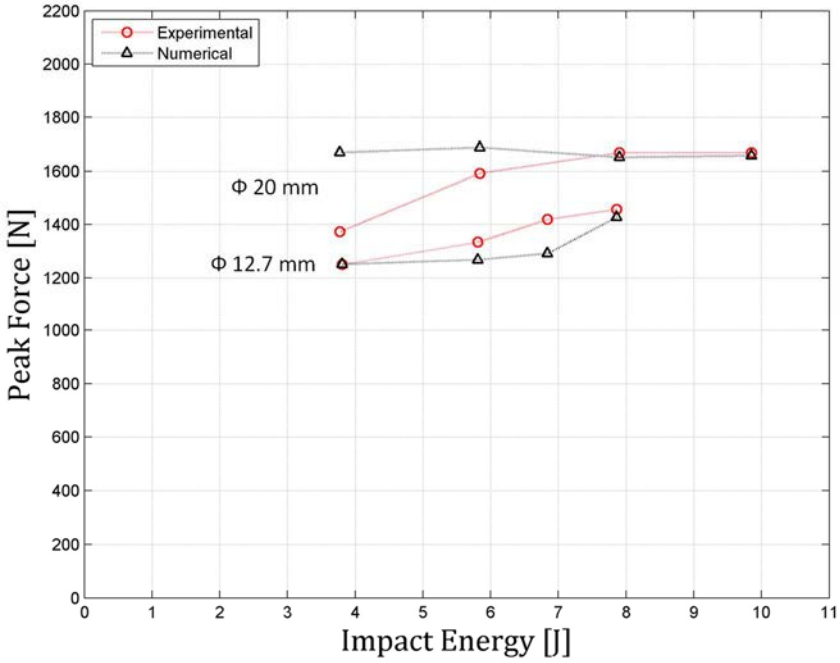

Figure 7.4. Peak force as a function of impact energy. Numerical predictions and experimental data.

In terms of absorbed energy evolution, see Figure 7.5, the numerical predictions agreed with the experimental results. The evolution of absorbed energy follows the well-known trend in low-velocity impacts. During the first stage, absorbed energy increases up to the value of impact energy. At this point, all the kinetic energy is absorbed by the composite plate and the impactor velocity is zero. Then, the absorbed energy decreases while impactor is bouncing back and, finally, the value of absorbed energy is constant after the separation of composite plate and impactor. The difference between the absorbed energy and the impact energy is the elastic energy that is converted again in the kinetic energy transferred to the impactor. FEM model reproduced accurately all these stages in absorbed energy evolution.

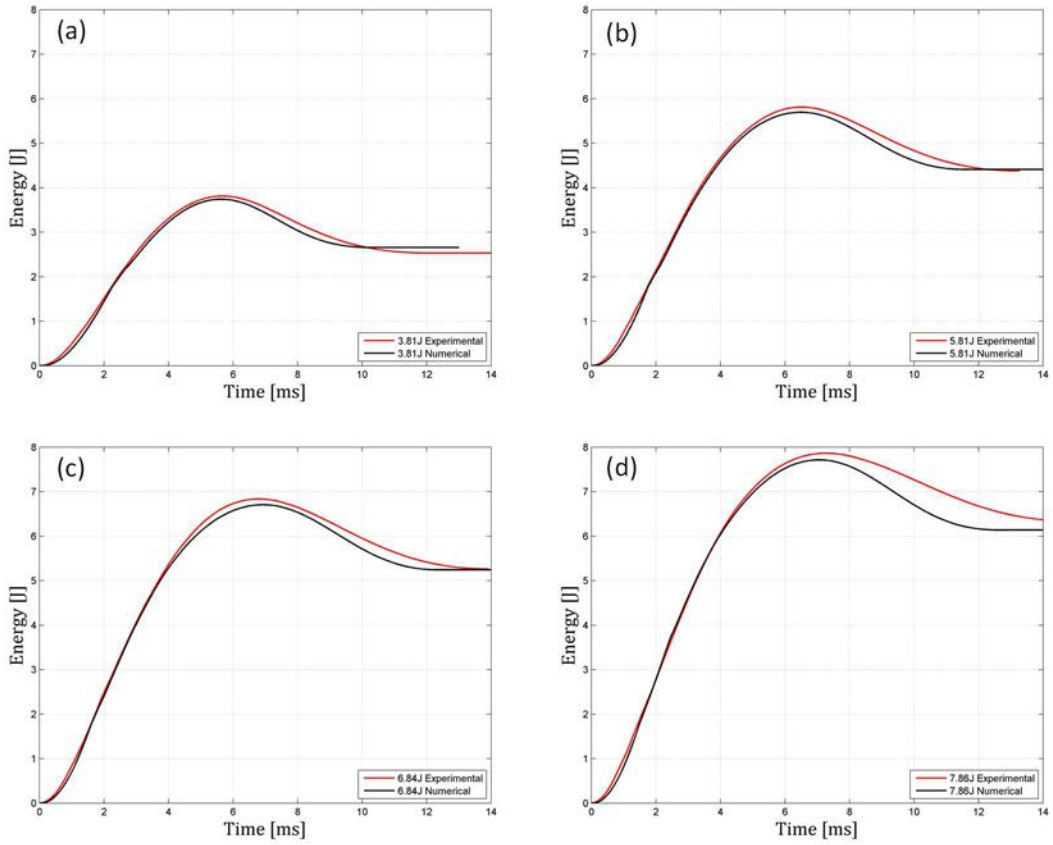

Figure 7.5. Evolution of absorbed energy for different impact energies. Impactor nose with ϕ 12.7 mm.

The results for impactor nose with ϕ 20 mm were similar to those shown in Figure 7.5 for ϕ 12.7 mm. The evolution of absorbed energy with impact energy is represented in Figure 7.6 for both impactors. Again, an excellent agreement was obtained when the experimental and numerical result were compared. An almost linear increment of absorbed energy with impact energy was observed. When comparing different impactor noses at the same impact energy, there is a clear difference in contact force but the absorbed energy is almost identical. The main difference is that the impactor with higher diameter can be subjected to a higher impact energy before penetration.

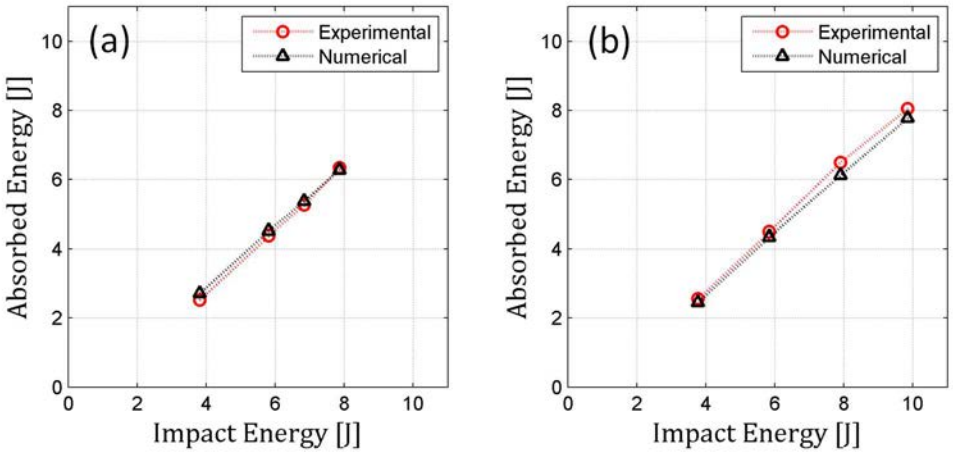

Figure 7.6. Absorbed energy as a function of impact energy. Numerical predictions and experimental data for a) impactor nose with ϕ 12.7 mm and b) impactor nose with ϕ 20 mm.

Not only global variables as contact force or absorbed energy were reproduced by FEM numerical model but also failure mode. When traditional composites are subjected to an impact energy lower than penetration energy the main failure modes are delamination and matrix cracking. However, damage modes in natural based composites are quite different, the main failure mode in the impacted specimens was fibre failure as was reported by Huber et al [15] on Cordenka fibres based composites. C-Scan ultrasonic inspection was used to analyse internal damage but no delamination was found in any impacted specimen. The failure mode was the formation of four petals due to two perpendicular cracks in a cross shape, see Figure 7.7, similar to that reported in [15]. The FEM model reproduced accurately the formation of the two perpendicular cracks and the petals. The cracks also grew along the fibres directions and the cracks length was similar to those found in experimental tests.

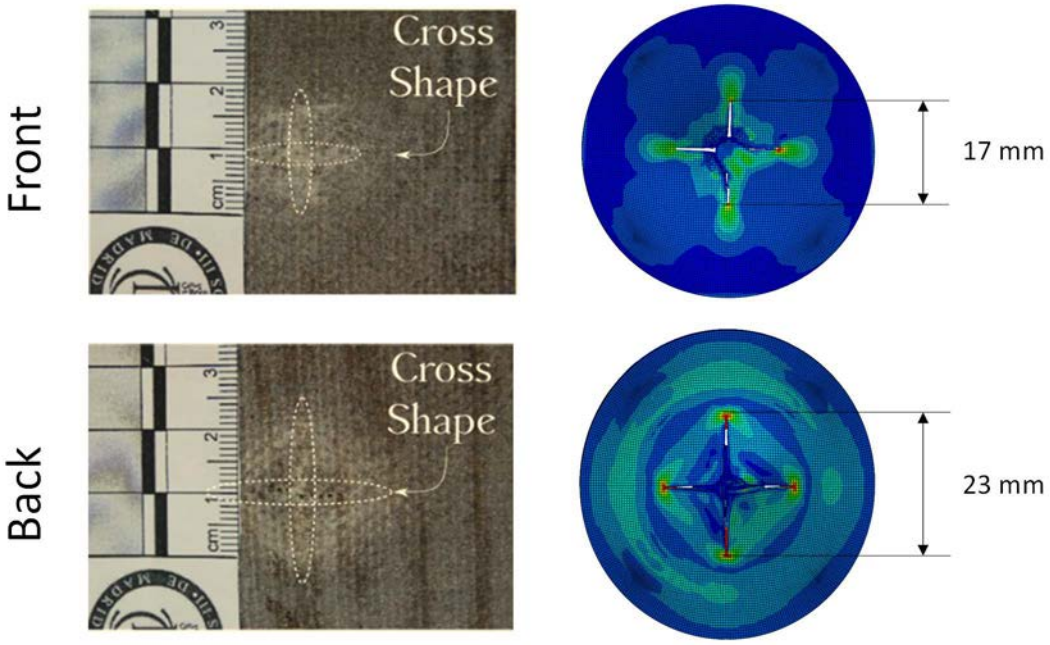

Fig. 7. Cross shape failure mode with an impact energy of 7.86 J and impactor nose of ϕ 12.7 mm. Experimental specimens and FEM model.

Since no delamination was observed in the impacted specimens, experimental values of damaged area were defined using the permanent deflection. The damaged area was defined as the points with a permanent deflection higher than 1mm. This area was assumed elliptical, so that two perpendicular axes were measured to calculate damaged area. The permanent deflection in the impacted face was measured by means of a laser extensometer MEL M27L/50. The laser was attached to an automatic positioning system to measure not only the maximum permanent deflection, but also the deflection along a path in the specimen. The damaged area in FEM results was also assumed elliptical. The lengths of the two cracks were used as the axes of the elliptical damaged area.

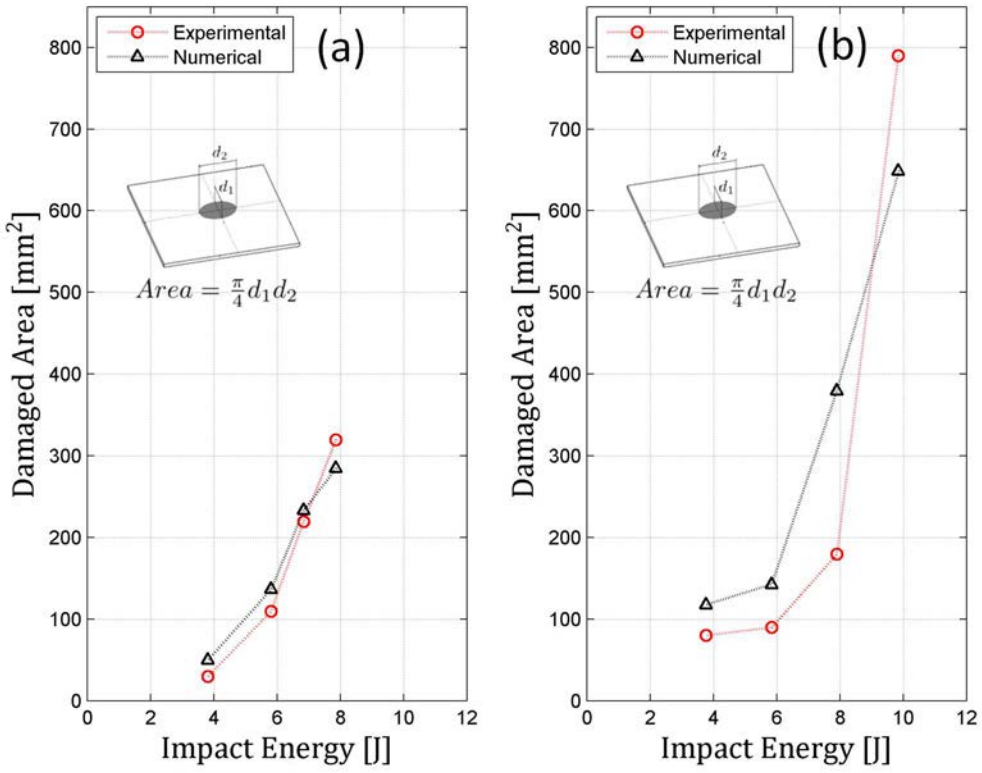

Figure 7.8. Damaged area as a function of impact energy. Numerical predictions and experimental data for a) impactor nose with ϕ 12.7 mm and b) impactor nose with ϕ 20 mm.

The evolution of the damaged area with impact energy for both impactor noses is shown in Figure 7.8. For both impactor noses damaged area increases with impact energy and the slope of the curves also increases with impact energy. Damaged areas are higher with the impactor nose of higher diameter as expected due to higher values of contact forces.

Numerical results are in a reasonable agreement with experimental data, the FEM model reproduced the trends observed experimentally. However, numerical results overestimated damaged area for lower impact energies and underestimated it for impact energy near to penetration energy. These differences can be neglected in the case of the impactor nose with ϕ 12.7 mm, but they are significant in the case of ϕ 20 mm. These differences can be attributed to the greater extension of damage with the impactor nose with ϕ 20 mm and the influence of boundary conditions. The composite plate was clamped between two steel rings leaving a free circular surface with a diameter of 55 mm. For sake of simplicity, only the free surface of the composite plate was modelled, considering that the external surface was perfectly clamped. This simplified hypothesis has been proved to be valid to analyse contact forces, absorbed energy and failure modes for both impactor noses but the estimation of damaged area is more sensible to boundary conditions.

7.5 Conclusions

The first FEM model for biodegradable composites considering viscoplastic behaviour has been developed and validated. The FEM model considers non-linear mechanical behaviour as a function of strain-rate and failure criterion based on maximum strains to delete damaged elements.

The results were validated through comparison with experimental tests conducted on a drop-weight tower with different impact energies and two impactor nose hemispherical sizes. Numerical predictions were in excellent agreement with experimental in terms of force history, evolution of absorbed energy and failure modes for all the impact energies analysed and both impactor noses. Only significant differences were found in the prediction of damage area with the impactor nose of ϕ 20mm at higher impact energies. These discrepancies can be attributed to the influence of boundary conditions when the extension of damage is near the plate edges.

The main contributions of the model are based on the differences between conventional composites and natural fibres based composites. Conventional composites can be considered linear-elastic up to failure and the influence of strain-rate is usually neglected. However, experimental tests conducted by different authors have shown the need to consider plastic behaviour and the influence of strain rate to predict the dynamic behaviour of biocomposites. The present work is the first attempt to include viscoplastic behaviour in a predictive FEM model. The accuracy of the results can open a promising line of research that can lead to a new generation of FEM models for natural fibres based composites. The introduction of biodegradable composites in industry can be benefit from the development of predictive tools.

References

[1] La Mantia FP, Morreale M. Green composites: a brief review. Compos Part A: Appl Sci Manuf 2011; 42: 579–88

[2] Lebrun G, Couture A, Laperriere L. Tensile and impregnation behavior of unidirectional hemp/paper/epoxy and flax/paper/epoxy composites. Compos Struct 2013;103: 151-60.

[3] Conzatti L, Giunco F, Stagnaro P, Capobianco M, Castellano M, Marsano E. Polyester-based biocomposites containing wool fibres. Compos Part A: Appl Sci Manuf 2012; 43: 1113-9

[4] Netravali AN, Chabba S. Composites get greener. Mater Today 2003;6(4): 22-9

[5] Song YS, Lee JT, Ji DS, Kim MW, Lee SH, Youn JR. Viscoelastic and thermal behavior of woven hemp fiber reinforced poly(lactic acid) composites. Compos Part B 2012; 43: 856-60.

[6] Bax B, Müssig J. Impact and tensile properties of PLA/Cordenka and PLA/flax composites. Compos Sci Technol 2008; 68(7): 1601–7

[7] Gurunathan T, Mohanty S, Nayak SK. A review of the recent developments in biocomposites based on natural fibres and their application perspectives. Compos Part A: Appl Sci Manuf 2015: 1-25

[8] Koronis G, Silva A, Fontul M. Green composites: a review of adequate materials for automotive applications. Compos Part B: Eng 2013; 44(1): 120–7.

[9] Jayakumar R, Menon D, Manzoor K, Nair SV, Tamura H. Biomedical applications of chitin and chitosan based nanomaterials—A short review. Carbohydr Polym, 2010; 82(2): 227–32.

[10] Santiuste C, Sanchez-Saez S, Barbero E. Residual flexural strength after low-velocity impact in glass/polyester composite beams. Compos Struct 2010; 92: 25-30

[11] Antonucci V, Caputo F, Ferraro P, Langella A, Lopresto V, Pagliarulo V, Ricciardi MR, Riccio A, Toscano C. Low velocity impact response of carbon fiber laminates fabricated by pulsed infusión: A review of damage investigation and semi-empirical models validation. Prog Aerosp Sci 2015; 81: 26-40

[12] Ivañez I, Santiuste C, Sanchez-Saez S. FEM analysis of dynamic flexural behaviour of composite sandwich beams with foam core. Compos Struct 2010; 92(9): 2285–91.

[13] Tan W, Falzon BG, Chiu LNS, Price M. Predicting low velocity impact damage and Compression-After-Impact (CAI) behaviour of composite laminates. Compos A Appl Sci Manuf 2015; 7: 212–26.

[14] Santiuste C, Sanchez-Saez S, Barbero E. A comparison of progressive-failure criteria in the prediction of the dynamic bending failure of composite laminated beams. Compos Struct 2010; 92(10): 2406–14.

[15] Huber T, Bickerton S, Müssig J, Pang S, Staiger MP. Flexural and impact properties of all-cellulose

composite laminates. Compos Sci Technol 2013; 88: 92–8.

[16] Dhakal HN, Skrifvars M, Adekunle A, Zhang ZY. Falling weight impact response of jute/methacrylated soybean oil bio-composites under low velocity impact loading. Compos Sci Technol 2014; 92: 134–41.

[17] Rubio-López A, Olmedo A, Santiuste C. Modelling impact behavior of allcellulose composite plates. Comp Struct 2015; 122: 139–43

[18] Rubio-López A, Hoang T, Santiuste C. Constitutive model to predict the viscoplastic behaviour of natural fibres based composites. Compos Struct 2016; 155: 8-18

[19] Poilâne C., Cherif ZE, Richard F, Vivet A, Doudou, BB, Chen J. Polymer reinforced by flax fibres as a viscoelastoplastic material. Compos Struct 2014; 112(1):100–12

[20] Rubio-López A, Olmedo A, Díaz-Álvarez A, Santiuste C. Manufacture of compression moulded PLA based biocomposites: a parametric study. Compos Struct 2015;131:995–1000

[21] Ochi S. Mechanical properties of kenaf fibers and kenaf/PLA composites. Mech mater 2008; 40(4): 446-52.

Chapter 8

Induced damage during drilling: Experimental study

Biodegradable composites are promising materials because of their acceptable mechanical properties and sustainable nature. Biocomposites are vulnerable to the generation of machining induced damage due to the nature of fibres and matrix. This paper focuses on the analysis of drilling induced damage on biocomposite (woven fibres of cotton, flax and jute combined with PLA as matrix). Contrarily to the behaviour commonly observed when drilling conventional composites, delamination was negligible. Entry and exit damage, quantified in terms of fraying extension were analysed demonstrating that the combination between cotton fibre and small drill angle showed the lowest level of damage. Composite reinforced with flax fibres showed the highest tensile strength and also the greatest damage extension, increasing with the number of layers of the composite. Concerning to the influence of cutting parameters, damage decreased when increasing cutting speed and feed rate. One of the main contribution of this chapter is the development of the first analysis of cutting parameter on fully biodegradable composites avoiding oil based polymeric matrices. These results can be used to optimize the production of components made of biodegradable composites.

8.1 Introduction

Composite components are usually made near net shape, however machining processes are usually needed to achieve dimensional tolerance and assembly requirements. Drilling is a common operation required for further mechanical joining of the components [1]. A significant percentage of the component rejection in composite manufacturing is due to damage induced during drilling, thus the optimization of drilling parameters can lead to a cleaner production of composites. Induced damage is one of the undesired effects of machining due to the use of inadequate cutting parameters or worn drill and has received extensive attention in the literature [2]. There are numerous studies focused on induced damage during machining of carbon and glass fibre composites [2-7]. According to these studies, induced damage during drilling of composite is mainly influenced by cutting parameters and drill geometry, including geometrical variations due to wear progression. Delamination is the main damage mechanism, and feed rate seems to be the most influencing factor in delamination (increasing with this parameter) in the case of CFRPs. The effect of cutting speed is not clear and seems to have a cross effect with thickness and spindle speed. Davim et al. [8] showed that delamination increased with cutting speed during conventional drilling. However Gaitonde et al. [9] showed an opposite effect when drilling at high spindle speed in thin woven-ply

CFRP composite laminates. Cutting speed shows in general much lower influence than feed rate and in some cases it was found to be negligible [10].

In the last few years, natural fibres based composites have been considered promising materials to replace traditional composites [11]. In terms of matrices, non-biodegradable polymeric materials (such as epoxy, polyethylene or polypropylene) are typically used with natural fibres [12]. However, biodegradable matrices (such as polysaccharides, proteins, polyesters, lignin, lipids, etc.) can also be used to obtain 100 % eco-sustainable composites [13]. The introduction of fully biodegradable composites reduces the use of non-biodegradable materials and non-renewable resources. Moreover, energy needed to produce natural fibres is really reduced (4 GJ/ton in plant fibres and 30 GJ/ton for fibreglass [14]) and they are less harmful for health and environment during its production and handling comparing with synthetic fibres. It also provides the opportunity to use waste from mills and farms [15] which in turn can be reused after the biocomposite lifecycle [16]. These advantages make biocomposites a real alternative to traditional composites [17,18].

On the other hand, some of the disadvantages of biodegradable composite are lower mechanical properties [13], low resistance to high temperatures [19], high flammability [20], and poor adhesion between polymeric matrix and fibres [21]. Considering this balance between benefits and drawbacks, biocomposites are suitable for numerous industrial applications as car panels [22,23], boats [24] or electronics applications [25] for instance.

Despite the great number of studies about the induced damage during drilling of conventional composites, there is a lack of research works focused on drilling of fully biodegradable composites. Only few researchers have analysed the drilling process of composites manufactured with natural fibres and non-degradable matrixes as polyester or epoxy [26-30].

Sidharan and Muthukrishnan [26] drilled a sisal/polyester composite with twist drill (point angle 118º, diameter 6 mm) in a Vertical Machining Centre. They conducted a parametric analysis observing that induced damage increased with feed rate and cutting speed. They identified delamination as the main damage mode. Abilash and Sivapragash [27] analysed drilling of composite based on polyester matrix and bamboo fibres, finding that feed rate is the main parameter to control induced damage. Damage extension was produced due to delamination. Ramesh et al. [28] carried out a parametric analysis, determining that fibre breakage was the main failure mode and finding that damage extension increases with feed rate and the convenience of using SC drill bit instead of HSS. Athijayamani et al. [29] proved that an alkali treatment during 8 hours on 30% wt. sisal fibres combined with polyester improves the drilled hole quality. Nasir et al. [30] manufactured a flax/epoxy composite by RTM, they found that induced damage increases with feed rate but decreases with cutting speed. They found that delamination was the main factor influencing damage extension. According to these studies the influence of cutting parameters and the failure modes mainly depends on the manufacturing route and the matrix type. None of these works analysed the behaviour of fully biodegradable composites manufactured with natural polymers.

The aim of this work is developing the first study focused on machining induced damage on fully biodegradable composites during drilling. There are two objectives behind this goal: first, the implementation of fully-biodegradable composites in industry because the combination of natural fibres with non-biodegradable polymeric matrices cannot be considered a clean final product; second, the optimization of the cutting parameter to reduce cost, energy consumption and CO2 emissions during machining of biocomposites.

The composites were based on three different types of natural fibres acting as reinforcement. Cotton, flax and jute woven fibres were combined with PLA (poly-lactic acid) matrix to manufacture the biocomposites by compression moulding method. The influence of the main process parameters; feed rate, cutting speed, plate thickness, drill tip and diameter; is analysed.

Interesting results, such as the occurrence of fraying as the dominant damage mechanism and the relationships between tensile strength and damage are explained in the following sections.

8.2 Experimental

8.2.1 Manufacturing route

Fully biodegradable composites were manufactured using compression moulding method. Four different woven fibres were used as reinforcement: plain weave jute (J); basket weave (2x1) cotton (C), basket weave (2x1) flax (BF); and plain weave flax (PF), which were cut into 150x150 mm plates. No chemical pre-treatment was applied to woven fibres. PLA was used as matrix; it is a thermoplastic resin, acquired in pellets form. Two kinds of PLA polymer were used: 3260HP (PLA 3) and 10361D (PLA 10), both provided by Natureworks LLC. 3260HP PLA is aimed to an extrusion process. 10361D PLA is specifically designed as a binder of natural fibres. The PLA density is 1.24 g/cm3 and the melting temperature is around 145-170ºC.

Compression moulding method includes several steps. First, PLA pellets are placed between two thermo-heated plates at a temperature equal to 185ºC in order to obtain a uniform film. Then, the matrix films are stacked alternatively with woven plies. The stacked plies are placed between the thermo-heated plates, also at temperature 185ºC. After a pre-heating time of 2 minutes, pressure of 16 MPa is applied during 3 minutes using a universal testing machine Servosis ME-404/100 + PCD-1065. Finally, the biocomposite panels were dried at room temperature.

All the composites were manufactured with 2, 3 and 4 layers with the objective of analysing the influence of thickness on the induced damage during drilling. Woven fibres and PLA plies were maintained in an oven under 95ºC during 30 minutes before the compression moulding processing to remove water content. All the materials were stored in stable constant conditions of 46% RH and 20ºC before and after the manufacturing process to control the environmental conditions influence. The biocomposites presented a resultant 65% weight reinforcement ratio, which is considered an optimum value as it was reported by Ochi [31]. Tensile strength of each manufactured composite is summarized in Table 8.1. More details concerning the manufacturing process and mechanical properties can be found in [13].

Material	*Tensile Strength (MPa)*	*Standard Deviation (MPa)*
BF/PLA 3	116.33	2.42
BF/PLA 10	103.98	4.71
PF/PLA 10	96.88	3.80
J/PLA 10	66.62	8.22
C/PLA 10	62.38	3.70

Table 8.1. Tensile strength of the manufactured biocomposites [12].

8.2.2 Drilling test

The drilling tests were carried out in a B500 KONDIA machining centre in dry conditions. A dynamometer (Kistler 9123C) was implemented in the machine tool (see Fig. 8.1) to measure thrust force and torque on the rotating tool. Drilling operations were carried out confined inside a special device allowing air entrance and connected to a vacuum with the aim of collecting the dust fibres generated during chip removal.

Three different values of cutting speed (V), ranging from 15 m/min to 25 m/min, and three values of feed rates (f), ranging from 0.03 mm/rev to 0.12 mm/rev, were analysed. Two different drill geometries were studied since drill geometry is a key parameter in damage generation in composites. Firstly, a HSS drill bit with 118º point angle, denoted Drill-A (3, 5 and 6 mm diameter, see Fig. 8.2a). Secondly, a custom HSS drill was manufactured for this study with 80º point angle and 40º helix angle, denoted Drill-B (6 mm diameter, see Fig. 8.2b). The cutting angles on Drill-B were selected close to the optimum point angle recommended for glass/carbon composites [4]. All these cutting parameters were stated in the range commonly defined for natural fibres based composites (see for instance [32]).

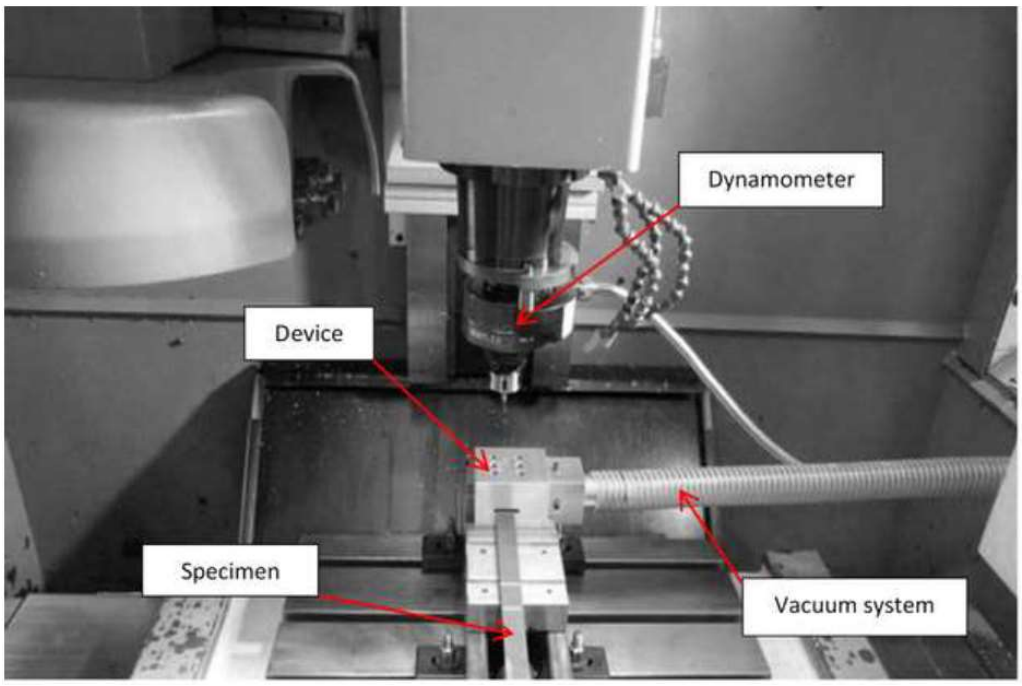

Figure 8.1. Machining centre used for drilling tests, showing Dynamometer Kistler 9123C and vacuum system for chip collection.

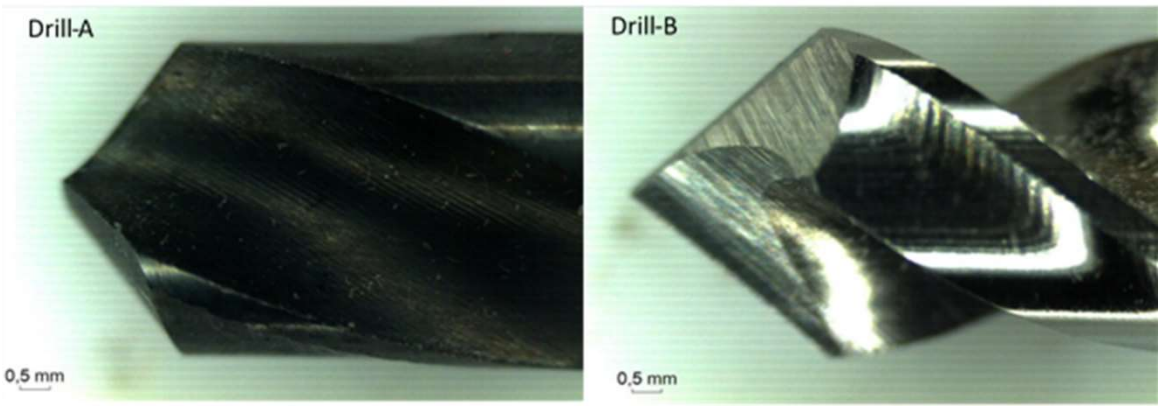

Figure 8.2. Drill-A: HSS drill (118º) and Drill-B: Custom HSS drill (80º).

8.2.3 Damage Factor

Damage extension was quantified in terms of the damage factor (F_d) defined as the ratio between the maximum diameter of the damaged area and the nominal diameter of the drill. Damaged area was obtained from the hole images captured with a stereo microscope (Optika SZR).The evaluation of F_d is illustrated in Fig. 8.3, where the difference between the nominal diameter and the maximum damaged diameter can be observed.

Damage factor was evaluated both at the entrance (peel up) and the exit (push out) of the drilled hole. The main failure mode originated by drilling was fraying, due to the fibres breakage, see Fig. 8.3, and there is no presence of delamination between adjacent layers, being the dominant damage mode observed in traditional glass or carbon fibre composites [2].

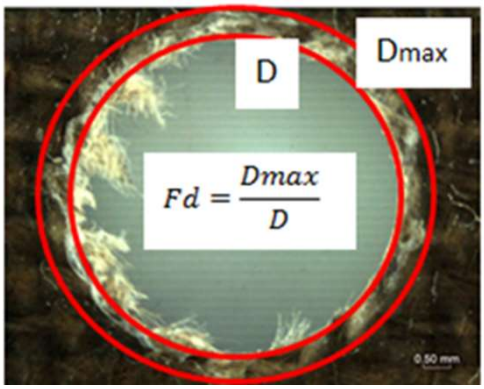

Figure 8.3. Example of the damage factor Fd calculation, being fraying the main damage mechanism. The image corresponds to the 2 Layers Jute and 10361D PLA biocomposite, drilled with drill-A.

8.3 Results and discussion

The parameters of drilling tests and results in terms of damage factor are summarized in Table 8.2. The parameters included in the analysis are: combination of fibre and matrix materials, laminate thickness, drill bit, drill diameter, cutting speed and feed rate. Three drilling tests were conducted

for each configuration, the repeatability of the results was excellent and standard deviation was negligible.

A general trend can be observed: push out damage is greater than peel up damage at the entrance in all tests. These results are in agreement with the behaviour observed when drilling CFRPs. Davim et al. [5] explained this phenomenon due to the compression of the plate leading to higher values of forces during drilling. The results for the drill-B showed a lower damage factor than drill-A type due to the smaller point angle of drill-B. Higher values of drill point angle are commonly related with increased thrust forces and enhanced delamination at the hole exit in conventional composites [33,34].

There are clear differences between results showed in Table 8.2 and those reported by other authors in natural based composited manufactured with non-degradable matrices. Damage factors obtained in this work are lower compared with drilling induced damage in composites manufactured with non-degradable matrixes. On the other hand, it is worth noting that the main damage mechanism reported in the second case is delamination [26,27,28,29]. For example, Abilash [27] studied a bamboo/polyester composite obtaining 1.14 and 1.23 damage factors in the drill entrance and exit, respectively, with 860 rpm cutting speed, 6 mm diameter drill, 26 mm/min feed rate. Sridharana et al. [26] also obtained higher damage factors drilling a sisal and polyester composite, as Ramesh et al. [28] (in the last case fibre breakage was the main failure mode, as it is observed in the present work). Nasir et al. [30] obtained results ranging from 1.09 to 1.2, when drilling a 6 layers flax/epoxy composite.

The influence of the different parameters in the machinability of the biocomposites is analysed in the following subsections. The drilling operation is evaluated in terms of trust force and damage factor. A trust force increment is related to an increase of delamination when machining conventional composites (see for instance [10,33]).

Layers	*Fibre/Matrix*	*Thickness [mm]*	*Ø [mm]*	*V [mm/min]*	*f [mm/rev]*	*Drill bit*	*Peel up [-]*	*Push out [-]*	*Test Number*
2	*C/PLA 10*	*1.53*	6	15	0,06	A	1,05	1,06	1
						B	1.04	1.05	
				20	0,03	A	1,04	1,05	2
						B	1.04	1.06	
					0,06	A	1,02	1,04	3
						B	1.03	1.05	
					0,12	A	1,02	1,03	4
						B	1.02	1.03	
				25	0,06	A	1,03	1,03	5
						B	*1.02*	*1.04*	
2	*J/PLA 10*	*1.25*	6	15	0,06	A	1,05	1,07	6
						B	*1.03*	*1.05*	
				20	0,03	A	1,05	1,07	7
						B	*1.04*	*1.05*	
					0,06	A	1,04	1,06	8
						B	*1.03*	*1.04*	
					0,12	A	1,03	1,04	9
						B	*1.03*	*1.05*	
				25	0,06	A	1,04	1,06	10
						B	*1.03*	*1.03*	
2	*PF/PLA 10*	*1.05*	6	15	0,06	A	1,07	1,08	11
						B	*1.05*	*1.07*	
				20	0,03	A	1,06	1,08	12
						B	*1.06*	*1.08*	
					0,06	A	1,05	1,06	13
						B	*1.05*	*1.06*	
					0,12	A	1,04	1,05	14
						B	*1.04*	*1.05*	
				25	0,06	A	1,05	1,07	15
						B	*1.04*	*1.05*	
2	*BF/PLA 10*	*1.4*	6	15	0,06	A	1,09	1,11	16
						B	*1.05*	*1.06*	
				20	0,03	A	1,07	1,08	17
						B	*1.05*	*1.06*	
					0,06	A	1,05	1,08	18
						B	*1.04*	*1.05*	
					0,12	A	1,03	1,05	19
						B	*1.03*	*1.04*	
				25	0,06	A	1,04	1,06	20
						B	*1.03*	*1.04*	
2	*BF/PLA 3*	*1.4*	6	15	0,06	A	1,11	1,12	21
				20	0,03	A	1,10	1,13	22
					0,06	A	1,09	1,10	23
					0,12	A	1,05	1,08	24
				25	0,06	A	1,07	1,09	25
3	*BF/PLA 10*	*2.14*	6	20	0,06	A	1,05	1,08	26
						B	*1.04*	*1.05*	
3	*C/PLA 10*	*2*	6	20	0,06	A	1,03	1,05	27
						B	*1.03*	*1.04*	
4	*BF/PLA 10*	*2.68*	6	20	0,06	A	1,06	1,11	28
						B	*1.04*	*1.06*	
4	*C/PLA 10*	*2.85*	6	20	0,06	A	1,04	1,08	29
						B	*1.04*	*1.06*	
4	*BF/PLA 10*	*2.68*	5	20	0,06	A	1,06	1,11	30
4	*C/PLA 10*	*2.85*	5	20	0,06	A	1,04	1,07	31
4	*BF/PLA 10*	*2.68*	3	20	0,06	A	1,06	1,10	32
4	*C/PLA 10*	*2.85*	3	20	0,06	A	1,03	1,06	33

Table 8.2. Damage Factor, F_d, at hole entrance (peel up) and exit (push out) measured in each test depending on woven fibres, PLA type, thickness and cutting parameters.

8.3.1 Cutting speed

The influence of cutting speed is analysed through the comparison of the tests denoted with numbers 1, 3, 5, 6, 8, 10, 11, 13, 15, 16, 18, 20, 21, 23 and 25 in Table 8.2. These tests were carried out on composites manufactured with 2 layers with nominal drill diameter equal to 6 mm and at constant feed rate equal to 0.06 mm/rev.

Peel up and push out damage factor *vs* cutting speed are graphically represented in Figure 8.4 for the different types of composites analysed. It is observed a general trend for all cases tested: damage decreases with cutting speed. This trend is observed in all the materials and with both drills and it was also reported by Nasir et al. [30] when drilling flax/epoxy composites.

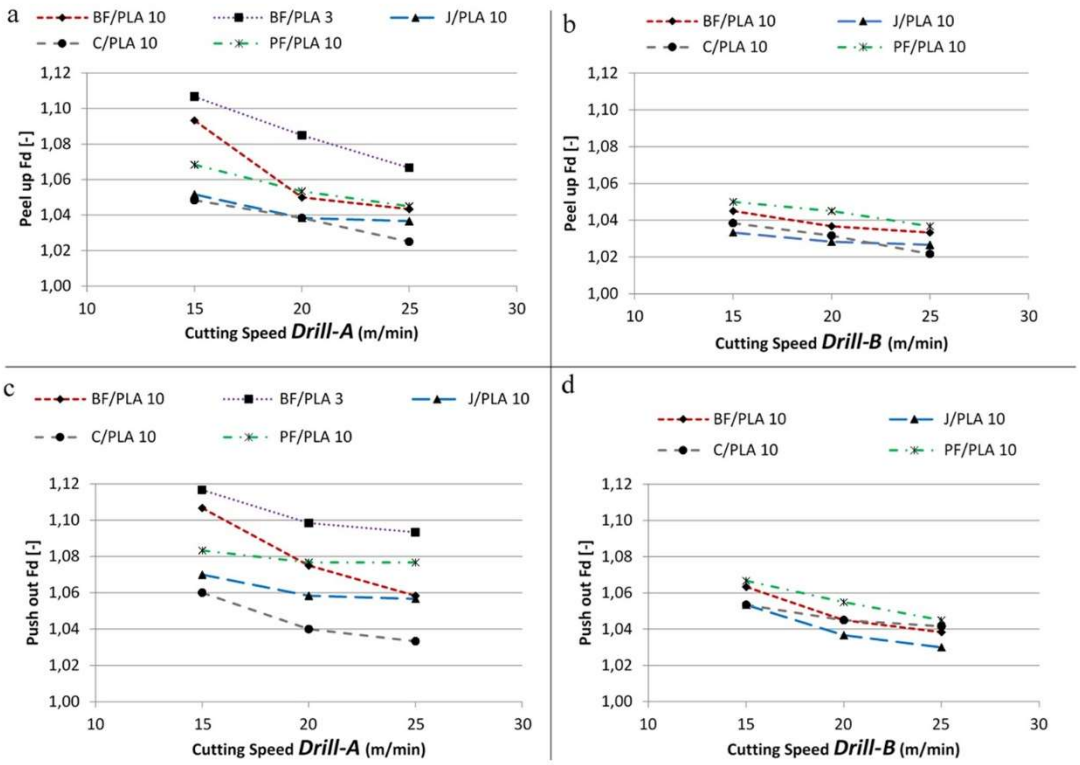

Figure 8.4. Damage factor vs cutting speed for all composites analysed (BF/PLA10, BK/PLA3, J/PLA10, C/PLA10, PF/PLA10). a) Peel up obtained with Drill-A, b) Peel up obtained with Drill-B, c) Push out obtained with Drill-A and d) Push out obtained with Drill-B.

This behaviour is different with respect to that observed when drilling conventional composites. As it was previously commented in the introduction, the effect of cutting speed is much lower than the influence of feed rate in conventional composites. Moreover, in recent works of the authors, it was reported the influence of drill geometry on the sensibility of delamination in CFRPs with cutting speed, observing negligible or significant influence for different drills configuration [10,33].

Figure 8.5 shows thrust forces as a function of cutting speed for all cases analysed. Thrust forces generated by the Drill-A were higher than those obtain with Drill-B. This is due to the higher point angle of Drill-A (118º) compared to Drill-B (80º). Thus a small point angle can be recommended to machine biocomposites in order to moderate thrust force (the same behaviour has been reported for conventional composites). However, the influence of cutting speed is found to be negligible on thrust force, although Figure 8.4 shows a clear

influence of cutting speed on induced damage. This is due to the nature of damage evaluated mainly consisting of frying commonly decreasing with cutting speed due to the cleaner cut produced at higher velocities. However, when the dominant damage is delamination the effect of thrust force is directly related with damage, being the case of conventional composites.

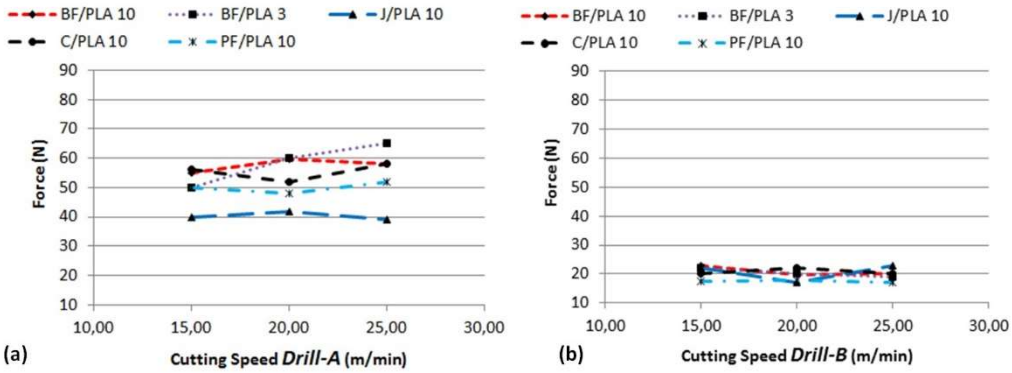

Figure 8.5. Thrust forces vs cutting speed for all composites analysed (BF/PLA10, BK/PLA3, J/PLA10, C/PLA10, PF/PLA10).a) Drill-A, b) Drill-B.

8.3.2 Feed rate

The influence of feed rate was observed analysing the tests denoted 2-4, 7-9, 12-14, 17-19, 22-24 in Table 8.2. These tests were carried out on composites manufactured with 2 layers with nominal drill diameter equal to 6 mm and at constant cutting speed equal to 20 m/min.

Figure 8.6 shows peel up and push out damage factor as a function of feed rate for the different types of composites analysed. It is clearly observed that induced damage decreases with feed rate. These results are in clear contradiction with those observed in carbon fibre composites [2,4,5], sisal/polyester composites [22], and flax/epoxy composites [27]. The disagreement is related to the different dominant failure modes, other authors identified delamination as the main failure mode while fibre breakage leading to fraying was the major failure mode found in the present work. Non-destructive tests were conducted by C-Scan ultrasonic inspection to confirm that delamination was not induced during drilling tests. In addition, a strong influence of strain rate on mechanical properties is well known in biocomposites [35]. A significant increment of biocomposites stiffness with strain rate can explain a more brittle behaviour for high feed rates.

Thrust forces as a function of feed rate are summarized in Figure 8.7. Thrust force increases with feed rate, as expected. In all cases thrust forces induced by Drill-A were higher than those produced by Drill-B. As it was explained previously, this fact can be explained by the higher point angle of Drill-A leading to lower values of thrust force independently of feed rate.

Moreover, the samples were observed in SEM-EDS through a transversal cutting along the drilled hole in order to analyse the damage generated during the process depending on feed rate. It was observed that for all materials hole quality surface is enhanced with the feed rate. Figure 8.8 shows an example of hole quality for the composite consisting of basket weave flax (BF) and 10361D (PLA 10), machined with Drill-A at cutting speed equal to 20 m/min, and feed rate equal to 0.03 (Figure 8.8a) and 0.12 (Figure 8.8b) mm/rev respectively. It is clear the enhanced hole surface quality with increments on the feed rate.

These results can help to reduce the energy consumption and cost of drilling operations in biocomposites. Drilling of conventional composites requires low values of feed rate but biocomposites can be drilled with higher feed rates leading to a better hole surface quality.

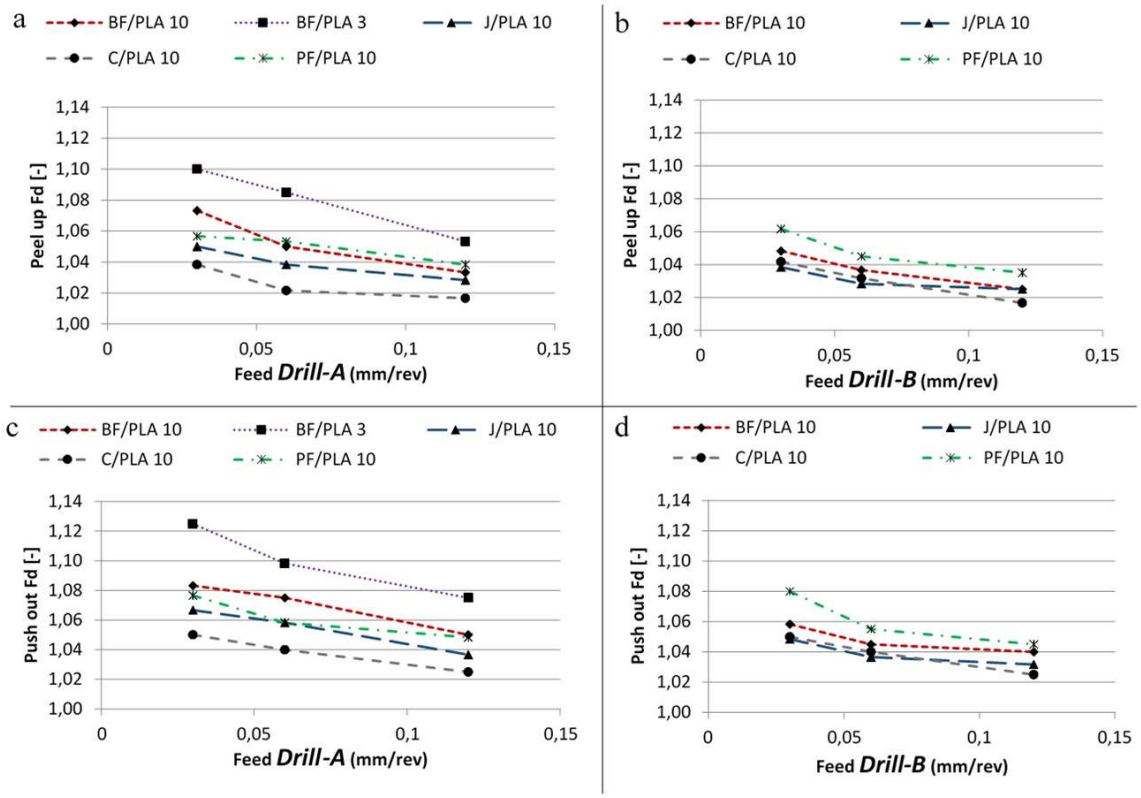

Figure 8.6. Damage factor vs feed rate for all composites analysed (BF/PLA10, BK/PLA3, J/PLA10, C/PLA10, PF/PLA10). a) Peel up obtained with Drill-A, b) Peel up obtained with Drill-B, c) Push out obtained with Drill-A and d) Push out obtained with Drill-B.

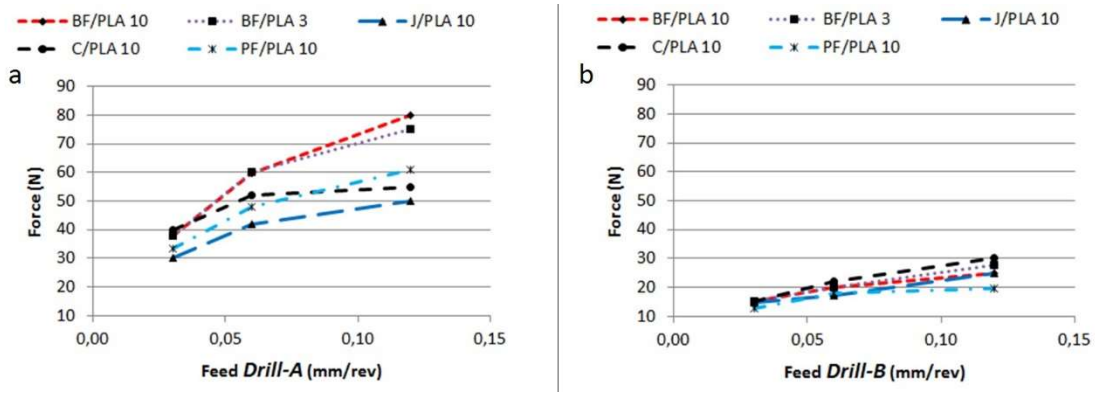

Figure 8.7. Thrust forces vs feed rate for all composites analysed (BF/PLA10, BK/PLA3, J/PLA10, C/PLA10, PF/PLA10).a) Drill-A, b) Drill-B.

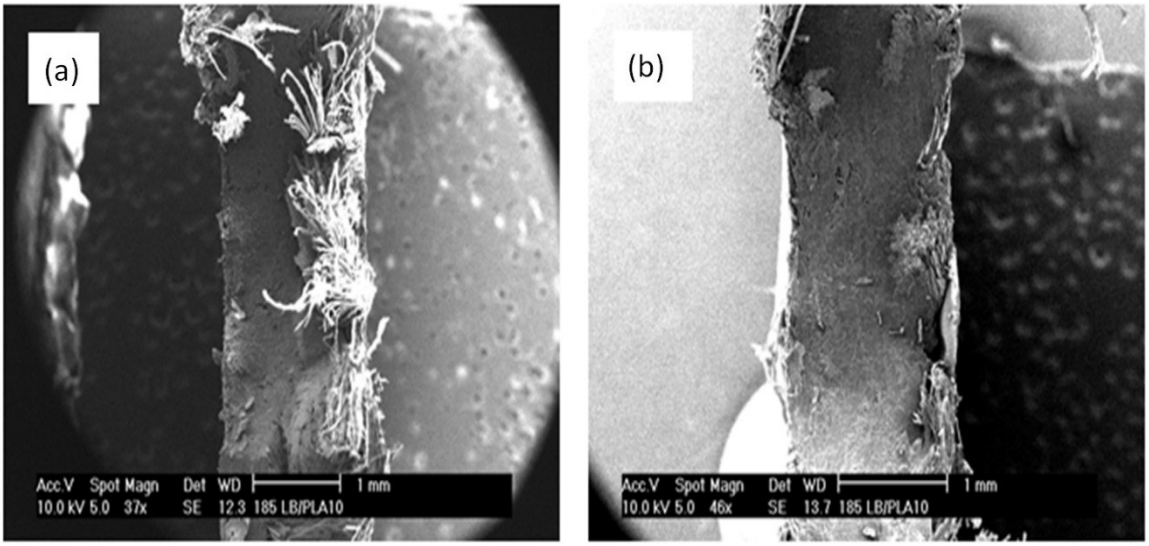

Figure 8.8. SEM- EDS image of transversal section of the drilled hole (biocomposite basket weave flax (BF) and 10361D PLA made of 2 layers), drilled with drill-A at cutting speed 20 m/min and feed rate 0.03 mm/rev (a) and 0.12 mm/rev (b) respectively.

8.3.3 Drill Diameter

Drill diameter was analysed trough the results obtained from tests 28-33. Two materials consisting of four layers were tested: basket (2x1) weave cotton (C) and basket (2x1) weave flax (BF) combined with 10361D PLA matrix. Both materials were drilled with drill-A with three different diameters equal to 3, 5 and 6 mm. Constant cutting speed equal to 20 m/min and feed rate equal to 0.06 mm/rev were established.

Figure 8.9 shows that push out damage increases in absolute terms with drill diameter during the drilling of biocomposites reinforced with basket weave flax fibres. However, the damage factor (ratio between diameter of damaged are and nominal diameter) is similar (around 1,1) in the range of diameters analysed. Similar results were obtained when analysing peel up damage extension in the case of testing cotton fibres biocomposites, see Figure 8.10. Both peel up and push out increase slightly with drill diameter in absolute terms, however the damage factor is similar. Thus the influence of drill diameter can be neglected comparing with the influence of other cutting parameters as feed rate or cutting speed.

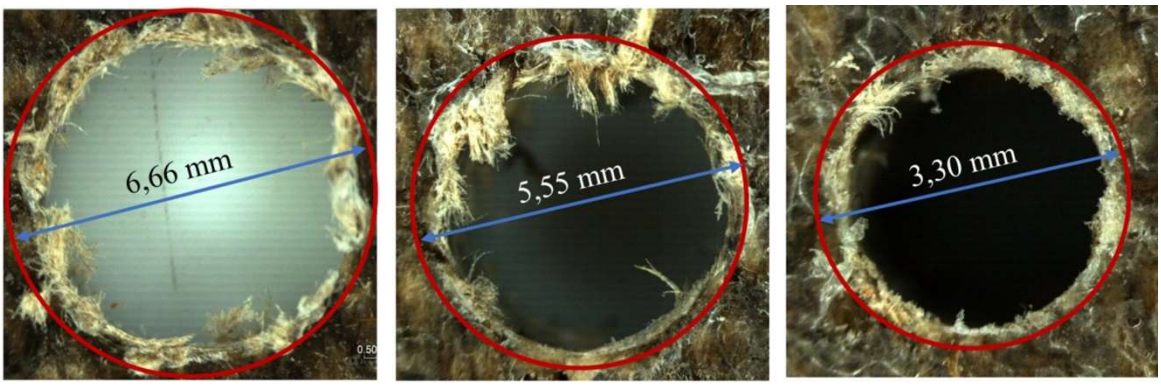

Figure 8.9. Hole quality (in terms of push out damage) of basket weave flax (BF) drilled by 3, 5 and 6 diameter drill-A.

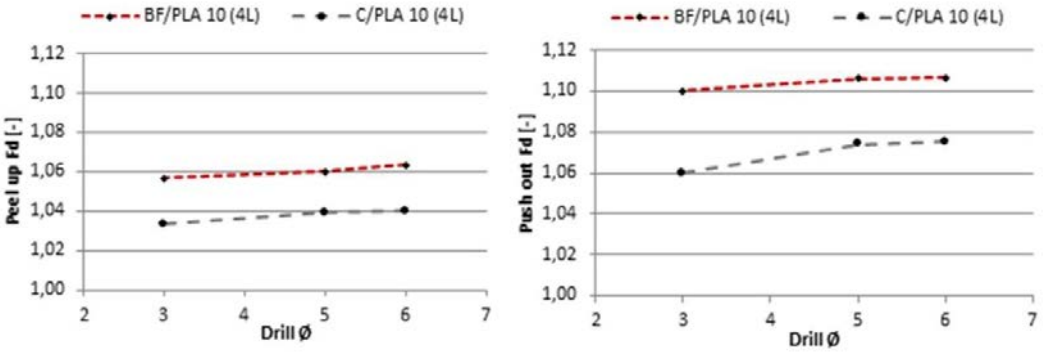

Figure 8.10. Peel up and Push out damage factor vs drill diameter (drill-A). Basket weave flax and cotton fibres with PLA10 matrix.

8.3.4 Plate thickness

The influence of the composite thickness on resultant damage was analysed for the cases corresponding to basket weave cotton (C) and the basket weave flax (BF) with 10361D PLA matrix, being both composites manufactured with 2, 3 and 4 layers and drilled both with Drill-A and Drill-B with diameter equal to 6 mm. Cutting speed equal to 20 m/min and feed rate equal to 0.06 mm/rev were established. Results of tests denoted 3, 13, 26-29 in Table 8.2 were compared for this analysis. Resulting damage factor (push out and peel up) are presented in Figure 8.11, showing that drilling induced damage increases with the number of layers. It should be noticed that the maximum thickness analysed was 2.85 mm, thus all the specimens analysed can be considered thin laminates. In this range of thicknesses, damage factor increases with plate thickness.

8.3.5 Drill geometry

The analysis described in previous sections have demonstrated that in general, the damage induced by drill-B (80º) was found to be lower than that produced by drill-A (118º). This behaviour is due to the lower value of drill point angle, also commonly related to decreased damage extension in conventional composites, see for instance a recent work of the authors [10].

Figure 8.4 shows that induced damage using drill-A is greater than that obtained with drill-B for different materials and cutting speed. Nevertheless, the sensibility of damage generation with drill point angle is not the same for all materials involved in the study and strongly depend on the nature of the reinforcement. In the case of biocomposites reinforced with basket weave flax, damage factor was reduced from 1.11 to 1.06 using drill-B instead of drill-A. On the other hand, the reduction of damage factor in biocomposites reinforced with cotton was almost negligible.

The results shown in Figure 8.6 confirm that damage factor is reduced using drill-B for different materials and feed rates. Figure 8.11 shows that drill-A lead to greater induced damage factor for different thicknesses, demonstrating the importance of selecting proper drill geometry in order to minimize damage extension. The selection of a lower drill point angle can help to obtain better results without an increment in cost or energy consumption.

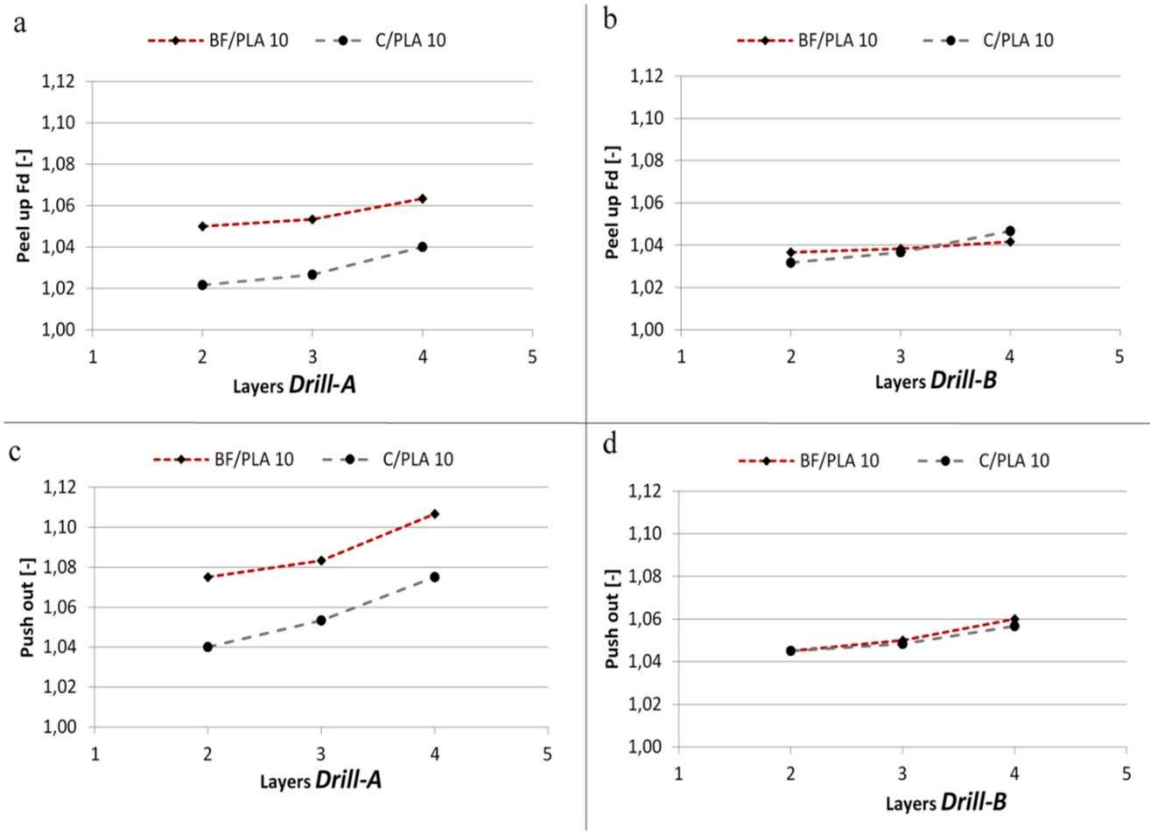

Figure 8.11. Damage factor vs number of layers for the composites BF/PLA10 and C/PLA10. a) Peel up obtained with Drill-A, b) Peel up obtained with Drill-B, c) Push out obtained with Drill-A and d) Push out obtained with Drill-B.

8.3.6 Type of biocomposite

Figure 8.12 shows a comparison of the push out damage produced on the five materials analysed made of two layers: basket weave flax and 3260HP PLA matrix (BF/PLA 3); basket weave flax and 10361D PLA matrix (BF/PLA 10); plain weave flax (PF/PLA10); plain weave jute (J/PLA10); and basket weave cotton (C/PLA10). These tests were conducted at a cutting speed equal to 20m/min and feed rate equal to 0.06 mm/rev, corresponding to tests denoted 5, 10, 15, 20, and 25 in Table 2.

The lowest values of damage factor were found in cotton based biocomposites, while the highest damage factor was found in basket weave flax (BF) using the 3260HP PLA. The influence of fibre material on damage factor can be related to the biocomposites tensile strength. An inverse relation between the tensile strength, see Table 8.1, and damage factor was found. Higher tensile strength leads to higher cutting forces and, consequently, greater induced damage.

Induced damage is lower in cotton and jute based biocomposites due to their lower tensile strength. However, different results were found comparing peel up and push out damage factors. In the peel up, induced damage in cotton was lower than in jute (see Figures 8.4 and 8.6), while push out damage factor is lower in the case of jute composite.

Concerning the influence of the matrix, damage factor in the composites manufactured with 101361D PLA, considering both peel up and push out, is lower than that observed in the composites based on 3260HP PLA. The polymer 10361D PLA is specifically designed as a binder of natural fibres and gives better interface cohesion resulting in reduced fraying.

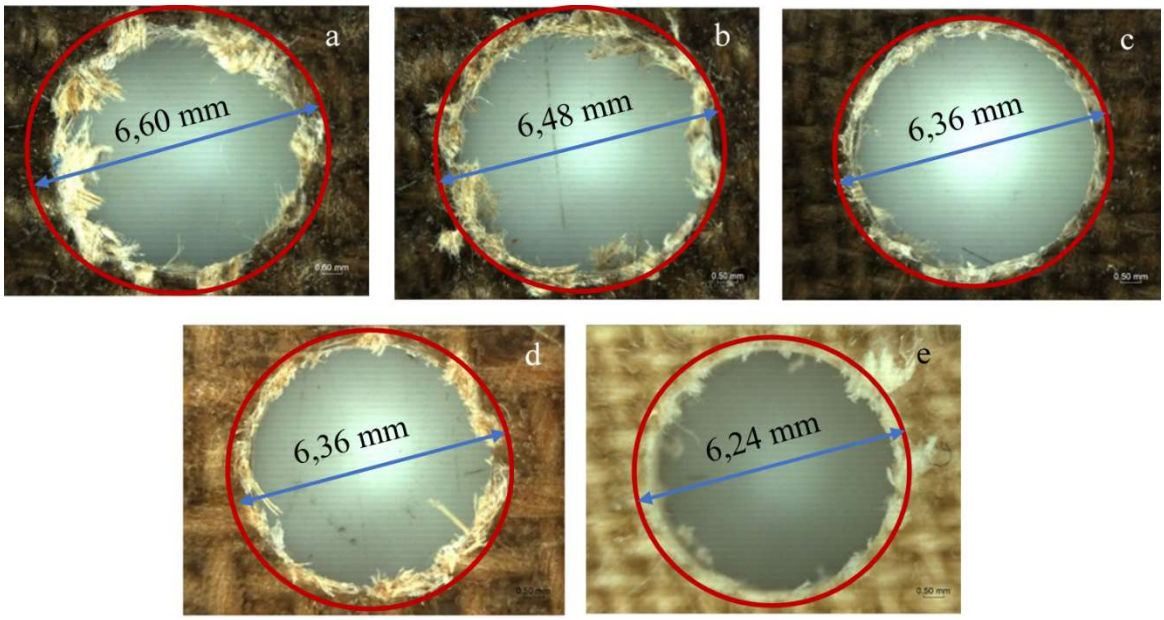

Figure 8.12. Push out induced damage obtained with Drill-A (2 layers, cutting speed 20 m/min, feed rate 0.06 mm/rev) in the five composites analysed: a) Basket weave flax with 3260HP PLA (BF/PLA 3); b) basket weave flax with 10361D PLA (BF/PLA 3); c) plain weave flax (PF/PLA10); d) plain weave jute (J/PLA10); e) basket weave cotton (C/PLA10) from left to right and up to down.

8.4 Conclusions

In this paper drilling of natural fibre fully biodegradable composites is analysed identifying the dominant damage mechanism. Fraying was the main damage mode while delamination was found to be negligible. Damage was evaluated in terms of damage factor (ratio between diameter of damaged area and hole nominal diameter) both at hole entry (peel up) and exit (push out).

The influence on the damage factor of the cutting parameters, drill diameter, thickness, fibre material and matrix was analysed in terms of damage extension and thrust force and concluding remarks are summarized below:

Concerning the influence of cutting parameters, it was found a decreasing damage extension when both cutting speed and feed rate increase. Although the former trend is in agreement with some works focused on CFRPs in the literature, the influence of the feed rate is in contradiction with that observed in CFRPs and other biocomposites. This behaviour can be related to the increment of biocomposites stiffness with strain rate explaining a more brittle behaviour for high feed rate and cutting speed that lead to a cleaner breakage of fibre and in consequence, decreased fraying.

The influence of cutting speed on thrust force was negligible, although cutting speed influenced induced damage. This is explained by the nature of damage mainly consisting of frying decreasing with cutting speed due to the cleaner cut produced at higher velocities. However, when

the dominant damage is delamination the effect of thrust force is directly related with damage, being the case of conventional composites.

Thrust force increases with feed rate, as expected. In all cases thrust forces induced by Drill-A were higher than those produced by Drill-B. As it was explained previously, this fact can be explained by the higher point angle of Drill-A leading to lower values of thrust force independently of feed rate.

The analysis of the geometrical parameters showed a negligible influence of drill diameter, while damage factor increases with plate thickness. The drill point angle was found to be an influencing geometrical parameter: the lower the drill point angle the lower the damage extension, both in the present work and also in conventional composites.

Finally, the damage extension was found to be influenced by fibre material. Induced damage is lower in cotton and jute based biocomposites due to their lower tensile strength. The matrix based on polymer 10361D PLA, recommended for natural fibres because of the better interface cohesion, resulted in reduced fraying.

The present study shows the importance of controlling process parameters in order to limit damage extension, giving valuable information for the industrial use of natural fibre fully biodegradable composites. The introduction of biodegradable composites in industry can be benefit from these recommendations of cutting parameters and tool angles to reduce energy consumption and cost of final product.

References

[1] Olmedo A, Santiuste C, Barbero E. An analytical model for predicting the stiffness and strength of pinned-joint composite laminates. Compos Sci Tech 2014;90:67-73.

[2] Feito N, López-Puente J, Santiuste C, Miguélez MH. Numerical prediction of delamination in CFRP drilling. Compos Struct 2014;108:677-683.

[3] Soldani X, Santiuste C, Muñoz-Sánchez A, Miguélez MH. Influence of tool geometry and numerical parameters when modeling orthogonal cutting of LFRP composites. Compos Part A: Appl Sci 2011;42(9):1205-1216.

[4] Gaitonde VN, Karnik SR, Rubio JC, Correia AE, Abrao AM, Davim JP. Analysis of parametric influence on delamination in high-speed drilling of carbon fiber reinforced plastic composites. J Mater Process Technol 2001;203(1):431-438.

[5] Davim JP, Rubio JC, Abrao AM. A novel approach based on digital image analysis to evaluate the delamination factor after drilling composite laminates. Compos Sci Tech 2007;67(9):1939-1945.

[6] Santiuste C, Olmedo A, Soldani X, Miguélez H. Delamination prediction in orthogonal machining of carbon long fiber-reinforced polymer composites. J Reinf Plast Compos 2012;31(13):875-885.

[7] Santiuste C, Díaz-Álvarez J, Soldani X, Miguélez H. Modelling thermal effects in machining of carbon fiber reinforced polymer composites. J Reinf Plast Compos 2014;33(8):758-766.

[8] Davim JP, Reis P. Study of delamination in drilling carbon fiber reinforced plastic (CFRP) using design experiments. Compos Struct 2003;59:481-7.

[9] Gaitonde VN, Karnik SR, Campos Rubio J, Esteves Correia A, Abrao AM, Paulo Davim J. Analysis of parametric influence on delamination in high-speed drilling of carbon fiber reinforced plastic composites. J Mater Process Technol 2008;203:431-8.

[10] Feito N, Díaz-Álvarez J, Díaz-Álvarez A, Cantero JL, Miguélez MH. Experimental Analysis of the Influence of Drill Point Angle and Wear on the Drilling of Woven CFRPs. Materials 2014;7(6):4258-4271

[11] Rubio-López A, Olmedo A, Santiuste C. Modelling impact behaviour of all-cellulose composite plates. Compos Struct 2015;122:139-43.

[12] Arbelaiz A, Fernandez B, Cantero G, Llano-Ponte R, Valea A, Mondragon I. Mechanical properties of flax fibre/polypropylene composites. Influence of fibre/matrix modification and glass fibre

hybridization. Comp Part A: Appl Sci 2005;36(12):1637-1644.

[13] Rubio-López A, Olmedo A, Díaz-Álvarez A, Santiuste C. Manufacture of compression moulded PLA based biocomposites: A parametric study. Compos Struct 2015;131:995-1000.

[14] Satyanarayana KG, Arizaga GG, Wypych F. Biodegradable composites based on lignocellulosic fibers—an overview. Prog Polym Sci 2009;34(9):982-1021.

[15] Gonzalez-Sanchez C, Martínez-Aguirre A, Pérez-García B, Martinez-Urreaga J, María U, Fonseca-Valero C. Use of residual agricultural plastics and cellulose fibers for obtaining sustainable eco-composites prevents waste generation. J Clean Prod 2014;83:228-237.

[16] Dittenber DB, GangaRao HV. Critical review of recent publications on use of natural composites in infrastructure. Compos Part A: Appl Sci 2012;43(8):1419-1429.

[17] Al-Oqla FM, Sapuan SM. (2014). Natural fiber reinforced polymer composites in industrial applications: feasibility of date palm fibers for sustainable automotive industry. J Clean Prod 2014;66:347-354.

[18] Zamri MH, Osman MR, Akil H, Shahidan MHA, Ishak ZM. Development of green pultruded composites using kenaf fibre: influence of linear mass density on weathering performance. J Clean Prod 2016;125:320-330.

[19] Pickering KL, Efendy MA, Le TM. A review of recent developments in natural fibre composites and their mechanical performance. Compos Part A: Appl Sci 2016;83,98-112.

[20] Kovacevic Z, Bischof S, Fan M. The influence of Spartium junceum L. fibres modified with montmorrilonite nanoclay on the thermal properties of PLA biocomposites. Compos Part B: Eng 2015;78:122-130.

[21] Huber T, Pang S, Staiger MP. All-cellulose composite laminates. Compos Part A: Appl Sci 2012;43(10):1738-1745.

[22] Summerscales J, Dissanayake N, Virk A, Hall W. A review of bast fibres and their composites. Part 2–Composites. Compos Part A: Appl Sci 2010;41(10):1336-1344.

[23] Alves C, Silva AJ, Reis LG, Freitas M, Rodrigues LB, Alves DE. Ecodesign of automotive components making use of natural jute fiber composites. J Clean Prod 2010;18(4):313-327.

[24] Brouwer WD. Natural Fiber Composites, Saving Weight and Cost with Renewable Materials. Thirteenth International Conference on Composite Materials 2001.

[25] Serizawa S, Inoue K, Iji M. Kenaf fiber reinforced poly (lactic acid) used for electronic products. J Appl Polym Sci 2006;100(1):618-24.

[26] Sridharana V, Muthukrishnanb N. Optimization of Machinability of Polyester/Modified Jute Fabric Composite Using Grey Relational Analysis (GRA). Proc Eng 2013;64:1003-1012.

[27] Abilash N, Sivapragash M. Optimizing the delamination failure in bamboo fiber reinforced polyester composite. Journal of King Saud University-Engineering Sciences 2013.

[28] Ramesh, M., Palanikumar, K., & Reddy, K. H. (2014). Influence of Tool Materials on Thrust Force and Delamination in Drilling Sisal-glass Fiber Reinforced Polymer (S-GFRP) Composites. Proc Mater Sci, 5, 1915-1921.

[29] Athijayamani A, Thiruchitrambalam M, Natarajan U, Pazhanivel B. Influence of alkali-treated fibers on the mechanical properties and machinability of roselle and sisal fiber hybrid polyester composite. Polym Compos 2010;31(4):723-731.

[30] Nasir AA, Azmi AI, Khalil ANM. Measurement and optimisation of residual tensile strength and delamination damage of drilled flax fibre reinforced composites. Measurement 2015;75:298-307.

[31] Ochi S. Mechanical properties of kenaf fibers and kenaf/PLA composites. Mech Mater 2008;40(4):446-52.

[32] Bajpai PK, Debnath K, Singh I. Hole making in natural fiber-reinforced polylactic acid laminates. Journal of Thermoplastic Composite Materials 2015

[33] Feito N, Diaz-Alvarez A, Cantero JL, Rodriguez-Millan M, Miguelez, H. Experimental analysis of special tool geometries when drilling woven and multidirectional CFRPs. Journal of Reinforced Plastics and Composites 2016;35(1):33-55.

[34] Durão P, Gonçalves JS, Tavares RS, Albuquerque C, Aguiar A, Torres A. Drilling tool geometry evaluation for reinforced composite laminates. Compos Struct 2010;92(7):1545–1550.

[35] Rubio-López A, Hoang T, Santiuste C. Constitutive model to predict the viscoplastic behaviour of natural fibres based composites. Compos Struct 2016; DOI: 10.1016/j.compstruct.2016.08.001.

Chapter 9
Conclusions

Summarizing the conclusions reached in each section, some general conclusions can be extracted.

A constitutive model for fully biodegradable composites was developed for the first time. The model, based on rheological elements, includes the consideration of non-linear elastic behaviour, viscous effects and plastic strains. The model was successfully validated for three different biocomposites: flax/PLA, jute/PLA, and cotton/PLA woven laminates. The model was validated for three different materials, what means that the model can help to bring some light to the physics behind the viscoplastic behaviour of biocomposites. Some hypotheses are proposed:

1- The plastic strains can be accurately predicted with a single friction element. This means that the yield point can be associated to a value of strain that initiates the plastic behaviour. One of the most probable reasons is the friction between fibres inside the yarns. The plastic behaviour of the matrix is an alternative explanation but it can be neglected due to the great differences in the values of yield strain for composites reinforced with different fibres.
2- The viscous effects can be attributed to fibres behaviour. The influence of matrix can be neglected again because the viscous effects are higher in the composites reinforced with stiffer fibres. Moreover, the influence of strain rate on the stiffness of flax/PLA composites is similar to that reported by other authors in flax/epoxy composites.
3- The non-linear elastic behaviour can be probably explained by a combination of woven fibres and matrix.

The present promising results can lead to get a better understanding of the mechanical behaviour of biocomposites and to increase their use in industrial applications to replace mineral fibres and oil-based polymer matrices.

The parametric analysis of the compression moulding manufacturing process revealed that PLA based biocomposites strength is directly related to fibre strength, what implies similar adhesion between the matrix and the different fibres. 10361D PLA produce better mechanical performance as the interface cohesion is enhanced. A 185ºC temperature and 8-32 MPa compression pressure were found as the optimum values for the process, producing a 100 MPa flax/PLA composite in a short time period of 5 minutes, what implies a significant advantage when compared with other procedures found in bibliography.

Delamination damage mechanism were not found in biocomposites. This is a particularity of the combination of natural fibres and bioplastics, what highly increase the interface adhesion. The principal damage mechanisms found were fibre breakage, matrix cracks and fraying. This result was obtained in the impacts tests done in flax/PLA composites and in the drilling studies realized using flax, cotton and jute combined with PLA matrix.

The impact test analysis results showed that fully biodegradable composites present some advantages when they are compared with traditional composites. Due to the absence of delamination and the ductile failure of the matrix, both absorbed energy and normalized residual strength of flax/PLA composites are higher than those obtained in carbon/epoxy laminates, in the range of studied impact energies.

The first FEM model for biodegradable composites considering linear-elastic up to failure behaviour was performed to study the limits of this assumption. Furthermore, viscoplastic behaviour has also been developed and validated with experimental results on flax/PLA composites for a second approach. This FEM model considers non-linear mechanical behaviour as a function of strain-rate and failure criterion based on maximum strains to delete damaged elements. Numerical predictions were in excellent agreement with experimental in terms of force history, evolution of absorbed energy and failure modes for all the impact energies analysed and both impactor noses of ϕ 12.7 mm and ϕ 20 mm. This model stablishes the basis for a future FEM implementation for biocomposites.

The main parameters of influence in the drilling process were studied manifesting another particularity of biocomposites, as it was found a decreasing damage extension when the feed rate increase, contradicting CFRPs behaviour. This behaviour can be related to the viscosity, as the increment of biocomposites stiffness with strain rate explains a more brittle behaviour for high feed rate, what leads to a cleaner breakage of fibre and in consequence, decreased fraying. The damage extension was found to be influenced by the type of reinforcement. Induced damage is lower in cotton and jute based biocomposites due to their lower tensile strength, while 10361D PLA matrix shows of the better interface cohesion, resulting in reduced fraying.

Chapter 10
Future works

As mentioned in the Introduction section, this Thesis is enveloped in a project work, which mission is to develop numerical models for the characterization and modelling of the behaviour of fully biodegradable composites. With this purpose, the next objectives are planned.

Optimization of the biocomposites manufacturing methods studied in this work in terms of ultimate strain or absorbed energy.

Development of a constitutive model for ACC as it presents a different behaviour that PLA based biocomposites.

The main limitation of the proposed constitutive model is its main unidimensional nature. A 3D model, considering orthogonal behaviour is the next step in the development of the model.

Implementation of the constitutive model described in this work in a user subroutine in order to have a more accurately integration in a FEM tool for the design of biocomposites components. This subroutine would allow the simulation of dynamic behaviour of biocomposites, so it could be validated under the impact and machining tests done in this work.

Analysis of the behaviour of biocomposites under other machining operations as orthogonal cutting. Development and validation of FEM tools for these operations.

Explore industrial applications of biocomposites and the behaviour of the materials under the conditions of these applications.

Global references

Abilash N, Sivapragash M. Optimizing the delamination failure in bamboo fiber reinforced polyester composite. Journal of King Saud University-Engineering Sciences 2013.

Akil HM, Omar MF, Mazuki AAM, Safiee S, Ishak ZAM, Abu Bakar A. Kenaf fiber reinforced composites: A review. Mater Des 2011;32(8-9):4107–4121.

Alibaba.com. Kevlar fabric price. 27/04/2016 <http://www.alibaba.com/product-detail/kevlar-fabric-price-of-kevlar-per_60373750766.html?spm=a2700.7724857.29.12.jhF0QT&smToken=49e884b2c2294ceb83904e936ca53e03&smSign=uJPT9xmHBhkwT5TFiTD3HQ%3D%3D>

Al-Oqla FM, Sapuan SM. (2014). Natural fiber reinforced polymer composites in industrial applications: feasibility of date palm fibers for sustainable automotive industry. J Clean Prod 2014;66:347-354.

Alves C, Silva AJ, Reis LG, Freitas M, Rodrigues LB, Alves DE. Ecodesign of automotive components making use of natural jute fiber composites. J Clean Prod 2010;18(4):313-327.

Andersons J, Modniks J, Spārniņš E. Modeling the nonlinear deformation of flax-fiber-reinforced polymer matrix laminates in active loading. J Reinf Plast Compos 2015; 34(3): 248-56

Antonucci V, Caputo F, Ferraro P, Langella A, Lopresto V, Pagliarulo V, Ricciardi MR, Riccio A, Toscano C. Low velocity impact response of carbon fiber laminates fabricated by pulsed infusión: A review of damage investigation and semi-empirical models validation. Prog Aerosp Sci 2015; 81: 26-40

Aramid (Kevlar) market price. 20/04/2016 <http://www.alibaba.com/product-detail/kevlar-fabric-price-of-kevlar-per_60373750766.html?spm=a2700.7724857.29.12.jhF0QT>

Aramid (Kevlar) market price. 20/04/2016 <http://www.clipcarbono.com/es/59-tejido-de-fibra-de-kevlar-1200-x-1000-mm.html>

Arbelaiz A, Fernandez B, Cantero G, Llano-Ponte R, Valea A, Mondragon I. Mechanical properties of flax fibre/polypropylene composites. Influence of fibre/matrix modification and glass fibre hybridization. Comp Part A: Appl Sci 2005;36(12):1637-1644.

Arbelaiz A, Orue A, Jauregi A, Mongragon G, Peña C, Eceiza A. Composites basados en fibras de sisal y matriz de poli(ácido láctico). Materiales Compuestos 2013;13:347-352.

Artengo TR890. 19/04/2016 <http://www.decathlon.es/raqueta-de-tenis-artengo-890-flax-fiber-id_8297316.html>

Artero-Guerrero JA, Pernas-Sánchez J, López-Puente J, Varas D. Experimental study of the impactor mass effect on the low velocity impact of carbon/epoxy woven laminates. Compos Struct 2015;133:774-81.

Athijayamani A, Thiruchitrambalam M, Natarajan U, Pazhanivel B. Influence of alkali-treated fibers on the mechanical properties and machinability of roselle and sisal fiber hybrid polyester composite. Polym Compos 2010;31(4):723-731.

B. Bax. J. Müssig , Impact and tensile properties of PLA/Cordenka and PLA/flax composites, Compos. Sci. Tech. 68(7) (2008) 1601-7.

Bajpai PK, Debnath K, Singh I. Hole making in natural fiber-reinforced polylactic acid laminates. Journal of Thermoplastic Composite Materials 2015

Bax B, Müssig J. Impact and tensile properties of PLA/Cordenka and PLA/flax composites. Compos Sci Technol 2008; 68(7): 1601–7

Be. E – Electric Bio-Scooter. 19/04/2016 <http://www.vaneko.com/the-be-e/>

Beakou A, Charlet K. Mechanical properties of interfaces within a flax bundle-Part II: Numerical analysis. Int J Adhes Adhes 2013; 43: 54–9

Blackbird El Capitan Guitar. 19/04/2016 <https://www.blackbirdguitar.com/products/el-capitan>

Bledzki AK, Faruk O, Sperber VE. Cars from BioFibres. Macromol Mater Eng 2006;291(5):449-57.

Bledzki AK, Jaszkiewicz A, Scherzer D. Mechanical properties of PLA composites with man-made cellulose and abaca fibres. Compos Part A: Appl S 2009;40(4):404-12.

Bledzki AK, Jaszkiewicz A. Mechanical performance of biocomposites based on PLA and PHBV reinforced with natural fibres – A comparative study to PP. Compos Sci Technol 2010;70(12):1687-1696.

Bocz K, Szolnoki B, Marosi A, Tábi T, Wladyka-Przybylak M, Marosi G. Flax fibre reinforced PLA/TPS biocomposites flame retarded with multifunctional additive system. Polym Degrad Stab 2013;106:63-73.

Bodros E, Pillin I, Montrelay N, Baley C. Could biopolymers reinforced by randomly scattered flax fibre be used in structural applications?. Compos Sci Technol 2007;67(3):462-70.

Brouwer WD. Natural Fiber Composites, Saving Weight and Cost with Renewable Materials Thirteenth International Conference on Composite Materials. 2001.

Buitrago BL, Santiuste C, Sánchez-Sáez S, Barbero E, Navarro C. Modelling of composite sandwich structures with honeycomb core subjected to high-velocity impact. Compos Struct 2010;92(9):2090-2096.

Caperlan. CAPERLAN BLYSS DEEP TEAM 5” FLAX Jig Fishing Rod. 19/04/2016 <https://www.decathlon.co.uk/blyss-deep-team-5-flax-fibre-id_8164177.html>

Carbon fibre market price. 20/04/2016 <http://www.build-on-prince.com/carbon-fiber.html#sthash.Ab1zqtdw.dpbs>

Charles, E. W., Charles, A. D., James, W. S., & Mark, T. B. (2005). PVC handbook.

Conzatti L, Giunco F, Stagnaro P, Capobianco M, Castellano M, Marsano E. Polyester-based biocomposites containing wool fibres. Compos Part A: Appl Sci Manuf 2012; 43: 1113-9

Davies, G. (2003). Future trends in automotive body materials. Mater Automob Bodies, 8, 252-269.

Davim JP, Reis P. Study of delamination in drilling carbon fiber reinforced plastic (CFRP) using design experiments. Compos Struct 2003;59:481-7.

Davim JP, Rubio JC, Abrao AM. A novel approach based on digital image analysis to evaluate the delamination factor after drilling composite laminates. Compos Sci Tech 2007;67(9):1939-1945.

Dhakal HN, Arumugam V, Aswinraj A, Santulli C, Zhang ZY, Lopez-Arraiza A. Influence of temperature and impact velocity on the impact response of jute/UP composites. Polym Test 2014;35:10-19.

Dhakal HN, Skrifvars M, Adekunle A, Zhang ZY. Falling weight impact response of jute/methacrylated soybean oil bio-composites under low velocity impact loading. Compos Sci Technol 2014; 92: 134–41.

Dhakal HN, Zhang ZY, Bennett N, Reis PNB. Low-velocity impact response of non-woven hemp fibre reinforced unsaturated polyester composites: Influence of impactor geometry and impact velocity. Compos Struct 2012;94(9):2756-63.

Dhakal HN, Zhang ZY, Richardson MOW, Errajhi OAZ. The low velocity impact response of non-woven hemp fibre reinforced unsaturated polyester composites. Compos Struct 2007;81(4):559-67.

Dittenber DB, GangaRao HV. Critical review of recent publications on use of natural composites in infrastructure. Compos Part A: Appl S 2010;43(8):1419-29.

Duchemin, B. J., Mathew, A. P., & Oksman, K. (2009). All-cellulose composites by partial dissolution in the ionic liquid 1-butyl-3-methylimidazolium chloride. Composites Part A: Applied Science and Manufacturing, 40(12), 2031-2037.

Duigou AL, Pillin I, Bourmaud A, Davies P, Baley C. Effect of recycling on mechanical behaviour of biocompostable flax/poly (l-lactide) composites. Compos Part A: Appl S 2008;39(9):1471-8.

Durão P, Gonçalves JS, Tavares RS, Albuquerque C, Aguiar A, Torres A. Drilling tool geometry evaluation for reinforced composite laminates. Compos Struct 2010;92(7):1545–1550.

Efunda. Mechanical properties of Polyester. 27/04/2016 <https://www.efunda.com/materials/polymers/properties/polymer_datasheet.cfm?MajorID=P-TP&MinorID=1>

Epoxy work tops. Epoxy Resin Mechanical properties. 27/04/2016 <http://plastics.ulprospector.com/generics/13/c/t/epoxy-properties-processing>

European Union. (2000). The Directive 2000/53/EC of the European Parliament and of the Council of 18 September 2000 on end-of-life vehicles. OJ L, 269 (34-49).

European Union. (2005). The Directive 2005/64/EC of the European Parliament and of the Council of 26 October 2005 on the type-approval of motor vehicles with regard to their reusability, recyclability and recoverability. OJ L, 310 (10–27).

Facca AG, Kortschot MT, Yan N. Predicting the elastic modulus of natural fibre reinforced thermoplastics. Compos Part A: Appl Sci Manuf 2006; 37: 1660–71.

Faruk O, Bledzki AK, Fink HP, Sain M. Biocomposites reinforced with natural fibers: 2000–2010. Prog Polym Sci 2012;37(11):1552–96.

Feito N, Diaz-Alvarez A, Cantero JL, Rodriguez-Millan M, Miguelez, H. Experimental analysis of special tool geometries when drilling woven and multidirectional CFRPs. Journal of Reinforced Plastics and Composites 2016;35(1):33-55.

Feito N, López-Puente J, Santiuste C, Miguélez MH. Numerical prediction of delamination in CFRP drilling. Compos Struct 2014;108:677-683.

Gaitonde VN, Karnik SR, Campos Rubio J, Esteves Correia A, Abrao AM, Paulo Davim J. Analysis of parametric influence on delamination in high-speed drilling of carbon fiber reinforced plastic composites. J Mater Process Technol 2008;203:431-8.

George J, Sreekala MS, Thomas S. A review on interface modification and characterization of natural fiber reinforced plastic composites. Polym Eng Sci. 2001;41(9):1471–85.

Gindl-Altmutter W, Keckes J, Plackner J, Liebner F, Englund K, Laborie MP. All-cellulose composites prepared from flax and lyocell fibres compared to epoxy–matrix composites. Compos Sci Technol 2012(11);72:1304–1309.

Gómez-del Rıo T, Zaera R, Barbero E, Navarro C. Damage in CFRPs due to low velocity impact at low temperature. Compos Part B: Eng 2005;36(1):41-50.

Gonzalez-Sanchez C, Martínez-Aguirre A, Pérez-García B, Martinez-Urreaga J, María U, Fonseca-Valero C. Use of residual agricultural plastics and cellulose fibers for obtaining sustainable eco-composites prevents waste generation. J Clean Prod 2014;83:228-237.

Graupner N, Herrmann AS, Müssig J. Natural and man-made cellulose fibre-reinforced poly (lactic acid)(PLA) composites: An overview about mechanical characteristics and application areas. Compos Part A: Appl S 2009;40(6):810-21.

Gurunathan T, Mohanty S, Nayak SK. A review of the recent developments in biocomposites based on natural fibres and their application perspectives. Compos Part A: Appl Sci Manuf 2015: 1-25

Hashin Z. Failure criteria for unidirectional fiber composites. Trans ASME J Appl Mech 1980;47(2):329–34.

Huber T, Bickerton S, Müssig J, Pang S, Staiger MP. Flexural and impact properties of all-cellulose composite laminates. Compos Sci Technol 2013; 88: 92–8.

Huber T, Bickerton S, Müssig J, Pang S, Staiger MP. Solvent infusion processing of all-cellulose composite materials. Carbohyd Polym 2012;90(1):730–733.

Huber T, Müssig J, Curnow O, Pang S, Bickerton S, Staiger MP. A critical review of all-cellulose composites. J Mater Sci 2012;47(3):1171–1186.

Huber T, Pang S, Staiger MP. All-cellulose composite laminates. Compos Part A: Appl S 2012;43(10):1738-45.

Ihueze CC, Okafor CE, Okoye CI. Natural fiber composite design and characterization for limit stress prediction in multiaxial stress state. J King Saud Univ-Eng Sci 2013; 27(2): 193-206

In'bô. Le Ventoux Bike. 20/04/2016 <http://inbo.fr/en/wood-and-bamboo-bikes/9-le-ventoux.html>

Ivañez I, Santiuste C, Sanchez-Saez S. FEM analysis of dynamic flexural behavior of composite sandwich beams with foam core. Compos Struct 2010;92(9):2285-2291.

Jang JY, Jeong TK, Oh HJ, Youn JR, Song YS. Thermal stability and flammability of coconut fiber reinforced poly (lactic acid) composites. Compos Part B: Eng 2012;43(5):2434-8.

Jayakumar R, Menon D, Manzoor K, Nair SV, Tamura H. Biomedical applications of chitin and chitosan based nanomaterials—A short review. Carbohydr Polym, 2010; 82(2): 227–32.

John MJ, Thomas S. Biofibres and biocomposites. Carbohydr Polym 2008; 71(3):343-64

Julkapli NM, Akil HM. Thermal properties of kenaf-filled chitosan biocomposites. Polym-Plast Tech Eng 2010;49(2):147-53.

Kim KM, Son JH, Kim SH, Weller CL, Hanna M. Properties of Chitosan Films as a Function of pH and Solvent Type. Biological Systems Engineering: Papers and Publications 2006; Paper 111.

Koronis G, Silva A, Fontul M. Green composites: a review of adequate materials for automotive applications. Compos Part B: Eng 2013; 44(1): 120–7.

Kovacevic Z, Bischof S, Fan M. The influence of Spartium junceum L. fibres modified with montmorrilonite nanoclay on the thermal properties of PLA biocomposites. Compos Part B: Eng 2015;78:122-130.

Ku H, Cheng YM, Snook C, Baddeley D. Drop weight impact test fracture of vinyl ester composites: micrographs of pilot study. J Compos Mater 2005;39(18):1607-1620.

Lebrun G, Couture A, Laperriere L. Tensile and impregnation behavior of unidirectional hemp/paper/epoxy and flax/paper/epoxy composites. Compos Struct 2013;103: 151-60.

Liang S, Guillaumat L, Gning PB. Impact behaviour of flax/epoxy composite plates. Int J Impact Eng 2015;80:56-64.

Lopez-Puente J, Zaera R, Navarro C. An analytical model for high velocity impacts on CFRPS woven laminates. Int Solids Struct 2007;44:2837-57.

Mantia FPL, Morreale M. Green composites: A brief review. Compos Part A: Appl S 2011;42(6):579-88.

Marsyahyo, E., & Rochardjo, H. S. B. (2009). Preliminary Investigation on Bulletproof Panels Made from Ramie Fiber Reinforced Composites for NIJ Level II, IIA, and IV. Journal of Industrial Textiles.

Mattrand C, Béakou A, Charlet K. Numerical modeling of the flax fiber morphology variability. Compos Part A: Appl Sci Manuf 2014; 63: 10-20.

Melo, J. D. D., Carvalho, L. F. M., Medeiros, A. M., Souto, C. R. O., & Paskocimas, C. A. (2012). A biodegradable composite material based on polyhydroxybutyrate (PHB) and carnauba fibers. Composites Part B: Engineering, 43(7), 2827-2835.

Milanese, AC, Cioffi MOH, Voorwald HJC. Thermal and mechanical behaviour of sisal/phenolic composites. Compos Part B: Eng 2012:43(7);2843-50.

Modniks J, Andersons J. Modeling the non-linear deformation of a short-flax-fiber-reinforced polymer composite by orientation averaging. Compos Part B: Eng 2013; 54: 188-93.

Mohanty AK, Misra M, Drzal LT (Eds.). Natural fibers, biopolymers, and biocomposites. CRC Press, 2005

Mohanty, A. K., Misra, M., & Hinrichsen, G. (2000). Biofibres, biodegradable polymers and biocomposites: an overview. Macromolecular materials and engineering, 276(1), 1-24.

Müssig J, Schmehl M, von Buttlar HB, Schönfeld U, Arndt K. Exterior components based on renewable resources produced with SMC technology—Considering a bus component as example. Ind crop Prod 2006;24(2):132-45.

Nasir AA, Azmi AI, Khalil ANM. Measurement and optimisation of residual tensile strength and delamination damage of drilled flax fibre reinforced composites. Measurement 2015;75:298-307.

Netravali AN, Chabba S. Composites get greener. Mater Today 2003;6(4): 22-9

Nishino T, Arimoto N. All-Cellulose Composite Prepared by Selective Dissolving of Fiber Surface. Biomacromolecules 2007;8(9):2712-2716.

Nishino, T., Matsuda, I., & Hirao, K. (2004). All-cellulose composite.Macromolecules, 37(20), 7683-7687.

O. Faruk, A.K. Bledzki, H.P. Fink, M. Sain, Biocomposites reinforced with natural fibers: 2000–2010, Prog. Polym. Sci. 37(11) (2012) 1552–96.

Ochi S. Development of high strength biodegradable composites using Manila hemp fiber and starch-based biodegradable resin. Compos Part A: Appl S 2006;37(11):1879-83.

Ochi S. Mechanical properties of kenaf fibers and kenaf/PLA composites. Mech mater 2008; 40(4): 446-52.

Oksman K. High quality flax fibre composites manufactured by the resin transfer moulding process. J Reinf Plast Compos 2001;20(7):621-7.

Olmedo A, Santiuste C, Barbero E. An analytical model for predicting the stiffness and strength of pinned-joint composite laminates. Compos Sci Tech 2014;90:67-73.

Ouajai, S., & Shanks, R. A. (2009). Preparation, structure and mechanical properties of all-hemp cellulose biocomposites. Composites Science and Technology, 69(13), 2119-2126.

Persson A, Karlsson F. Modelling non-linear dynamics of rubber bushings-parameter identification and validation. PhD thesis, Lund University 2003.

Petrucci R, Santulli C, Puglia D, Nisini E, Sarasini F, Tirillò J, Kenny JM. Impact and post-impact damage characterisation of hybrid composite laminates based on basalt fibres in combination with flax, hemp and glass fibres manufactured by vacuum infusion. Compos Part B: Eng 2015;69:507-15.

Pickering KL, Efendy MA, Le TM. A review of recent developments in natural fibre composites and their mechanical performance. Compos Part A: Appl Sci 2016;83,98-112.

Pil, L., Bensadoun, F., Pariset, J., & Verpoest, I. (2015). Why are designers fascinated by flax and hemp fibre composites?. Composites Part A: Applied Science and Manufacturing.

Plackett, D., Andersen, T. L., Pedersen, W. B., & Nielsen, L. (2003). Biodegradable composites based on L-polylactide and jute fibres. Composites Science and Technology, 63(9), 1287-1296.

Plant/Crop-based renewable resources 2020, a Vision to Enhance U.S. Economic Security Through Renewable Plant/Crop-based Resource Use (1998), www.nrel.gov/docs/legosti/fy98/24216.pdf

Poilâne C., Cherif ZE, Richard F, Vivet A, Doudou, BB, Chen J. Polymer reinforced by flax fibres as a viscoelastoplastic material. Compos Struct 2014; 112(1):100–12

Porras A, Maranon A. Development and characterization of a laminate composite material from polylactic acid (PLA) and woven bamboo fabric. Compos Part B: Eng 2012;43(7):2782-8.

Ramesh, M., Palanikumar, K., & Reddy, K. H. (2014). Influence of Tool Materials on Thrust Force and Delamination in Drilling Sisal-glass Fiber Reinforced Polymer (S-GFRP) Composites. Proc Mater Sci, 5, 1915-1921.

Rubio-López A, Hoang T, Santiuste C. Constitutive model to predict the viscoplastic behaviour of natural fibres based composites. Compos Struct 2016; 155: 8-18

Rubio-López A, Olmedo A, Díaz-Álvarez A, Santiuste C. Manufacture of compression moulded PLA based biocomposites: a parametric study. Compos Struct 2015;131:995–1000

Rubio-López A, Olmedo A, Santiuste C. Modelling impact behavior of allcellulose composite plates. Comp Struct 2015; 122: 139–43

Sánchez-Sáez S, Barbero E, Zaera R, Navarro C. Compression after impact of thin composite laminates. Compos Sci Tech 2005;65(13):1911-9.

Santiuste C, Barbero E, Miguélez MH. Computational analysis of temperature effect in composite bolted joints for aeronautical applications. J Reinf Plast Compos 2001;30(1):3-11.

Santiuste C, Díaz-Álvarez J, Soldani X, Miguélez H. Modelling thermal effects in machining of carbon fiber reinforced polymer composites. J Reinf Plast Compos 2014;33(8):758-766.

Santiuste C, Olmedo A, Soldani X, Miguélez H. Delamination prediction in orthogonal machining of carbon long fiber-reinforced polymer composites. J Reinf Plast Compos 2012;31(13):875-885.

Santiuste C, Sanchez-Saez S, Barbero E. A comparison of progressive-failure criteria in the prediction of the dynamic bending failure of composite laminated beams. Compos Struct 2010; 92(10): 2406–14.

Santiuste C, Sanchez-Saez S, Barbero E. Residual flexural strength after low-velocity impact in glass/polyester composite beams. Compos Struct 2010; 92: 25-30

Santiuste C, Soldani X, Miguélez MH. Machining FEM model of long fiber composites for aeronautical components. Compos Struct 2010;92(3):691-8.

Santiuste C, Thomsen OT Frostig Y. Thermo-mechanical load interactions in foam cored axi-symmetric sandwich circular plates–High-order and FE models. Compos Struct 2011; 93(2): 369-76.

Satyanarayana KG, Arizaga GG, Wypych F. Biodegradable composites based on lignocellulosic fibers—an overview. Prog Polym Sci 2009;34(9):982-1021.

Serizawa S, Inoue K, Iji M. Kenaf fiber reinforced poly (lactic acid) used for electronic products. J Appl Polym Sci 2006;100(1):618-24.

Shibata, M., Teramoto, N., Nakamura, T., & Saitoh, Y. (2013). All-cellulose and all-wood composites by partial dissolution of cotton fabric and wood in ionic liquid. Carbohydrate polymers, 98(2), 1532-1539.

Sliseris J, Yan L, Kasal B. Numerical modelling of flax short fibre reinforced and flax fibre fabric reinforced polymer composites. Compos Part B: Eng 2016; 89: 143-54.

Soldani X, Santiuste C, Muñoz-Sánchez A, Miguélez MH. Influence of tool geometry and numerical parameters when modeling orthogonal cutting of LFRP composites. Compos Part A: Appl Sci Manuf 2011: 42(9): 1205-16

Song YS, Lee JT, Ji DS, Kim MW, Lee SH, Youn JR. Viscoelastic and thermal behavior of woven hemp fiber reinforced poly(lactic acid) composites. Compos Part B 2012; 43: 856-60.

Song, Y. S., Lee, J. T., Ji, D. S., Kim, M. W., Lee, S. H., & Youn, J. R. (2012). Viscoelastic and thermal behavior of woven hemp fiber reinforced poly (lactic acid) composites. Composites Part B: Engineering, 43(3), 856-860.

Soykeabkaew N, Arimoto N, Nishino T, Peijs T. All-cellulose composites by surface selective dissolution of aligned ligno-cellulosic fibres. Compos Sci Technol 2008;68(10-11):2201–2207.

Soykeabkaew, N., Nishino, T., & Peijs, T. (2009). All-cellulose composites of regenerated cellulose fibres by surface selective dissolution. Composites Part A: Applied Science and Manufacturing, 40(4), 321-328.

Sridharana V, Muthukrishnanb N. Optimization of Machinability of Polyester/Modified Jute Fabric Composite Using Grey Relational Analysis (GRA). Proc Eng 2013;64:1003-1012.

Steel mechanical properties. 20/04/2016 <http://www.steelconstruction.info/Steel_material_properties>

SteelConstruction.info. Steel properties 27/04/2016 <http://www.steelconstruction.info/Steel_material_properties#Other_mechanical_properties_of_steel>

Summerscales J, Dissanayake N, Virk A, Hall W. A review of bast fibres and their composites. Part 2–Composites. Compos Part A: Appl S 2010;41(10):1336-44.

Summerscales J, Dissanayake N, Virk A, Hall W. A review of bast fibres and their composites. Part 2–Composites. Compos Part A: Appl Sci 2010;41(10):1336-1344.

Tan W, Falzon BG, Chiu LNS, Price M. Predicting low velocity impact damage and Compression-After-Impact (CAI) behaviour of composite laminates. Compos A Appl Sci Manuf 2015; 7: 212–26.

Tawakkal ISMA, Talib RA, Abdan K, Ling CN. Mechanical and physical properties of Kenaf-derived Cellulose (KDC)-filled polylactic acid (PLA) composites. Bioresources 2012;7(2):1643-4655.

Virk AS, Hall W, Summerscales J. Modelling tensile properties of jute fibres. Mater Sci Technol 2011; 27(1): 458-60.

Virk AS, Hall W, Summerscales J. Modulus and strength prediction for natural fibre composites. Mater Sci Technol 2012; 28(7): 864-71.

Voorn BV, Smit HHG, Sinke RJ, Klerk BD. Natural fibre reinforced sheet moulding compound. Compos Part A: Appl S 2001;32(9):1271-9.

Wambua P, Ivens J, Verpoest I. Natural fibres: can they replace glass in fibre reinforced plastics? Compos Sci Technol 2003; 63(9):1259–64.

WS Hampshire Inc. Mechanical properties of Polyethylene. 27/04/2016 <http://www.wshampshire.com/pdf/psg_uhmw_polyethylene.pdf>

Xiao-Yun W, Qiu-Hong W, Gu H. Research on Mechanical Behaviors of the Flax/Polyactic Acid Composites . Journal of Reinforced Plastics and Composites 2010;29(17):2561-2567.

Yeoh OH. Some forms of the strain energy function for rubber. Rubber Chem technol 1993; 66(5): 754-71

Zamri MH, Osman MR, Akil H, Shahidan MHA, Ishak ZM. Development of green pultruded composites using kenaf fibre: influence of linear mass density on weathering performance. J Clean Prod 2016;125:320-330.

Zhao, Q., Yam, R. C., Zhang, B., Yang, Y., Cheng, X., & Li, R. K. (2009). Novel all-cellulose ecocomposites prepared in ionic liquids. Cellulose, 16(2), 217-226.

List of publications

Journal publications

Rubio-López A, Hoang T, Santiuste C. Constitutive model to predict the viscoplastic behaviour of natural fibres based composites. Compos Struct 2016; 155: 8-18

Rubio-López A, Olmedo A, Díaz-Álvarez A, Santiuste C. Manufacture of compression moulded PLA based biocomposites: a parametric study. Compos Struct 2015; 131:995–1000

Rubio-López A, Olmedo A, Santiuste C. Modelling impact behavior of allcellulose composite plates. Comp Struct 2015; 122: 139–43

Rubio-López A, Artero-Guerrero J, Pernas-Sánchez J, Santiuste C. Compression after impact of flax/PLA biodegradable composites. Under review

Hoang T, Rubio-López A, Santiuste C. Viscoplastic fem model to predict the impact behaviour of flax/PLA composites. Under review

Díaz-Álvarez A, Rubio-López A, Santiuste C, Miguélez MH. Experimental analysis of drilling induced damage in biocomposites. Under review

Book chapter

Rubio-López A, Olmedo A, Díaz-Álvarez A, Santiuste C. Parametric Study on the Manufacturing of Biocomposite Materials. In Natural Fibres: Advances in Science and Technology Towards Industrial Applications (pp. 243-254). Springer Netherlands 2016.

Conference papers

Rubio-López A, Hoang-Hoang VT, Díaz-Álvarez A, Escobar E, Santiuste C. Simulation of the Impact behavior of PLA/Flax biocomposites. 19th International Conference on Composites Structures. Porto 2016.

Rubio-López A, Pernas-Sánchez J, Artero-Guerrero JA, Díaz-Álvarez A, Santiuste C. Impact and Compression after Impact (CAI) behavior of PLA/Flax biocomposites. 2nd International Conference on Mechanics of Composites. Porto 2016.

Rubio-López A, Hoang-Hoang T, Díaz-Álvarez A, Santiuste C. Modeling of viscoelastoplastic behavior of Flax/PLA biodegradable Composites. 2nd International Conference on Mechanics of Composites. Porto 2016.

Rubio-López A, Díaz-Álvarez A, Olmedo A, Santiuste C. Study of induced damage during drilling on natural fibre based biocomposites. International Conference on Advances in Composite Materials and Structures. Istanbul 2015.

Rubio-López A, Olmedo A, Díaz-Álvarez A, Santiuste C. Parametric study on the manufacturing of biodegradable composites 2nd International Conference on Natural Fibers. Azores 2015

Rubio-López A, Olmedo A, Díaz-Álvarez A, Santiuste C. Fabricación de materiales compuestos biodegradables con matriz de ácido poliláctico. 3º Encontro Português de Materiais e Estruturas Compósitas. Lisbon 2014.

Rubio-López A, Olmedo A, Santiuste C. Modelización de impactos de baja velocidad sobre placas de material compuesto biodegradable. 3º Encontro Português de Materiais e Estruturas Compósitas. Lisbon 2014